Environmental controls on the distribution of bacterial membrane lipids

by

Emily D. Matys

B.S., University of Vermont, 2009

Submitted to the Department of Earth, Atmospheric and Planetary Sciences

in partial fulfillment of the requirements for the degree of

Doctor of Philosophy

at the

MASSACHUSETTS INSTITUTE OF TECHNOLOGY

September 2018

Author: Signature redacted

Department of Earth, Atmospheric and Planetary Sciences

August 31, 2018

Certified by: Signature redacted

Roger E. Summons

Schlumberger Professor of Geobiology

Thesis Supervisor

Accepted by: Signature redacted

Robert D. van der Hilst

Schlumberger Professor of Earth and Planetary Sciences

Head of Department

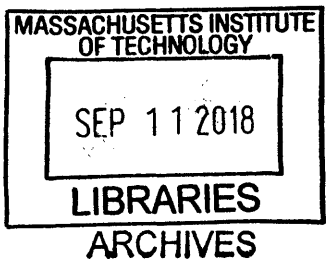

Environmental controls on the distribution of bacterial membrane lipids

by

Emily D. Matys

Submitted to the Department of Earth, Atmospheric, and Planetary Sciences

on August 31, 2018 in Partial Fulfillment of the

Requirements for the Degree of Doctor of Philosophy

THESIS ABSTRACT

Since their discovery in ancient sediments, hopanes and their biological precursors, bacteriohopanepolyols (BHPs), have been of great interest for their potential to serve as proxies for bacteria in the geological record. The validation of these and other biomarkers have implications for understanding the coevolution of organisms and the environment throughout Earth's history. 2-Methylhopanoids are of particular interest because their occurrence may be confined to cyanobacteria and alphaproteobacteria. Similarly, a stereoisomer of bacteriohopanetetrol (BHT), BHT II, has been identified exclusively in anaerobic ammonium oxidation (anammox) bacteria. However, the interpretation of sedimentary hopanoids is presently limited by an incomplete understanding of their phylogenetic associations, biological functions, and spatial and temporal disposition throughout diverse environments. I address some of these shortcomings through lipid biomarker characterization of water column and benthic microbial mat samples collected across geochemical and physiochemical gradients in the Eastern Tropical South Pacific oxygen minimum zone off the coast of northern Chile and in two ice-covered lakes of the McMurdo Dry Valleys, Antarctica. The results will enhance our ability to interpret the molecular fossil record, particularly those biomarkers that might preserve evidence of ancient marine and glacial environments. I will provide evidence that supports the use of BHT II as a biomarker for suboxia/anoxia, confirm the biosynthesis of 2-MeBHT in cyanobacteria as a response to photosynthetic stress, and describe improved methods that allow us to better detect, quantify, and interpret these markers in modern environments.

Thesis Supervisor: Roger E. Summons
Schlumberger Professor of Geobiology, MIT

Acknowledgements

This thesis would not have been possible without the unwavering support of my advisor, Roger E. Summons. Roger has not only provided me with the means necessary to choose and pursue the research described here, but has also encouraged me to seek unique field and laboratory opportunities and collaborate with world renowned experts. It has been an honor to learn from him, as an advisor and friend.

I would like to ackowneldge and thank my committee members, Tanja Bosak, Anne Junblut, and David McGee for their time, support, guidance and feedback. Their perspectives and expertise have been essential to the successful completion of my thesis. Additionally, I thank the MIT faculty who taught the courses that provided the foundation for my research.

I would also like to thank my friends and colleagues within the Department of Earth, Atmospheric, and Planetary Sciences. In particular, friends on the sixth floor of E25 have taught me so much and made my time at MIT both enjoyable and memorable.

Last, but certainly not least, I would like to thank my family. My mother, father, and brother have been a consistent source of support and encouragement for the past 32 years. I will be forever grateful for their love, support, and positivity. And finally, words cannot express how grateful I am for my partners in life (human and dog), their patience, encouragement, and unconditional love.

This research was supported by the NASA Astrobiology Institute (NNA13AA90A) and a grant from NASA Exobiology (NNX09AM88G). Travel support was provided by the MISTI Global Seed Funds grant program (MIT-Chile, MIT-Germany, and MIT-New Zealand).

Table of Contents

List of Figures

List of Tables

Chapter 1.

Introduction

Lipids have been widely used to evaluate the compositions of benthic and planktonic microbial communities (Allen et al., 2010; Castañeda and Schouten, 2011; Herndl et al., 2005; Jahnke et al., 2001, 2004; Jungblut et al., 2009; Sinninghe Damsté et al., 1995, 2005; Wakeham et al., 2003, 2007). While other biochemicals such as carbohydrates, proteins, and nucleic acids are promptly degraded after cell death, lipids are of significant interest due to the preservation potential of their hydrocarbon cores and their utility as molecular markers in modern environments and ancient sediments.

Hopanoids are well-established biomarkers for bacteria (Handley et al., 2010; Rohmer et al., 1984; Talbot and Farrimond, 2007). Hopanoids have been proposed as bacterial sterol surrogates (Rohmer et al., 1979; Ourisson et al., 1987), assisting in membrane organization (Sáenz et al., 2015) and fluidity (Sáenz et al., 2012; Wu et al., 2015). Bacteria produce a great diversity of composite haopanoids, bacteriohopanepolyols (BHPs). While bacteriohopanetetrol (BHT) is produced by diverse bacteria and is ubiquitous in modern environments (e.g. lakes, soils, marine), other structural variations are associated with particular taxonomic or environmental sources. For example, amino-BHPs are prevalent in methanotrophs (Blumenberg et al., 2006; Rush et al., 2016), a stereoisomer of BHT (BHT II) has been associated with anammox bacteria and suboxic-anoxic environments (Sáenz et al., 2011; Rush et al., 2014; Matys et al., 2017), and hopaneribonolactone and anhydrobacteriohopanetetrol have been used as indicators of oxidizing and reducing environments, respectively (Bradley et al., 2010).

BHPs are abundant in modern environments and their degradation products, geohopanoids or hopanes, have been called the most abundant natural products on Earth (Ourisson and Albrecht, 1992). In fact, intact BHPs have been reported in sediments as old as the Jurassic (Bednarczyk et al., 2005) and their recalcitrant carbon skeletons are stable in sedimentary records over timescales of up to 1.64 Ga (e.g., Summons et al., 1988; Brocks et al., 2005). However, interpretations of sedimentary hopanoids are currently impeded by an incomplete understanding of the sources, biological functions, and spatial and temporal distribution of BHPs throughout diverse environments (e.g., Newman et al., 2016). Furthermore, analytical limitations have until recently (Wu et al., 2015) precluded reliable

quantification of BHPs, which is necessary for comparison between laboratories and robust correlations between BHP compounds and particular biological sources and environmental conditions.

While this thesis does not resolve all these shortcomings, it contributes in significant ways to the understanding and application of hopanoid (and hopane) biomarkers. In particular, the chapters of this thesis focus on two biomarkers that, if substantiated, would greatly increase our understanding of microbial ecology throughout the geological record: 2-methylhopanoids and bacteriohopanetetrol isomer (BHT II).

2-Methylhopanoids (2-MeBHPs) have been of particular interest to organic geochemists and geobiologists due to their preservation potential and ubiquity in ancient sediments. During diagenesis, hopanoid parent molecules lose many of their differentiating features, such as hydroxyl and amine groups. Methylations of the hydrocarbon backbone at C-2 or C-3 position, however, are preserved for extended periods of time. In fact, 2-methylhopanes, the stable degradation products of 2-MeBHP, are among the oldest and most abundant syngenetic biomarkers, dating back to 1.64 Ga (Brocks et al., 2005). However, the interpretation of sedimentary 2-methylhopanes has been the topic of much debate. Originally proposed as biomarkers for cyanobacteria and by extension oxygenic photosynthesis (Summons et al., 1999), some alphaproteobacteria have since been shown to produce 2-MeBHPs in abundance (Rashby et al., 2007; Welander et al., 2010; Ricci et al., 2015). As a result, 2-MeBHP have more recently been investigated as markers of particular ecological niches (Ricci et al., 2014) and environmental stressors, such as increased temperature (Doughty et al., 2011; Poralla et al., 1984; Kulkarni et al., 2013), nutrient limitation (Doughty et al., 2009), pH and osmotic tension (Poralla et al., 1984; Kulkarni et al., 2013; Welander et al., 2009), and desiccation (Poralla et al., 2000). However, few studies have tested the preferential production of 2-MeBHP over des-methyl counterparts in the environment, where complex microbial communities are responding to natural environmental variability.

Chapter 2 describes BHP profiles of benthic microbial mats, which span environmental gradients throughout a unique ice-covered lake environment in the McMurdo Dry Valleys of Antarctica. 2-MeBHPs were abundant in whole mat samples, individual microbial mat laminae and sediment core samples throughout Lake Vanda, particularly where photosynthetically active radiation (PAR) was lowest. In fact, many C-2 methylated hopanoids were present without their des-methyl counterparts, a striking feature that has not been reported before now. Microbial communities present in Lake Vanda have adapted in many ways to thrive in this environment, with pigment and bacteriohopanepolyol adaptations among them. Notably, the

relative abundance of 2-MeBHT in relation to BHT was linearly correlated with PAR in isolated mat layers across a shading gradient, where other environmental parameters would have varied only slightly. This correlative data immediately suggests testable hypotheses about 2-MeBHP functions. One such hypothesis is that the production of 2-MeBHP in cyanobacteria reflects a particular environmental stressor, that is, low and fluctuating PAR, and provides valuable insight for examining 2-methylhopane patterns in the rock record.

Given the abundance 2-MeBHP production in low light environments described in Chapter 2 and the localization of 2-MeBHP in the thylakoid membrane of vegetative cell types in some bacteria (Doughty et al., 2009), we sought to further investigate the expression of 2-MeBHP by cyanobacteria in response to photosynthetic stress in Chapter 3. This chapter describes the production of 2-MeBHP by two filamentous cyanobacteria, *Nostoc punctiforme* and *Phormidium luridum*, grown under 1-12 hours of light exposure during 24-hour cycles. The relative abundance of 2-MeBHP in relation to des-methyl counterparts increases with decreased light duration in both *N. punctiforme* and *P. luridum*. These results are the first empirical evidence of the production of 2-MeBHP over des-methyl counterparts in response to limited light and reduced photosynthetic activity. Although we have demonstrated a trigger for the production of 2-MeBHP, a more complete understanding of the physiological function of 2-MeBHP is essential if we are to confidently interpret 2-methylhopanes in sedimentary archives.

While significant progress has been made toward the interpretation of long-standing biomarkers such as 2-methylhopanes, the full diversity of hopanoid-based biomarkers remains to be determined. Analytical advancements such as the development of high precision liquid chromatography mass spectrometry (HPLC-MS) methods for the analysis of intact BHPs (Talbot et al., 2001, 2003) and compound-specific response factors (Wu et al., 2015) have enabled robust identification and semi-quantification of BHPs in complex samples from a range of modern environments. For example, it is now possible to separate, identify, and quantify composite BHPs and some stereoisomers.

A stereoisomer of bacteriohopanetetrol (BHT), BHT II, was identified and proposed as a biomarker for water column hypoxia/anoxia in 2011 (Sáenz et al., 2011). BHT II had been identified exclusively in marine oxygen minimum zones (OMZs) of the Eastern Tropical Pacific, Cariaco Basin, and the Arabian and Baltic Seas (Berndmeyer et al., 2014; Kharbush et al., 2013; Sáenz et al., 2011; Wakeham et al., 2012). Although its phylogenetic association was unknown at that time, it was suggested that a "BHT II ratio" (BHT II/total BHT) could serve as a useful proxy for suboxic to anoxic conditions (Sáenz et al., 2011). More recently, BHT II

was unequivocally identified in culture enrichments of the anammox bacterium "*Candidatus* Scalindua profunda" and in sediments from Golfo Dulce, an anoxic marine fjord-like enclosure, at depths where anammox bacteria proliferate (Rush et al., 2014). Notably, BHT II has been detected in ancient sapropel sediments (2.97 Ma; Rush, *unpublished data*), which suggests that BHT II may serve as a proxy for anammox bacteria over much longer timescales than is currently possible using ladderane lipids, another biomarker for anammox bacteria.

In Chapter 4, BHT II is examined as a proxy for suboxia/anoxia and anammox bacteria in suspended organic matter across OMZ waters of the Humboldt Current System off northern Chile, as well as in surface and deeply buried sediments (125–150 ky) to examine the biological sources, transport, and fate of BHT II in the environment. It was found that the BHT II ratio increased as oxygen content decreased through the water column, consistent with previous results from Perú, the Cariaco Basin and the Arabian Sea, and in line with microbiological evidence indicating intense anammox activity in the Chilean OMZ. Notably, BHT II was transported from the water column to surface sediments, and preserved in deeply buried strata, where the BHT II ratio correlated with changes in $\delta^{15}N$ sediment values during glacial–interglacial transitions. As a result, it was concluded that BHT II offers a proxy for past changes in the relative importance of anammox, and fluctuations in nitrogen cycling in response to ocean redox changes through the geological record.

It is unclear whether additional sources of BHT II exist, if it is produced in non-marine environments, and what the implications such findings would have on interpretations of the rock record. In Chapter 5 the presence of BHT II is investigated in Lake Fryxell, Antarctica. Lake Fryxell is a perennially ice-covered lake with a sharp oxycline in a density stabilized water column. Benthic microbial communities are structured by local environmental conditions, such as oxygenation. Accordingly, we described the diversity and abundance of BHPs and possible source organisms in benthic microbial mats along a transect from oxic to anoxic conditions. Of particular interest is the ubiquity of BHT II in mats underlying both oxic and anoxic portions of the water column. This study suggests that BHT II is produced at least in part by anammox bacteria, which populate anoxic mats and may exploit anaerobic microenvironments in otherwise oxygenated mats. These results are examined in the context of BHPs as biomarkers in modern and ancient environments. It is suggested that, while BHT II ratios <0.3 may suggest the presence of anammox bacteria in benthic microbial mats or sediments, only BHT II ratio values >0.3 indicate influence from marine oxygen minimum zones and other environments supporting intense anammox activity.

References

Allen, M.A., Burns, B.P., Neilan, B.A., Jahnke, L.L., Summons, R.E., 2010. Lipid biomarkers in Hamelin Pool microbial mats and stromatolites. Organic Geochemistry 41, 1207-1218.

Bednarczyk, A., Hernandez, T.C., Schaeffer, P., Adam, P., Talbot, H.M., Farrimond, P., Riboulleau, A., Largeau, C., Derenne, S., Rohmer, M., Albrecht, P., 2005. 32,35-Anhydrobacteriohopanetetrol: an unusual bacteriohopanepolyol widespread in recent and past environments. Organic Geochemistry 36, 673–677.

Berndmeyer, C., Thiel, V., Schmale, O., Wasmund, N., Blumenberg, M., 2014. Biomarkers in the stratified water column of the Landsort Deep (Baltic Sea). Biogeosciences 11, 7009-7023.

Blumenberg, M., Kruger, M., Nauhaus, K., Talbot, H.M., Oppermann, B.I., Seifert, R., Pape, T., Michaelis, W., 2006. Biosynthesis of hopanoids by sulfate-reducing bacteria (genus Desulfovibrio). Environmental Microbiology 8, 1220–1227.

Bradley, A.S., Pearson, A., Sáenz, J.P., Marx, C.J., 2010. Adenosylhopane: the first intermediate in hopanoid side chain biosynthesis. Organic Geochemistry 41, 1075–81.

Brocks, J.J., Pearson, A., 2005. Building the Biomarker Tree of Life. Reviews in Mineralogy and Geochemistry 59, 233-258.

Castañeda, I.S., Schouten, S., 2011. A review of molecular organic proxies for examining modern and ancient lacustrine environments. Quaternary Science Reviews 30, 2851-2891.

Doughty, D.M., Hunter, R.C., Summons, R.E., Newman, D.K., 2009. 2-Methylhopanoids are maximally produced in akinetes of Nostoc punctiforme: geobiological implications. Geobiology 7, 524–532.

Doughty M.D., Coleman, M.L., Hunter, R.C., Sessions, A.L., Summons R.E., Newman D.K., 2011. The RND-family transporter, HpnN, is required for hopanoid localization to the outer membrane of Rhodopseudomonas palustris TIE-1. PNAS 108, E1045-E1051.

Handley, L., Talbot, H.M., Cooke, M.P., Anderson, K.E., Wagner, T., 2010. Bacteriohopanepolyols as tracers for continental and marine organic matter supply and phases of enhanced nitrogen cycling on the late Quaternary Congo deep sea fan. Organic Geochemistry 41, 910-914.

Herndl, G.J., Reinthaler, T., Teira, E., van Aken, H., Veth, C., Pernthaler, A., Pernthaler, J. 2005. Contribution of Archaea to total prokaryotic production in the deep Atlantic Ocean. Applied and Environmental Microbiology 71, 1715-1726.

Jahnke, L.L., Eder, W., Huber, R., Hope, J.M., Hinrichs, K.-U., Hayes, J.M., Des Marais, D.J., Cady, S.L., Summons, R.E., 2001. Signature lipids and stable carbon isotope analyses of Octopus Spring hyperthermophilic communities compared to those of Aquificales representatives. Applied and Environmental Microbiology 67, 5179-5189.

Jahnke, L.L., Embaye, T., Hope, J.M., Turk, K.A., van Zuillen, M., Des Marais, D.J., Farmer, J.D., Summons, R.E., 2004. Lipid Biomarker and Carbon Isotopic Signatures for Stromatolite-Forming, Microbial Mat Communities and Phormidium cultures from Yellowstone National Park. Geobiology 2, 31-47.

Jungblut, A.-D., Allen, M.A., Burns, B.P, Neilan, B.A., 2009. Lipid biomarker characterization of cyanobacterial mat communities in meltwater ponds of the McMurdo Ice Shelf, Antarctica. Organic Geochemistry 40, 258-269.

Kharbush, J.J., Ugalde, J.A., Hogle, S.L., Allen, E.E., Aluwiharea, L.I., 2013. Composite bacterial hopanoids and their microbial producers across oxygen gradients in the water column of the California Current. Applied and Environmental Microbiology 79, 7491-7501.

Kulkarni, G., Wu, C.-H., Newman, D.K., 2013. The general stress response factor EcfG regulates expression of the C-2 hopanoid methylase HpnP in Rhodopseudomonas palustris TIE-1. Journal of Bacteriology 195, 2490–2498.

Matys, E.D., Sepúlveda, J., Pantoja, S., Lange, C.B., Caniupan, M., Lamy, F., Summons, R. E., 2017. Bacteriohopanepolyols along redox gradients in the Humboldt Current System off northern Chile. Geobiology 15, 844-857.

Newman, D.K., Neubauer, C., Ricci, J., Wu, C-H., Pearson, A., 2016. Cellular and molecular biological approaches to interpreting ancient biomarkers. Annual Reviews Earth Planetary Sciences 44, 493–522.

Ourisson, G., Albrecht, P., 1992. Geohopanoids: The most abundant natural products on Earth? Accounts of Chemical Research 25, 398-402.

Poralla, K., Härtner, T., Kannenberg, E., 1984. Effect of temperature and pH on the hopanoid content of Bacillus acidocaldarius. FEMS Microbiology Letters 23, 253–256.

Poralla, K., Muth, G., Härtner, T., 2000. Hopanoids are formed during transition from substrate to aerial hyphae in Streptomyces coelicolor A3(2). FEMS Microbiology Letters 189, 93–95.

Rashby, S.E., Sessions, A.L., Summons, R.E., Newman, D.K., 2007. Biosynthesis of 2-methylbacteriohopanepolyols by an anoxygenic phototroph. PNAS 104, 15099–15104.

Ricci, J.N., Michel, A.J., Newman, D.K., 2015. Phylogenetic analysis of HpnP reveals the origin of 2-methylhopanoid production in Alphaproteobacteria. Geobiology 13, 267–77.

Ricci, J.N., Coleman, M.L., Welander, P.V., Sessions, A.L., Summons, R.E., Spear, J.R., Newman, D.K., 2014. Diverse capacity for 2-methylhopanoid production correlates with a specific ecological niche. The ISME Journal 8, 675-684.

Rohmer, M., Bouvier-Nave, P., Ourisson, G., 1984. Distribution of hopanoid triterpanes in prokaryotes. Journal of General Microbiology 130, 1137-1150.

Rush, D., Sinninghe Damsté, J.S., Poulton, S.W., Thamdrup, B., Garside, A.L., González, J. A., Schouten, S., Jetten, M.S.M., Talbot, H.M., 2014. Anaerobic ammonium-oxidising bacteria: A biological source of the bacteriohopanetetrol stereoisomer in marine sediments. Geochimica Et Cosmochimica Acta 140, 50–64.

Rush, D., Osborne, K.A, Birgel, D., Kappler, A., Hirayama, H., Peckmann, J., ... Talbot, H. M., 2016. The Bacteriohopanepolyol Inventory of Novel Aerobic Methane Oxidising Bacteria Reveals New Biomarker Signatures of Aerobic Methanotrophy in Marine Systems. PLOS ONE 11, e0165635.

Sáenz, J.P., Wakeham, S.G., Eglinton, T.I., Summons, R.E., 2011. New constraints on the provenance of hopanoids in the marine geologic record: Bacteriohopanepolyols in marine suboxic and anoxic environments. Organic Geochemistry 42, 1351–1362.

Sinninghe Damsté, J.S., Kenig, F., Koopmans, M.P., Koster, J., Schouten, S., Hayes, J.M., de Leeuw, J.W., 1995. Evidence for gammacerane as an indicator of water column stratification. Geochimica et Cosmochimica Acta 59, 1895-1900.

Sinninghe Damsté, J.S., Rijpstra, W.I.C., Geenevasen, J.A.J., Strous, M., Jetten, M.S.M., 2005. Structural identification of ladderane and other membrane lipids of planctomycetes capable of anaerobic ammonium oxidation (anammox). Federation of European Biochemical Societies Journal 272, 4270-4283.

Summons R.E., Powell T.G. and Boreham C.J., 1988. Petroleum geology and geochemistry of the Middle Proterozoic McArthur Basin, Northern Australia: III. Composition of extractable hydrocarbons. Geochimica et Cosmochimica Acta 52, 1747-1763.

Summons, R.E., Jahnke, L.L., Hope, J.M., Logan, G.A., 1999. 2-Methylhopanoids as biomarkers for cyanobacterial oxygenic photosynthesis. Nature 400, 554–557.

Talbot, H.M., Farrimond, P., 2007. Bacterial populations recorded in diverse sedimentary biohopanoid distributions. Organic Geochemistry 38, 1212-1225.

Talbot, H.M., Watson, D.F., Murrell, J.C., Carter, J.F., Farrimond, P., 2001. Analysis of intact bacteriohopanepolyols from methanotrophic bacteria by reversed-phase high-performance

liquid chromatography-atmospheric pressure chemical ionization mass spectrometry. Journal of Chromatography A 921, 175-185.

Talbot, H.M., Squier, A.H., Keely, B.J., Farrimond, P., 2003. Atmospheric pressure chemical ionisation reversed-phase liquid chromatography/ion trap mass spectrometry of intact bacteriohopanepolyols. Rapid Communications in Mass Spectrometry 17, 728 –737.

Wakeham, S.G., Amann, R., Freeman, K.H., Hopmans, E.C., Jorgensen, B.B., Putnam, I.F., Schouten, S., Sinninghe Damsté, J.S., Talbot, H.M., Woebken, D., 2007. Microbial ecology of the stratified water column of the Black Sea as revealed by a comprehensive biomarker study. Organic Geochemistry 38, 2070-2097.

Wakeham, S.G., Lewis, C.M., Hopmans, E.C., Schouten, S., Sinninghe Damsté, J.S., 2003. Archaea mediate anaerobic oxidation of methane in deep euxinic waters of the Black Sea. Geochimica et Cosmochimica Acta 67, 1359-1374.

Wakeham, S.G., Turich, C., Schubotz, F., Podlaska, A., Li, X.N.N., Varela, R., Astor, Y., Sáenz, J.P., Rush, D., Sinninghe Damsté, J.S., Summons, R.E., Scranton, M.I., Taylor, G.T., Hinrichs, K.-U., 2012. Biomarkers, chemistry and microbiology show chemoautotrophy in a multilayer chemocline in the Cariaco Basin. Deep-Sea Research I 63, 133–156.

Welander, P.V., Hunter, R.C., Zhang, L.C., Sessions, A.L., Summons, R.E., Newman, D.K., 2009. Hopanoids play a role in membrane integrity and pH homeostasis in Rhodopseudomonas palustris TIE-1. Journal of Bacteriology 191, 6145–6156.

Welander, P.V., Coleman, M.L., Sessions, A.L., Summons, R.E., Newman, D.K., 2010. Identification of a methylase required for 2-methylhopanoid production and implications for the interpretation of sedimentary hopanes. PNAS 107, 8537–8542.

Wu, C.-H., Bialecka-Fornal, M., Newman, D.K., 2015. Methylation at the C-2 position of hopanoids increases rigidity in native bacterial membranes. eLIFE e05663.

Wu, C.-H., Kong, L., Bialecka-Fornal, M., Park, S., Thompson, A.L., Kulkarni, G., … Newman, D.K., 2015. Quantitative hopanoid analysis enables robust pattern detection and comparison between laboratories. Geobiology 13, 391–407.

Chapter 2.

Bacteriohopanepolyols across environmental gradients in Lake Vanda, Antarctica

This chapter has been accepted at Geobiology by Wiley-Blackwell.

Bacteriohopanepolyols across environmental gradients in Lake Vanda, Antarctica

Emily D. MATYS[1*], Tyler MACKEY[1*], Christen GRETTENBERGER[2], Elliott MUELLER[1], Dawn Y. SUMNER[2], Ian HAWES[3], and Roger E. SUMMONS[1]

1. Department of Earth, Atmospheric and Planetary Sciences, Massachusetts Institute of Technology, 77 Massachusetts Avenue, Cambridge, MA 02139, USA
2. Department of Earth and Planetary Sciences, University of California, Davis, CA 95616, United States
3. University of Waikato, Tauranga, New Zealand

Abstract

Bacteriohopanepolyols (BHPs) are bacterial membrane lipids that may be used as phylogenetic or environmental biomarkers. Previous studies have described the diversity, distribution, and abundance of BHPs in a variety of modern environments. However, the regulation of BHP production in polar environments is not well understood. Benthic microbial mats from ice-covered lakes of the McMurdo Dry Valleys, Antarctica provide an opportunity to investigate the sources, the physiological roles, and preservation of BHPs in icy worlds. Lake Vanda is one of the most stable lakes on Earth, with microbial communities existing at specific positions along environmental gradients. We describe the influence of mat morphology and local environmental conditions on the diversity and distribution of BHPs and possible source organisms in benthic microbial mats from Lake Vanda. The abundance and diversity of C-2 methylated hopanoids (2-MeBHP) is of particular interest, given that their stable degradation products, 2-methylhopanes, are among the oldest and most prevalent syngenetic biomarkers. Furthermore, the interpretation of sedimentary 2-methylhopanes has been the topic of much debate. We identify cyanobacteria as the sole source of 2-MeBHP in benthic microbial mats from Lake Vanda and assess the hypothesis that 2-MeBHP are regulated in response to particular environmental conditions, such as irradiance.

Keywords: 2-Methylhopane, 2-Methylhopanoid, Bacteriohopanepolyol, Biomarker, McMurdo Dry Valleys

2.1 Introduction

Bacteriohopanepolyols (BHPs) comprise a structurally diverse group of pentacyclic triterpenoids and a biomarker class that is widely used for environmental, paleoceanographic and paleo-reconstruction studies (i.e. Talbot and Farrimond, 2007; Wakeham et al., 2012; Blumenberg et al., 2013). BHPs have long been considered bacterial sterol surrogates (Rohmer et al., 1979; Ourisson et al., 1987), assisting in membrane organization (Sáenz et al., 2015) and fluidity (Sáenz et al., 2012; Wu et al., 2015). However, the exact phylogenetic function of particular BHPs remains uncertain. While bacteriohopanetetrol (BHT) is produced by diverse bacteria and is ubiquitous in modern environments (e.g. lakes, soils, marine), other structural variations are associated with particular taxonomic or environmental sources. For example, amino-BHPs are prevalent in methanotrophs (Blumenberg et al., 2006; Rush et al., 2016), a stereoisomer of BHT (BHT II) has been associated with anammox bacteria and suboxic-anoxic environments (Sáenz et al., 2011; Rush et al., 2014; Matys et al., 2017), and hopaneribonolactone and anhydrobacteriohopanetetrol have been used as indicators of oxidizing and reducing environments, respectively (Bradley et al., 2010). Identifying and understanding taxonomic sources and environmental conditions that prompt the production of particular hopanoids in diverse modern environments continues to be a geobiologically-significant research topic.

2-Methylhopanoids (2-MeBHPs) are of particular interest due to their preservation potential and limited number of known biological sources. Through diagenesis, functionalized hopanoids may lose their differentiating features. However, hydrocarbon backbone methylations at the C-2 (2-MeBHP) or C-3 (3-MeBHP) position may be preserved. In fact, 2-methylhopanes, the stable degradation products of 2-MeBHP, are prevalent in sediments dating back to 1.64 Ga (Brocks et al., 2005). The interpretation of sedimentary 2-methylhopanes continues to be debated. Originally proposed as biomarkers for cyanobacterial oxygenic photosynthesis (Summons et al., 1999), some alphaproteobacteria have since been shown to produce 2-MeBHPs in abundance (Rashby et al., 2007; Welander et al., 2010; Ricci et al., 2015). 2-MeBHP have more recently been investigated as markers of particular ecological niches (Ricci et al., 2017) and environmental conditions such as nutrient limitation (Doughty et al., 2009), pH and osmotic tension (Poralla et al., 1984; Welander et al., 2009; Kulkarni et al., 2013, 2015; Garby et al. 2017), and desiccation (Poralla et al., 2000). However, few studies have examined the regulation of 2-MeBHP as a response to environmental conditions in natural systems.

Benthic microbial ecosystems are abundant in ice-covered lakes of Antarctica's McMurdo Dry Valleys (e.g. Wharton et al., 1993; Wharton, 1994; Paerl and Priscu, 1998; Priscu et al., 1998, 2005; Quesada et al., 2008) and provide a unique opportunity to examine hopanoid source organisms and the BHPs they produce in response to environmental conditions. Due to the oligotrophic nature of the water column (Vincent and Vincent, 1982) and limited influx of organic matter (McKnight et al., 1993) into Lake Vanda, the organic content of benthic microbial mats is a result of *in situ* growth rather than sedimentary processes. Furthermore, Lake Vanda is one of the most physically stable lakes on Earth (Vincent et al., 1981). Microbial communities exist at specific positions across persistent environmental gradients in response to local environmental conditions, including low light levels (Hawes et al., 2011, 2013; Zhang et al., 2015).

Lakes of the McMurdo Dry Valleys can be characterized as extreme shade environments due to perennial ice cover and winter darkness. The ice cover affects the quantity and spectral quality of light available to photosynthetic communities below. Lake Vanda has the thinnest ice cover (3.5-4 m; Sumner et al., 2016) and highest transmittance ($K_{ice} = 0.6$ m^{-1}) of any McMurdo Dry Valley lake (Howard-Williams, 1998). Light is scattered within the ice, creating a diffuse light environment below. Approximately 15-20% of incident photosynthetically active radiation (PAR) reaches the water column (Howard-Williams, 1998; Hawes and Schwarz, 2000). Light at the red end of the spectrum (>750 nm) is attenuated by the ice, leaving the transmitted light closer to the blue end of the spectrum (400-700 nm; Howard-Williams et al., 1998; Hawes and Schwarz, 2001). The water column is characterized by extreme clarity due to low suspended solids (<0.1 g m^{-3}) and few sources of terrestrial dissolved organic carbon (Howard-Williams et al., 1998).

Shade-adapted benthic microbial mats dominated by cyanobacteria are responsible for the majority of primary production in Lake Vanda (Hawes and Schwarz, 2001; Quesada et al., 2008; Zhang et al., 2015). The microbial communities are organized within pinnacles and prostrate mats (Hawes and Schwarz, 2001; Hawes et al., 2013; Sumner et al., 2016), contributing to the development of and exploiting steep environmental gradients. For example, the mats are finely laminated and contain characteristic pigmented zones (from orange to green and pink) that reflect acclimation to changing spectral characteristics with depth into the mats through the synthesis of particular pigments (from carotenoids to phycocyanin and phycoerythrin; Hawes et al., 2013).

BHPs may also be regulated in response to environmental conditions, as previously described. This study is the first comprehensive characterization of BHPs and their source

organisms in Antarctica. We describe the abundance and diversity of BHPs and their source organisms in whole microbial mats (prostrate and pinnacle morphologies) and sub-sectioned mat laminae from Lake Vanda, Antarctica. The analyzed samples span stable environmental gradients, from 9 m to 27 m depth and through microbial mat structures. We specifically focus on the abundance and diversity of 2-MeBHP across environmental gradients such as irradiance, and consider hopanoid C-2 methylation as an adaptation to membrane stress in polar environments.

2.2 Methods

2.2.1 Study area

Lake Vanda (77.52° S, 161.67° E) is a perennially ice-covered lake in Wright Valley, one of the McMurdo Dry Valleys in southern Victoria Land, Antarctica (Fig. 1). The ice cover (approx. 4 m thick in January 2011) minimizes wind mixing, which, in addition to strong salinity gradients, results in a stratified water column with two convecting cells in the upper part of the lake (Howard-Williams et al., 1998). Convecting cells are individually mixed by thermohaline convection. The upper convection cell (UCC; ca. 4-23 m) is well mixed with relatively consistent conductivity (~900 µs/cm), dissolved oxygen (~16 mg/L), temperature (~4.5 °C), and pH (8-8.5; Zhang et al., 2015; Castendyk et al., 2016). The upper and lower (28-45 m) convection cells are separated by a pycnocline (23-28 m), where conductivity increases rapidly with depth.

Lake Vanda is one of the most oligotrophic lakes in the world due to the low supply and efficient scavenging of phosphorus (Vincent and Vincent, 1982). Communities of phytoplankton in the water column are limited by but are highly specialized to nutrient availability, low and seasonal photosynthetically active radiation (PAR) and temperature (Vincent and Vincent, 1982). Instead, benthic microbial mats play a major role in carbon and nutrient cycling and are responsible for the majority of primary production in Lake Vanda (Hawes and Schwarz, 2001; Quesada et al., 2008). The mats are volumetrically dominated by mainly filamentous cyanobacteria including taxa within the *Leptolyngbya*, *Phormidium*, and *Tychonema* genera with lesser representation by *Pseudanabaena* and *Synechococcus* sp. (Hawes et al., 2013; Zhang et al., 2015; Sumner et al., 2016).

The cyanobacterial mats have complex topography, including prostrate forms and pinnacles that are from <1 mm to 30 cm tall (Love et al., 1983; Wharton et al., 1994; Sumner et al., 2016). They are internally laminated with organic-rich hyaline layers alternating with thin (~0.4 mm) mud-rich laminae that form annually (Hawes et al., 2001, 2013; Sumner et al.,

2016). The outermost mat layers are brown, and their geometry mimics the outer morphology of the pinnacle. Inner laminae of large pinnacles have thicker hyaline layers (0.5-3.0 mm) between mud laminae, and these areas contain green or purple pigments. The geometry of the subsurface green and purple laminae, their response to pulse amplitude modulated (PAM) photometry, and light penetration measurements all suggest active net photosynthetic carbon fixation within the large pinnacles by cyanobacteria (Sumner et al., 2016), to ~5 mm depth. These subsurface photosynthetic zones have significantly greater populations of *Phormidium* and other *Oscillatoriales* sp. than the surface brown layers, which are dominated by *Leptolyngbya* (Hawes et al., 2013; Sumner et al., 2016). The subsurface photosynthesis contributes significantly to the biomass of pinnacles colonized by the *Phormidium* and other *Oscillatoriales*. The cyanobacterial composition of sample types is consistent across individual pinnacles, including ones of different sizes (Sumner et al., 2016).

A flood in summer of 2001-2002 deposited a thick layer of mud in Lake Vanda, and that horizon can be used to constrain the age of pinnacles (Hawes et al., 2013; Sumner et al., 2016). The age of pinnacles can be determined by counting their subsurface laminae, but the organics composing laminae span the time range from capture of the mud at the pinnacle surface to the time of collection due to the abundance of internal photosynthesis (Sumner et al., 2016).

2.2.2 Sample Collection

SCUBA divers sampled benthic microbial mats during austral summer (December 2013; Table 1). The divers entered the lake through an access hole melted in the ice cover at 77° 31.6' S, 161° 36.6' E.

Whole prostrate mat samples

Whole prostrate mat samples were collected in duplicate from the UCC (11-19 m) and pycnocline (23-27 m) of Lake Vanda (Fig. 2). Prostrate mat between pinnacles was generally flat-lying but contained centimeter-scale mounds and lows with relief of a few millimeters (Hawes et al., 2013). The samples consist of the upper cohesive layers (brown surface and green and purple subsurface laminae) of prostrate microbial mats, which were cut from the surrounding mat and delaminated from underlying organic material and sediment, all younger than the 2001 flood. Samples were originally collected in Falcon tubes, and were transferred to combusted mason jars with foil between glass and rubber seal approximately 1 hour after sample collection. Jars were placed in a freezer approximately 2 hours after sampling.

Individual pinnacles

Individual pinnacles (small, medium, and large) were collected from within the UCC (19 m depth; Fig. 3). Small sized pinnacles were defined as containing two or more hyaline-sediment laminae while medium sized pinnacles were defined as being larger than small pinnacles but lacking internal green and purple pigmented areas (Sumner et al., 2016). Thus, both small and medium sized pinnacles had low populations of *Phormidium* and other *Oscillatoriales*. All of these pinnacles grew after 2001 flood (Sumner et al., 2016).

One large (~20 mm tall) pinnacle was dissected in the field. Subsamples collected include surface, green, purple, and interior mat components (Fig. 3). The "surface" subsample consisted of the outer brown surface mat. The "green" subsample consisted of green-pigmented areas in the pinnacle subsurface. The "purple" subsample consisted of pink-purple pigmented areas underlying green-pigmented areas in the pinnacle subsurface. The "interior" subsample was the central part of the pinnacle. The surface, green, and purple subsamples all grew between 2001 and 2013, whereas the interior sample grew before the 2001 flood (Sumner et al., 2016). Pinnacles and subsamples were transferred directly into combusted glass vials using a metal spatula. The vials were placed in the freezer within 2 hours of sampling.

Shading transect

At 9 m depth, microbial mats grew around and under cobbles and boulders that represent the remnants of a paleo-shoreline (Fig. 4; Mackey et al., 2017). Some rocks created overhangs that produced gradients in light and sand sedimentation for the mats growing under them (Mackey et al., 2017). Suspended mud-sized sediment was deposited on these mats (Mackey et al., 2017), demonstrating that the water under rocks was mixed with open lake water, which is the source of mud. Thus, no gradients in water chemistry or temperature are expected under overhangs, in contrast to significant light gradients. A cohesive mat unit (10.5 x 15 cm) was collected from below an overhanging rock that partially shaded the mat from ambient irradiance, as described by Mackey et al. (2017). The mat was cut and delaminated from underlying rocks, likely along the 2001 flood sediment layer. Photosynthetically active radiation (PAR) contours were calculated across the mat sample, through the generation of a 3D point cloud reconstruction of the mat and surrounding environment (Mackey et al., 2017).

The microbial mat was subsampled across a transition from a region under the overhanging rock (<10% relative PAR) to open water (>80% relative PAR). Subsamples were cut from flat-lying prostrate mats between pinnacles using sharpened metal rings with areas of 0.5 and 0.95 cm^2. Pinnacles were avoided due to their relatively complex internal structure.

Individual subsamples (~0.5-1 mm thick) were delaminated according to pigmentation: brown surface layer, green subsurface layer, and an interior layer comprised of a combination of green and purple pigmented communities plus degraded organic material. All subsamples were approximately 0.5 mm thick. Sample size was chosen to maximize the number of samples collected across the transect, while still being able to detect and quantify BHT and 2-MeBHT, which are the most abundant compounds present. As a result, BHT and 2-MeBHT are the only compounds described across the transect.

Maximum absolute PAR values of approximately 180 μmol photon m^{-2} s^{-1} were extrapolated for open water top mat samples at 9 m depth assuming a January peak incident irradiance of 1200 μmol photon m^{-2} s^{-1} (Hawes and Howard-Williams, 1998) and ice thickness of 4 m resulting in 20% light transmission through the ice cover (Hawes and Schwarz, 2000). Absolute PAR received by subsurface laminae (green and bottom) is less due to adsorption by pigments in the mat with approximately 1-5% transmission of 455 nm and 16-22% transmission of 580 nm light to 2.5 mm depth into the mat (Sumner et al., 2016). Given these constraints, BHP diversity and abundance were interpreted in the context of relative PAR values across the transect at 5% extrapolated surface PAR intervals with reductions in PAR from the surface to subsurface mat layers. It is assumed that all other ambient environmental parameters would have remained relatively consistent overlying the mat (Mackey et al., 2017).

Core Samples

A core (~5 cm) was collected from the lower convection cell (31 m depth) using a polycarbonate sampling tube (38 mm diameter). The core included a cohesive pinnacle mat (~1 cm), underlying organic material (~1 cm), and sediments below (3 cm; Fig. 5). The core was extruded and sectioned approximately 2 hours after sampling. The samples were then homogenized in a falcon tube and stored in glass scintillation vials. Samples were placed in the freezer approximately 3.5 hours after collection of the core.

2.2.3 Lipid extraction and analysis

Microbial biomass and sediment core samples were placed in combusted glass centrifuge vials and homogenized. Total lipid extracts (TLEs) were achieved through the extraction of the samples using a modified Bligh and Dyer method (Bligh and Dyer, 1959) as reported by Matys et al. (2017). Dichloromethane (DCM) was used as a replacement for chloroform. Samples were ultrasonicated (30 min. at room temperature) initially (2x) with a methanol (MeOH)/DCM/phosphate buffer (2:1:0.8, v/v/v) solution, and then (2x) with a

MeOH/DCM/trichloroacetic acid buffer (2:1:0.8, v/v/v) solution. Following each extraction, supernatants were transferred to respective separatory funnels (phosphate vs. trichloroacetic acid buffer). The supernatants were subjected to liquid-liquid extractions with DCM and water (1:1). Extracts were combined only after the TCA was removed through the liquid-liquid extraction. The TLEs were stored at -20 °C pending analysis.

The TLE was acetylated with pyridine/acetic anhydride (1:1, v/v) for 1 h at 70 °C. The acetylated TLEs were stored at -20 °C until analyzed by high-performance liquid chromatography – atmospheric pressure chemical ionization – mass spectrometry (HPLC-APCI-MS) as described in Matys *et al.* (2017). The LC-MS system included a 1200 Series HPLC (Agilent Technologies, Santa Clara, CA, USA) outfitted with an auto sampler and binary pump. The LC was linked to a Q-TOF 6520 mass spectrometer (Agilent Technologies) through an APCI interface (positive ion mode). The APCI parameters were set to the following: gas temperature, 325 °C; vaporizer temperature, 350 °C; drying gas (N_2) flow, 6 l/min; nebulizer (N_2) flow, 30 l/min; capillary voltage, 1200 V; corona needle, 4 μA; fragmentor, 150 V. A Poroshell 120 EC-C18 column (2.1 x 150 mm, 2.7 μm; Agilent Technologies) was set to 30 °C and provided fast and high-resolution separations of small molecules at low pressure. The eluent flow was held constant at 0.19 ml/min. Eluent A comprised MeOH: water (95:5, v/v) and eluent B was pure isopropyl alcohol (IPA). The HPLC gradient was as follows: isocratic flow of 100% eluent A (0-2 min.), a linear ramp of eluent B from 0-20% (2-20 min.), isocratic flow of 20% eluent B (20-30 mins), a linear ramp of eluent B from 20-30% (30-40 mins), a linear ramp of eluent B from 30-0% (40-45 mins), isocratic flow of 100% eluent A for 5 min. Following the run, the column was conditioned for 5 min. at 100% A.

BHPs were identified through the accurate mass measurements of protonated molecular ions, fragmentation patterns in MS-MS mode and assessment of relative retention times (Talbot et al., 2003, 2007; Welander et al., 2012). Quantification was completed through external standard calibration curves of 3α,12α-Dihydroxy-5β-pregnan-20-one,3,12-diacetate (PD) and authentic bacteriohopane-32,33,34,35-tetrol (BHT), 2-methylbacteriohopane-32,33,34,35-tetrol (2-MeBHT), diplopterol, 2-Mediplopterol, and 35-amino-bacteriohopane-32,33,34-triol (aminoBHT). PD was also used as an internal standard due to its structural similarity to hopanoids and because it elutes prior to BHPs of interest. Calibrations with authentic BHP standards were conducted since they are necessary to account for variations in ionization efficiencies of different BHPs (Wu et al., 2015; Garby et al. 2017).

2.2.4 Loss on ignition

Samples vary in supplementary constituents, including carbonates and silicates (Mackey et al., 2017), which bias bulk weight. Therefore, all quantitative BHP analysis was normalized to total organic carbon (TOC) measured for each sample. All extracted material was dried, weighed, and combusted at 450 °C for 4 hours in accordance with Mackey et al. (2017).

2.2.5 Genomic analyses

Several relevant samples from Lake Vanda were sequenced by the Joint Genome Institute (JGI) for a different project. Assembled metagenomes and coverage files were downloaded from JGI IMG. Metagenomes represent four individual samples: bulk prostrate mat (300022222) and pinnacle subsamples including green (3300030596) and pink (3300020201) subsurface and interior (3300020057) components (Fig. 6). We retrieved sequences that were annotated with KEGG enzyme EC:5.4.99.17 (squalene hopene cyclase). Because EC:5.4.99.17 is also used to annotate tetraprenyl-beta-curcumene cyclase, retrieved sequences were also blasted against the NCBI database and all sequences that hit non-targeted gene products were removed. Taxonomy was assigned to each sequence based on the best blast hit. Custom protein BLAST database was created for *hpn*P genes using the makeblastdb command in blast+ 2.2.29. The database contained all sequences used in the phylogenetic reconstruction of *hpnP* excluding the two environmental sequences (Ricci et al., 2015). Each assembled metagenome was blasted against the *hpnP* database using blastx with an e-value of 1E-30. The sequences retrieved from the *hnpP* database were blasted against the NCBI database, but the top results only indicated that they were in the radical SAM family which includes non-target protein products. Therefore, the retrieved sequences and database sequences were aligned in MEGA7 (Kumar et al., 2016) with Muscle (Edgar, 2004) using default parameters. A maximum likelihood tree was built in MEGA7 based on the JTT matrix-based model (Jones et al., 1992), with 1000 bootstrap replicates. The analysis involved 138 amino acid sequences with a total of 420 positions. All positions containing gaps and missing data were eliminated. Sequences that fell outside the *hpnP* clade defined by Ricci et al. (2015) were removed. Phylum level taxonomy was assigned to each remaining sequence based on the nearest relative in the phylogenetic tree. The fold-coverage *(# reads * read length/ contig length)* was used as the abundance of each sequence. The relative abundance of each *shc* sequence is defined as *fold coverage sequence/* $\sum$*fold coverage shc sequences.*

2.3 Results

2.3.1 Diversity and abundance of BHPs in whole prostrate mats

The abundance and diversity of BHPs varied with depth in whole prostrate mat samples collected at 5 depths, between 11-27 m (Fig. 2). All quantitative BHP analysis was normalized to total organic carbon (TOC; mg), which ranged from 14.4-71.2 mg. Percent TOC ranged from 3.9-32.2% (mg TOC/mg sample) in whole mat samples. Total BHP (n= 10), the summed concentration of all BHPs identified, varied with depth in no particular trend (*mean*= 36.26 ng/mg, *standard deviation (SD)*= 10.86). Bacteriohopanetetrol (BHT; Supplementary Fig. 1 **1a**; *m/z* 655) and 2-methylbacteriohopanetetrol (2-MeBHT; **2a**; *m/z* 669) were the most abundant compounds in all samples, ranging from 6.5-50 ng/mg and 2.5-17.9 ng/mg, respectively. 2-Methylbacteriohopanepentol (2-MeBHpentol; **2b**; *m/z* 727) was also identified in all whole mat samples (0.1-0.9 ng/mg). Ribonylhopane (**1e**; *m/z* 627) was identified in only one sample from 19 m depth (1 ng/mg). Aminotriol (**1c**; *m/z* 714) was detected in low abundance at 15 m (0.1 ng/mg) and at all depths greater than 19 m (1-3.3 ng/mg), within the pycnocline.

2.3.2 Diversity and abundance of BHPs in whole pinnacles

BHP abundance in individual pinnacles was normalized to TOC, which averaged 5.2 mg (*SD*= 2.2; n= 3) in small and 7.5 mg (*SD*= 3.5; n= 3) in medium sized pinnacles. BHP abundance and diversity were higher in medium than small sized pinnacles (Fig. 3). The mean of total BHP was 64.7 ng/mg (*SD*= 16.3; n= 3) in small sized pinnacles. BHPs present included ribonylhopane, BHT, 2-MeBHT, aminotriol, 2-MeBHpentol, and 3-Meaminotetrol (**3d**; *m/z* 786). Total BHP averaged 118.4 ng/mg (*SD*= 15.7; n= 3) in medium sized pinnacles and included all of the BHPs present in small sized pinnacles in addition to unsaturated BHpentose (**4e**; *m/z* 941). BHT and 2-MeBHT were the most abundant compounds present in all small and medium sized pinnacles, accounting for up to 96% of the total BHP. Minor compounds accounted for an average of 7.38% of the total BHP in small sized pinnacles and 12.24% of the total BHP in medium sized pinnacles.

2.3.3 Diversity and abundance of BHPs in pinnacle subsamples

BHP abundance and diversity generally decreased with depth into the large pinnacle, which was collected from 19 m depth (Fig. 3). BHP abundance was normalized to TOC, which ranged from 3.5-38 mg (41-100% TOC). Total BHP was 98.8 ng/mg in the brown surface sample, 158.6 ng/mg in the green subsurface sample, 81.4 ng/mg in the purple subsurface sample, and 10.9 ng/mg in the pinnacle interior. Seven compounds were identified in the brown

surface layer of the pinnacle, 6 in the green subsurface, 6 in the purple subsurface, and 3 in the pinnacle interior. BHT and 2-MeBHT were the most abundant compounds present in all pinnacle subsamples, ranging from 93-99% of the total BHP.

2.3.4 Hopanoid producers in whole prostrate mat and pinnacle subsamples

Using genetic data for similar samples from JGI IMG, hopanoid producers were identified based on the *shc* gene, essential for the cyclization of squalene to produce the basic hopanoid structure (Seckler and Poralla, 1986). Samples included: one bulk prostrate mat and pinnacle subsamples (green, purple, and interior) from 19 m depth (Fig. 6). The bulk microbial mat sample comprised 127 unique hopanoid producers. Cyanobacteria (*Synechococcales*, *Nostocales*, and *Oscillatoriales*) made up the majority (36-42%) of potential hopanoid producers in green and purple subsurface regions and 8% in the pinnacle interior. 2-Methylhopanoid producers were identified based on the *hpnP* gene, required for methylation of hopanoids at the C-2 position (Welander et al., 2010). We retrieved three unique HpnP sequences from the metagenomic data all of which are phylogenetically placed in the cyanobacterial phylum (Supplementary Fig. 2). The community from the purple laminae contained copies of all three unique HpnP sequences, whereas the communities from the bulk sample and green laminae only contained two, and the beige interior community contained a single sequence (Supplementary Fig. 2).

2.3.5 Relative abundance of 2-MeBHT across a PAR transect

Sample size was small in order to maximize the number of data points generated across the PAR transect. As a result, minor BHP components were not always detected and we describe only the most abundant compounds present, BHT and 2-MeBHT. The 2-MeBHT ratio (2-MeBHT/total BHT) was used to identify the relative contribution of 2-MeBHT in respect to its desmethyl counterpart (BHT) within individual mat layers (Fig. 4). Generally, the 2-MeBHT ratios were lowest in the top mat layer (0.13-0.23) and increased with depth into the mat, with the highest 2-MeBHT ratios measured in the bottom mat layer (0.32-0.44). The 2-MeBHT ratio and relative PAR values exhibit positive linear relationships in top brown (R^2= 0.27) and middle green mat (R^2= 0.79) layers and showed no particular trend in the bottom mat layer (*mean*= 0.38, *SD*= 0.04, *n*= 8,).

2.3.6 Core Data

BHP abundance was normalized to TOC, which ranged from 3.77-81.9 mg (2.88-20.12% TOC). Total BHP measured within each 0.5 cm sample generally decreased with depth into the core, from 26.1-11.2 ng/mg in the top layers (pinnacle mat and underlying organic material) to 1.4-9.3 ng/mg in the sediment below. However, BHP diversity and relative abundance were invariable throughout the core (Fig. 5). BHPs present included BHT, $\Delta^{6/11}$ BHT (**4/5a**; *m/z* 653), 2-MeBHT, 2-MeBHpentol, and aminotriol.

2.4 Discussion

Bacteriohopanepolyol diversity and abundance varied at multiple scales in Lake Vanda, with local environmental conditions, mat morphology, and between mat laminae. Due to the absence of a significant organic matter influx into Lake Vanda (McKnight et al., 1993) and age constraints on the growth of the mats (Hawes et al., 2013; Sumner et al., 2016), the organic contents of benthic microbial mats analyzed are a result of *in situ* growth rather than sedimentary processes. Consequently, BHP abundance and diversity were interpreted as markers of active microbial communities that reflect and respond to local environmental conditions.

BHP diversity in whole prostrate mat samples reflected ambient environmental conditions, which vary with depth into Lake Vanda. Samples collected from the upper convection cell (UCC; 4-23 m) experienced relatively similar environmental conditions (conductivity, DO, temperature, pH, and nutrients) and exhibited similar BHP profiles, comprising BHT, 2-MeBHT and 2-MeBHpentol (Fig. 2). The lack of variation suggests stable community structure and function across the UCC. However, whole mat BHP analyses described here homogenized and averaged internal mat layers with their own microenvironments, which differ in light, oxygen, and nutrient availability. Therefore, it is unclear as to how the absolute or relative abundance of these compounds change throughout the mat structure with depth in the UCC. Aminotriol was detected in one sample within the UCC at 15 m in low concentrations but only in abundance within the pycnocline (23-28 m), amounting to up to 17.9% of the total BHP. The abundance of aminotriol in the pycnocline suggests a shift in bacterial community structure and/or hopanoid production in response to environmental conditions (Supplementary Table 1). However, the hopanoids identified (BHT, 2-MeBHT, 2-MeBHpentol, and aminotriol) are produced by diverse bacteria and do not signify any unambiguous shift in community structure that we know of.

BHP abundance and diversity were higher in pinnacles than prostrate whole mat samples, likely due to diverse bacteria that colonize within and develop the pinnacle morphology. Sumner et al. (2016) described the growth of pinnacles in Lake Vanda as proceeding through several steps: Tufts initiate from random irregularities in prostrate mat, which may grow into small sized pinnacles with annual laminae. As pinnacles develop in size, to medium sized pinnacles, an increasingly diverse microbial community colonizes the mat interior. Complex bacterial communities develop in response to physical and chemical gradients within the pinnacles. As a result, medium sized pinnacles contained more abundant and diverse hopanoids than small sized pinnacles (Fig. 3).

Increased sampling resolution, such as by zones distinguishable by pigmentation, through microbial mats is essential to constraining the sources and production of the compounds identified. The occurrence of the *shc* gene and BHP abundance and diversity were similar among photosynthetically active mat laminae (Fig. 3). However, the relative abundance of BHPs and their source organisms varied. Notably, the relative abundance of 2-MeBHP increased with depth into the pinnacle in line with the number of unique sources of cyanobacteria capable of hopanoid C-2 methylation. BHP abundance and diversity decreased substantially below the photosynthetically active mat laminae, in the pinnacle interior. However, possible hopanoid producers were most diverse (142 unique sources) in this region, suggesting that possible hopanoid producers were in low abundance, were inactive, or did not experience environmental conditions that necessitate the production of BHP.

2-MeBHP have previously been identified in sessile microbial communities (Summons et al., 1999; Talbot et al., 2008; Blumenberg et al., 2013) but are particularly abundant in benthic mats subjected to low-light conditions. For example, 2-MeBHP account for up to 42% of the total BHP in Lake Vanda, 60% of the total BHP in Little Salt Spring, FL (Hamilton et al., 2016), and 54.8% of the total BHP in Mars Oasis mat, Antarctica (Talbot et al., 2008). Furthermore, we have identified 2-MeBHpentol and 2-MeBHpentose without detectable desmethyl counterparts (BHpentol and BHpentose), a rare feature. We hypothesize that shade-adapted communities in the pinnacle subsurface produce an abundance of 2-MeBHP in response to the low light environment. 2-MeBHPs act as membrane rigidifiers (Wu *et al.*, 2015), which in turn can influence membrane protein function and transport. 2-MeBHP have been shown to localize in the thylakoid membrane of vegetative cell types of *Nostoc punctiforme* (Doughty et al., 2009). Thylakoid membranes host the light-dependent reactions of photosynthesis, and their organization and structural dynamics are essential for the success of cyanobacteria (Mullineaux and Kirchhoff, 2009). It is possible that an abundance of C-2

methylated hopanoids advantageously alter physical properties of the thylakoid membrane (Iwai et al., 2014; Stingaciu et al., 2016).

The association between PAR and 2-MeBHP production was assessed through the characterization of the 2-MeBHT ratio for individual mat laminae spanning a PAR transect at a single depth with consistent water chemistry (Mackey et al., 2017). The 2-MeBHT ratio was inversely correlated with relative PAR across the transect in both the top (R^2= 0.27) and middle mat layers (R^2= 0.79). Furthermore, the 2-MeBHT ratio was consistently higher in the middle mat layer (0.22-0.38) as compared to the top mat layer (0.13-0.23). These values are consistent with results from the large pinnacle, where the 2-MeBHT ratio increased with depth into the structure. Our results suggest that C-2 methylation is advantageous in low light environments. Culture experiments have shown that 2-MeBHP are produced in abundance in the akinete cell type of *Nostoc punctiforme* in low light treatments (Doughty et al., 2009). However, akinete forming cyanobacteria are sparse if not absent from benthic mats in Lake Vanda (Hawes et al., 2013; Zhang et al., 2015; Sumner et al., 2016), which implies that 2-MeBHP in Lake Vanda are associated with cyanobacterial vegetative cell types.

It is possible that other environmental conditions prompted the production of 2-MeBHP over desmethyl counterparts. Growth temperature may encourage the development of a more rigid thylakoid membrane (Várkonyi et al., 2002). Other studies have shown that C-2 methylation may be a response to nitrogen limitation (Doughty et al., 2009). However, it is unlikely that temperature and nutrient availability change significantly across the PAR transect. Furthermore, C:N ratios for the mats are all close to ten and would not appear to indicate any nitrogen limitation (Zhang et al., 2015). In fact, the decay of mat biomass may act as a source of nutrients (Hawes et al., 2001; Sumner et al., 2016), partially alleviating any nutrient limitation of biomass accrual.

BHP signatures, including the 2-MeBHT ratio, produced in benthic microbial mats from Lake Vanda may be preserved in sedimentary archives, as exhibited in the analysis of a core collected at 31 m depth. While total BHP decreased with depth, the relative abundances of BHPs remained relatively stable throughout the core, likely reflecting the recycling and degradation of organic material. This suggests that hopanoids may be useful tools for monitoring environmental change over time in Lake Vanda. However, this would require age constraints on preserved organic material, not available for this study.

2.5 Conclusions

Bacteriohopanepolyols (BHPs) and are potentially valuable phylogenetic and environmental biomarkers due to the regulation of some hopanoids in response to particular environmental conditions. BHPs are diverse and abundant in Lake Vanda, varying with microbial community structure and environmental conditions present. As a result, BHP abundance and diversity reflect mat morphology and depth in which whole mat samples were collected along a depth transect, spanning the upper convection cell and pycnocline. Of particular interest is the abundance and diversity of 2-MeBHP. The results of this study suggest that cyanobacteria, the sole source of 2-MeBHP in Lake Vanda, produce 2-MeBHP in abundance, possibly in response to this low light environment. For example, the relative abundance of 2-methylbacteriohopanetetrol (i) increased with depth into benthic microbial mats where irradiance decreased and (ii) is inversely correlated with photosynthetically active radiation in isolated mat layers across a shading gradient, where other environmental parameters would have varied only slightly. This correlative data should be further investigated in laboratory experiments that examine the production of 2-MeBHP by non-akinete forming cyanobacteria exposed to low light environments and are essential in further elucidating the physiological function of 2-MeBHP.

2.6 Acknowledgements

We would like to acknowledge the logistic support of the US Antarctic Program and Antarctica New Zealand. Anne Jungblut and Dale Andersen provided substantial support as field team members.

2.7 Funding

This research was supported by the NASA Astrobiology Institute through an award (NNA13AA90A) to RES. Field data and sample collection for this study were supported by funds from the NASA Exobiology Program (NNX13AI60G and NNX08AO19G) and the New Zealand Foundation for Research, Science and Technology (CO1X0306). EDM and RES also thank the MIT-NZ MISTI Global Seed Funds grant program for additional support.

2.8 References

Bligh, E.G., Dyer, W.J., 1959. A rapid method of total lipid extraction and purification. Canadian Journal of Biochemistry and Physiology 37, 911–917.

Blumenberg, M., Berndmeyer, C., Moros, M., Muschalla, M., Schmale, O., Thiel, V., 2013. Bacteriohopanepolyols record stratification, nitrogen fixation and other biogeochemical

perturbations in Holocene sediments of the central Baltic Sea. Biogeosciences 10, 2725–35.

Blumenberg, M., Kruger, M., Nauhaus, K., Talbot, H.M., Oppermann, B.I., Seifert, R., ... Michaelis, W., 2006. Biosynthesis of hopanoids by sulfate-reducing bacteria (genus Desulfovibrio). Environmental Microbiology 8, 1220–27.

Bradley, A.S., Pearson, A., Sáenz, J.P., Marx, C.J., 2010. Adenosylhopane: the first intermediate in hopanoid side chain biosynthesis. Organic Geochemistry 41, 1075–81.

Brocks, J.J., Pearson, A., 2005. Building the Biomarker Tree of Life. Reviews in Mineralogy and Geochemistry 59, 233-258.

Brocks, J.J., Love, G.D., Summons, R.E., Knoll, A.H., Logan, G.A., Bowden, S.A., 2005. Biomarker evidence for green and purple sulphur bacteria in a stratified Palaeoproterozoic sea. Nature 437, 866-70.

Castendyk, D.N., Obryk, M.K., Leidman, S.Z., Gooseff, M., Hawes, I., 2016. Lake Vanda: A sentinel for climate change in the McMurdo Sound Region of Antarctica. Global and Planetary Change 144, 213-227.

Doughty, D.M., Hunter, R.C., Summons, R.E., Newman, D.K., 2009. 2-Methylhopanoids are maximally produced in akinetes of Nostoc punctiforme: geobiological implications. Geobiology 7, 524–32.

Edgar, R.C., 2004. MUSCLE: multiple sequence alignment with high accuracy and high throughput. Nucleic Acids Research 32, 1792–1797.

Garby, T.J., Matys, E.D., Ongley, S.E., Salih, A., Larkum, A.W. D., Walter, M.R., ... Neilan, B.A., 2017. Lack of methylated hopanoids renders the cyanobacterium Nostoc punctiforme sensitive to osmotic and pH Stress. Applied Environmental Microbiology 83, e00777-17.

Gibson, J.A.E, Roberts, D., Van de Vijver, B., 2006. Salinity control of the distribution of diatoms in lakes of the Bunger Hills, East Antarctica. Polar Biology 29, 694-704.

Hamilton, T.L., Welander, P.V., Albrecht, H.L., Fulton, J.M., Schaperdoth, I., Bird, L.R., ... Macalady, J.L., 2017. Microbial communities and organic biomarkers in a Proterozoic-analog sinkhole. Geobiology 15, 784–797.

Hawes, I., Howard-Williams, C., 1998. Primary Production Processes in Streams of the McMurdo Dry Valleys, Antarctica. In: J. C. Priscu (Ed.), Ecosystem Dynamics in a Polar Desert: the McMurdo Dry Valleys, Antarctica.

Hawes, I., Moorhead, D., Sutherland D., Schmeling, J., Schwarz, A.-M., 2001. Benthic primary production in two perennially ice-covered Antarctic Lakes: patterns of biomass accumulation with a model of community metabolism. Antarctic Science 13, 18-27.

Hawes, I., Schwarz, A.–M., 2001. Absorption and utilization of irradiance by cyanobacterial mats in two ice-covered Antarctic lakes with contrasting light climates. Journal of Phycology 37, 5-15.

Hawes, I., Sumner, D.Y., Andersen, D.T., Jungblut, A.D., Mackey, T.J., 2013. Timescales of growth response of microbial mats to environmental change in an ice-covered Antarctic lake. Biology, Special Issue on Polar Microbiology 2, 151-176.

Hawes, I., Sumner, D.Y., Andersen, D.T., Mackey, T.J., 2011. Legacies of recent environmental change in the benthic communities of Lake Joyce, a perennially ice covered, Antarctic lake. Geobiology 9, 394-410.

Howard-Williams, C., Schwarz, A.-M., Hawes, I., Priscu, J.C., 1998. Optical properties of the McMurdo Dry Valley lakes, Antarctica. Antarctic Research Series 72, 189-203.

Iwai, M., Yokono, M., Nakano, A., 2013. Visualizing structural dynamics of thylakoid membranes. Scientific reports 4, 3768.

Jungblut, A.D., Hawes, I., Mackey, T.J., Krusor, M., Doran, P.T., Sumner, D.Y., ... Goroncy, A.K., 2016. Microbial Mat Communities along an Oxygen Gradient in a Perennially Ice-Covered Antarctic Lake. Applied and Environmental Microbiology 82, 620-630.

Kulkarni, G., Busset, N., Molinaro, A., Gargani, D., Chaintreuil, C., Silipo, A., Giraud, E., 2015. Specific hopanoid classes differentially affect free-living and symbiotic states of Bradyrhizobium diazoefficiens. mBio 6:e01251–15.

Kulkarni, G., Wu, C.-H., Newman, D.K., 2013. The general stress response factor EcfG regulates expression of the C-2 hopanoid methylase HpnP in Rhodopseudomonas palustris TIE-1. Journal of Bacteriology 195, 2490–2498.

Kumar, S., Stecher, G., Tamura, K., 2016. MEGA7: molecular evolutionary genetics analysis version 7.0 for bigger data sets. Molecular Biology and Evolution 33, 1870–1874.

Love, F.G., Simmons, G.M., Parker, B.C., Wharton, R.A., Seaburg, K.G., 1983. Modern conophyton-like microbial mats discovered in Lake Vanda, Antarctica. Geomicrobiology Journal 3, 33-48.

Mackey, T.J., Sumner, D.Y., Jungblut, A.D., 2017. Morphological signatures of microbial activity across sediment and light microenvironments of Lake Vanda, Antarctica. Sedimentary Geology 361, 82-92.

Matys, E.D., Sepúlveda, J., Pantoja, S., Lange, C.B., Caniupan, M., Lamy, F., Summons, R.E., 2017. Bacteriohopanepolyols along redox gradients in the Humboldt Current System off northern Chile. Geobiology 15, 844-857.

Mcknight, D.M., Aiken, G.R., Andrews, E.D., Bowles, E.C., Harnish, R.A., 2013. Dissolved Organic Material in Dry Valley Lakes: A Comparison of Lake Fryxell, Lake Hoare and Lake Vanda. In: W. J. Green and E. I. Friedmann (Eds.), Physical and Biogeochemical Processes in Antarctic Lakes.

Mullineaux, W.C., Kirchhoff, H., 2009. Role of Lipids in the Dynamics of Thylakoid Membranes. Lipids in Photosynthesis 30, 283-294.

Ourisson, G., Rohmer, M., Poralla, K., 1987. Prokaryotic hopanoids and other polyterpenoid sterol surrogates. Annual Review of Microbiology 41, 301–333.

Paerl, H.W., Priscu, J.C., 1998. Microbial phototrophic, heterotrophic, and diazotrophic activities associated with aggregates in the permanent ice cover of Lake Bonney, Antarctica. Microbial Ecology 36, 221-230.

Poralla, K., Härtner, T., Kannenberg, E., 1984. Effect of temperature and pH on the hopanoid content of Bacillus acidocaldarius. FEMS Microbiology Letters 23, 253–256.

Poralla, K., Muth, G., Härtner, T., 2000. Hopanoids are formed during transition from substrate to aerial hyphae in Streptomyces coelicolor A3(2). FEMS Microbiology Letters 189, 93–95.

Priscu, J.C., Fritsen, C.H., Adams, E.E., Giovannoni, S.J., Paerl, H.W., McKay, C.P., ... Pinckney, J.L., 1998. Perennial Antarctic lake ice: an oasis for life in a polar desert. Science 280, 2095-2098.

Priscu, J.C., Fritsen, C.H., Adams, E.E., Paerl, H.W., Lisle, J.T., Dore, J.E., ... Mikucki, J.A., 2005. Perennial Antarctic lake ice: a refuge for cyanobacteria in an extreme environment. In: Castello, J.D. and Rogers, S.O. (Eds.), Life in ancient ice. Princeton Press, p. 22-49.

Quesada, A., Fernández-Valiente, E., Hawes, I., Howard-Williams, C., 2008. Benthic primary production in polar lakes and rivers. In: Vincent, W.F., and Laybourn-Parry, J. (Eds.), Polar Lakes and Rivers. Oxford Scholarship Online Monographs, p. 329.

Rashby, S.E., Sessions, A.L., Summons, R.E., Newman, D.K., 2007. Biosynthesis of 2-methylbacteriohopanepolyols by an anoxygenic phototroph. PNAS 104, 15099-15104.

Ricci, J.N., Michel, A.J., Newman, D.K., 2015. Phylogenetic analysis of HpnP reveals the origin of 2-methylhopanoid production in Alphaproteobacteria. Geobiology 13, 267–77.

Ricci, J.N., Morton, R., Kulkarni, G., Summers, M.L., Newman, D.K., 2017. Hopanoids play a role in stress tolerance and nutrient storage in the cyanobacterium Nostoc punctiforme. Geobiology 15, 173-183.

Rohmer, M., Bouvier, P., Ourisson, G., 1979. Molecular evolution of biomembranes—structural equivalents and phylogenetic precursors of sterols. PNAS 76, 847–51.

Rush, D., Osborne, K.A, Birgel, D., Kappler, A., Hirayama, H., Peckmann, J., ... Talbot, H.M., 2016. The Bacteriohopanepolyol Inventory of Novel Aerobic Methane Oxidising Bacteria Reveals New Biomarker Signatures of Aerobic Methanotrophy in Marine Systems. PLOS ONE 11, e0165635.

Rush, D., Sinninghe Damsté, J.S., Poulton, S.W., Thamdrup, B., Garside, A.L., Acuña González, J., ... Talbot, H.M., 2014. Anaerobic ammonium-oxidising bacteria: A biological source of the bacteriohopanetetrol stereoisomer in marine sediments. Geochimica et Cosmochimica Acta 140, 50-64.

Sáenz, J.P., Grosser, D., Bradley, A.S., Lagny, T.J., Lavrynenko, O., Broda, M., Simons, K., 2015. Hopanoids as functional analogues of cholesterol in bacterial membranes. PNAS 112, 11971–76.

Sáenz, J.P., Sezgin, E., Schwille, P., Simons, K., 2012. Functional convergence of hopanoids and sterols in membrane ordering. PNAS 109, 14236-14240.

Sáenz, J.P., Wakeham, S.G., Eglinton, T.I., Summons, R.E., 2011. New constraints on the provenance of hopanoids in the marine geologic record: Bacteriohopanepolyols in marine suboxic and anoxic environments. Organic Geochemistry 42, 1351-1362.

Seckler, B., Poralla, K., 1986. Characterization and partial purification of squalene-hopene cyclase from *Bacillus acidocaldarius*. Biochimica et Biophysica Acta (BBA) - General Subjects 881, 356-363.

Stingaciu, L.-R., O'Neill, H., Liberton, M., Urban, V.S., Pakrasi, H., Ohl, M., 2016. Revealing the Dynamics of Thylakoid Membranes in Living Cyanobacterial Cells. Scientific Reports 6, 19627.

Sumner, D.Y., Hawes, I., Andersen, D.T., Jungblut, A.-D., Mackey, T., Wall, K., 2016. Growth model for microbial pinnacles in Lake Vanda, Antarctica. Geobiology 14, 556-574.

Summons, R.E., Jahnke, L.L., Hope, J.M., Logan, G.A., 1999. 2-Methylhopanoids as biomarkers for cyanobacterial oxygenic photosynthesis. Nature 400, 554-556.

Talbot, H.M., Summons, R.E., Jahnke, L., Farrimond, P., 2003. Characteristic fragmentation of bacteriohopanepolyols during atmospheric pressure chemical ionisation liquid

chromatography/ion trap mass spectrometry. Rapid Communications in Mass Spectrometry 17, 2788-2796.

Talbot, H.M., Farrimond, P., 2007. Bacterial populations recorded in diverse sedimentary biohopanoid distributions. Organic Geochemistry 38, 1212-1225.

Talbot, H.M., Rohmer, M., Farrimond, P., 2007. Structural characterization of unsaturated bacterial hopanoids by atmospheric pressure chemical ionization liquid chromatography/ion trap mass spectrometry. Rapid Communications in Mass Spectrometry 21, 1613-1622.

Talbot, H.M., Summons, R.E., Jahnke, L.L., Cockell, C.S., Rohmer, M., Farrimond, P., 2008. Cyanobacterial bacteriohopanepolyol signatures from cultures and natural environmental settings. Organic Geochemistry 39, 232-263.

Várkonyi, Z., Masamoto, K., Debreczeny, M., Zsiros, O., Ughy, B., Gombos, Z., ... Szalontai, B., 2002. Low-temperature-induced accumulation of xanthophylls and its structural consequences in the photosynthetic membranes of the cyanobacterium Cylindrospermopsis raciborskii: An FTIR spectroscopic study. PNAS 99, 2410-5.

Vincent, W.F., 1981. Production strategies in Antarctic inland waters: phytoplankton eco-physiology in a permanently ice-covered lake. Ecology 62, 1215-1224.

Vincent, W.F., James, M.R., 1996. Biodiversity in extreme aquatic environments: lakes, ponds and streams of the Ross Sea sector, Antarctica. Biodiversity and Conservation 5, 1451-1471.

Vincent, W.F., Vincent, C.L., 1982. Factors controlling phytoplankton producers in Lake Vanda (77°S). Canadian Journal of Fisheries and Aquatic Sciences 39, 1602-1609.

Wakeham, S.G., Turich, C., Schubotz, F., Podlaska, A., Li, X.N., Varela, R., ... Hinrichs, K.-U., 2012. Biomarkers, chemistry and microbiology show chemoautotrophy in a multilayer chemocline in the Cariaco Basin. Deep-Sea Research I 63, 133-156.

Welander, P.V., Coleman, M., Sessions, A.L., Summons, R.E., Newman, D.K., 2010. Identification of a methylase required for 2-methylhopanoid production and implications for the interpretation of sedimentary hopanes. PNAS 107, 8537–8542.

Welander, P.V., Doughty, D.M., Wu, C.-H., Mehay, S., Summons, R.E., Newman, D.K., 2012. Identification and characterization of Rhodopseudomonas palustris TIE-1 hopanoid biosynthesis mutants. Geobiology 10, 163-177.

Welander, P.V., Hunter, R.C., Zhang, L., Sessions, A.L., Summons, R.E., Newman, D.K., 2009. Hopanoids play a role in membrane integrity and pH homeostasis in Rhodopseudomonas palustris TIE-1. Journal of Bacteriology 191, 6145-6156.

Wharton, R.A., Jr., 1994. Stromatolitic mats in Antarctic lakes. In: Bertrand-Sarfati, J. and Monty, C. (Eds.), Phanerozoic Stromatolites II. Springer Netherlands, p. 5370.

Wharton, R.A., McKay, C.P., Clow, G.D., Andersen, D.T., 1993. Perennial ice covers and their influence on Antarctic lake ecosystems. In: Green, W. (Ed.), Physical and Geochemical Processes in Antarctic Lakes. AGU Studies in Antarctic Meteorology p. 53-70.

Wu, C.-H., Kong, L., Bialecka-Fornal, M., Park, S., Thompson, A.L., Kulkarni, G., … Newman, D.K., 2015. Quantitative hopanoid analysis enables robust pattern detection and comparison between laboratories. Geobiology 13, 391–407.

Zhang, L., Jungblut, A.D., Hawes, I., Andersen, D.T., Sumner, D.Y., Mackey, T.J., 2015. Cyanobacterial diversity in benthic mats of the McMurdo Dry Valley Lakes, Antarctica. Polar Biology 38, 1097-1110.

2.9 Figures

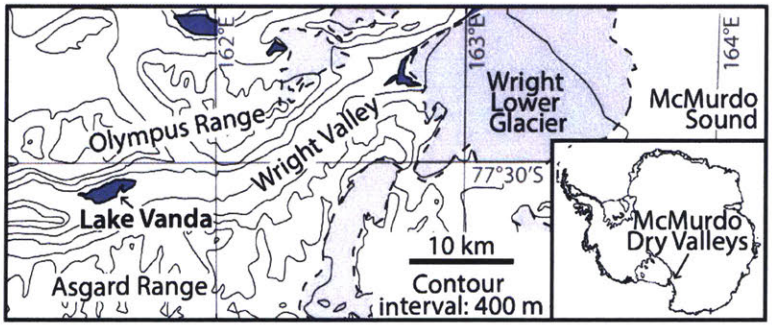

Figure 1. Map of the McMurdo Dry Valleys, Antarctica, including Lake Vanda (adapted from Sumner et al., 2016).

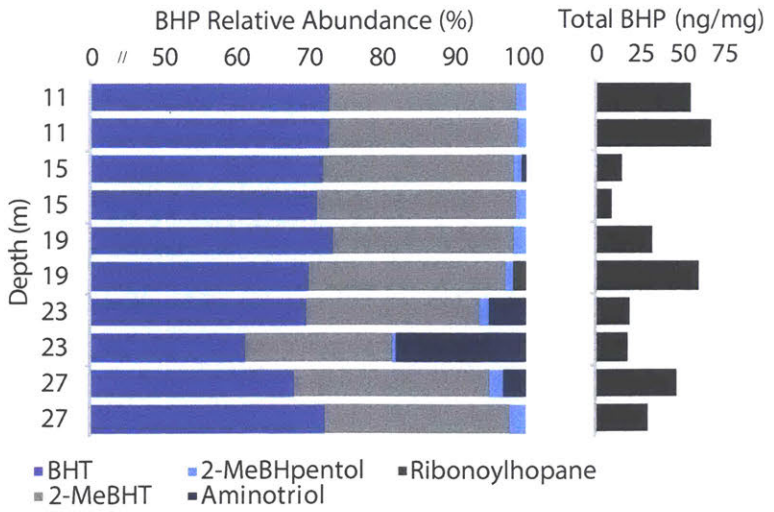

Figure 2. Bacteriohopanepolyol relative (%) and total abundance (ng BHP/mg total organic carbon) in whole prostrate mat samples collected from 11-27 m depth in Lake Vanda.

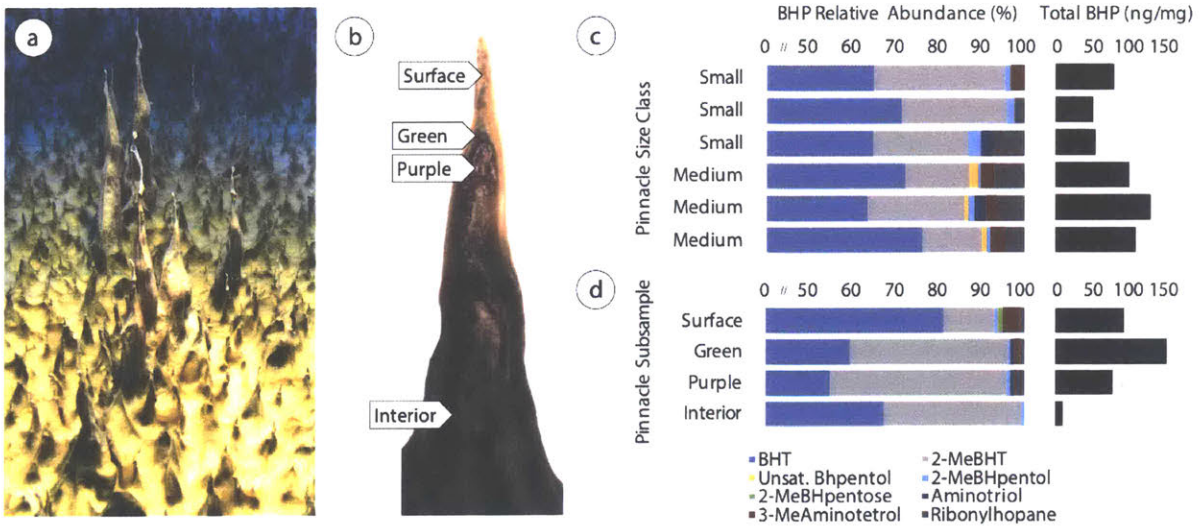

Figure 3. Well-developed pinnacle mats (a) at 19 m depth in Lake Vanda. Large pinnacles have complex internal structures (b) which include surface, green- and purple-pigmented subsurface, and interior zones. Bacteriohopanepolyol relative (%) and total abundance (ng BHP/mg total organic carbon) vary with pinnacle size (c) due to differences in bacteriohopanepolyol profiles present throughout individual pinnacle structures (d).

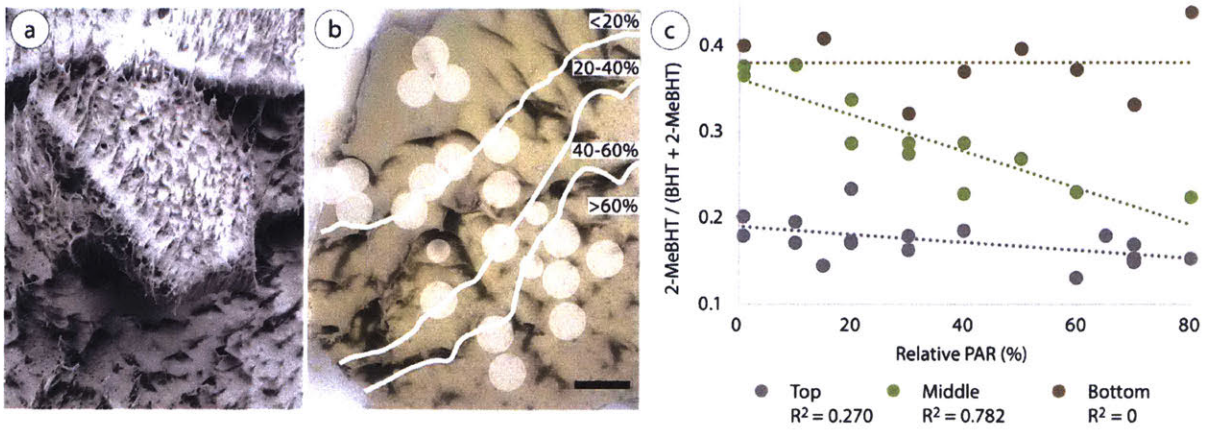

Figure 4. Microbial mats grew under boulders at 9 m depth in Lake Vanda (a). Mat subsamples (white circles) were collected and analyzed across a photosynthetically active radiation (PAR) gradient (b) which extended from below the boulder to ambient irradiance. Relative PAR contours (white lines; <20 to >60 %) were defined by Mackey et al. (2017). 2-MeBHT ratio values (2-MeBHT/BHT + 2-MeBHT) were calculated for top, middle, and bottom subsamples and plotted against relative PAR (%; c).

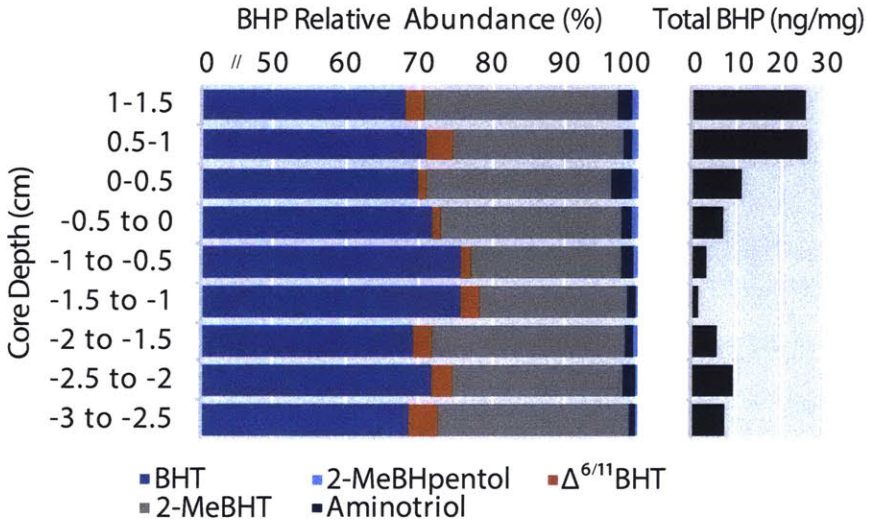

Figure 5. Bacteriohopanepolyol relative (%) and total (ng BHP/mg total organic carbon) abundance in a core collected from 31 m depth in Lake Vanda. The core comprised whole pinnacle mat (1-1.5 cm), underlying organic material (0-1 cm), and sediments below (0 to -3 cm).

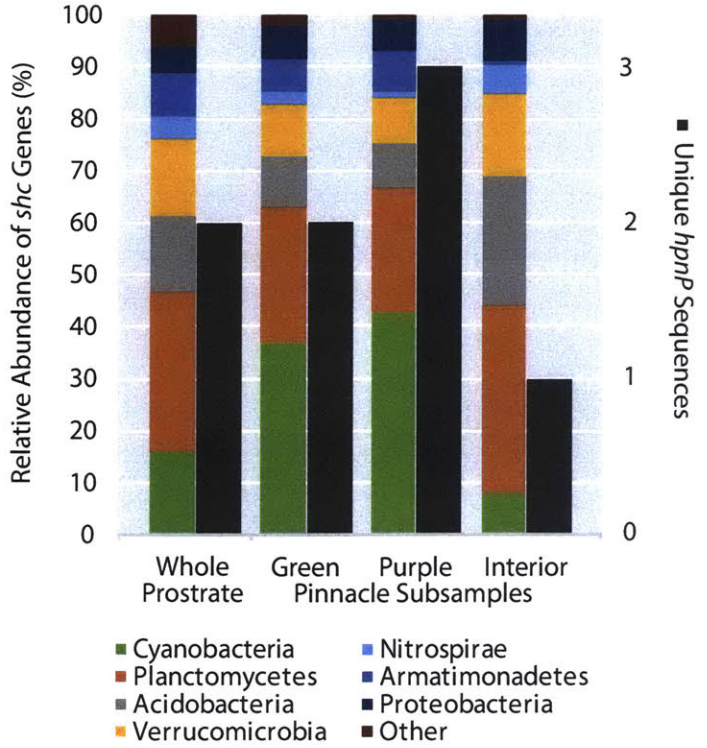

Figure 6. Occurrence of *shc* (relative abundance; %) and *hpnP* (unique sequences) genes in whole prostrate mat and green, purple, and interior pinnacle mat subsamples from 19 m depth in Lake Vanda. All unique *hpnP* sequences belong to Cyanobacteria.

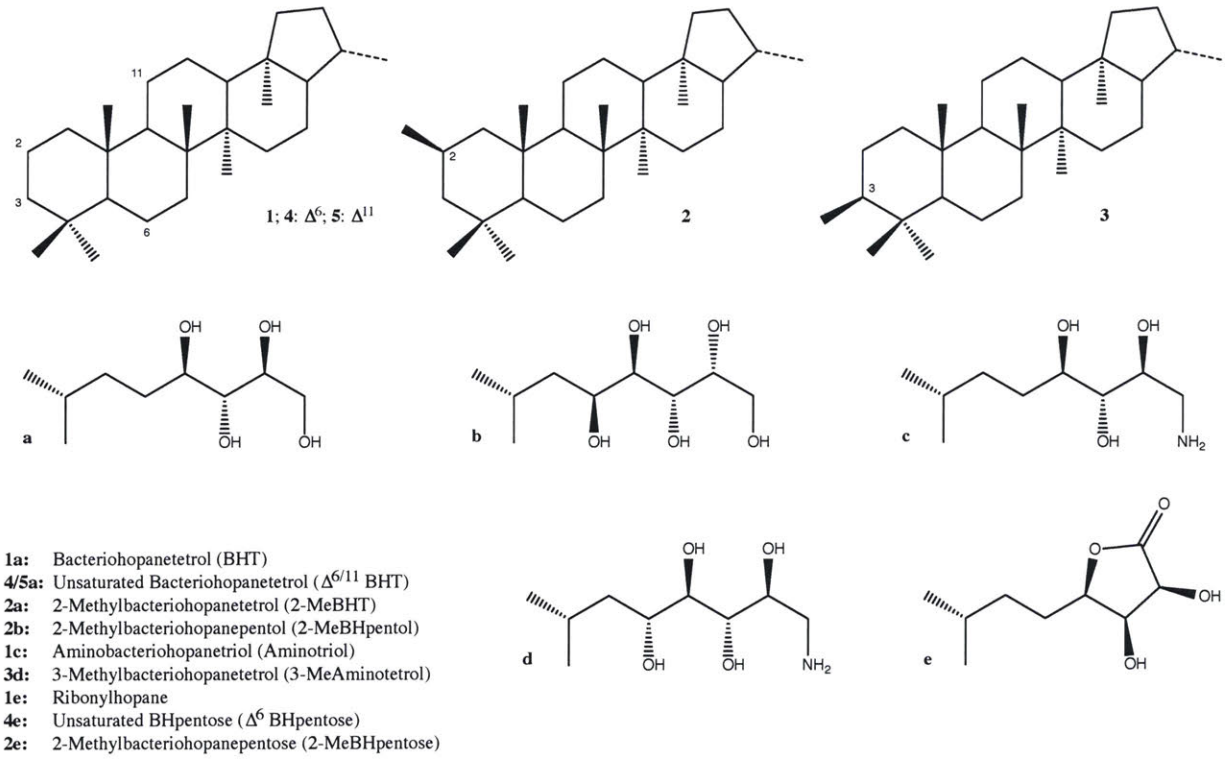

1a: Bacteriohopanetetrol (BHT)
4/5a: Unsaturated Bacteriohopanetetrol ($\Delta^{6/11}$ BHT)
2a: 2-Methylbacteriohopanetetrol (2-MeBHT)
2b: 2-Methylbacteriohopanepentol (2-MeBHpentol)
1c: Aminobacteriohopanetriol (Aminotriol)
3d: 3-Methylbacteriohopanetetrol (3-MeAminotetrol)
1e: Ribonylhopane
4e: Unsaturated BHpentose (Δ^{6} BHpentose)
2e: 2-Methylbacteriohopanepentose (2-MeBHpentose)

Supplementary Figure 1. Bacteriohopanepolyols described in this study.

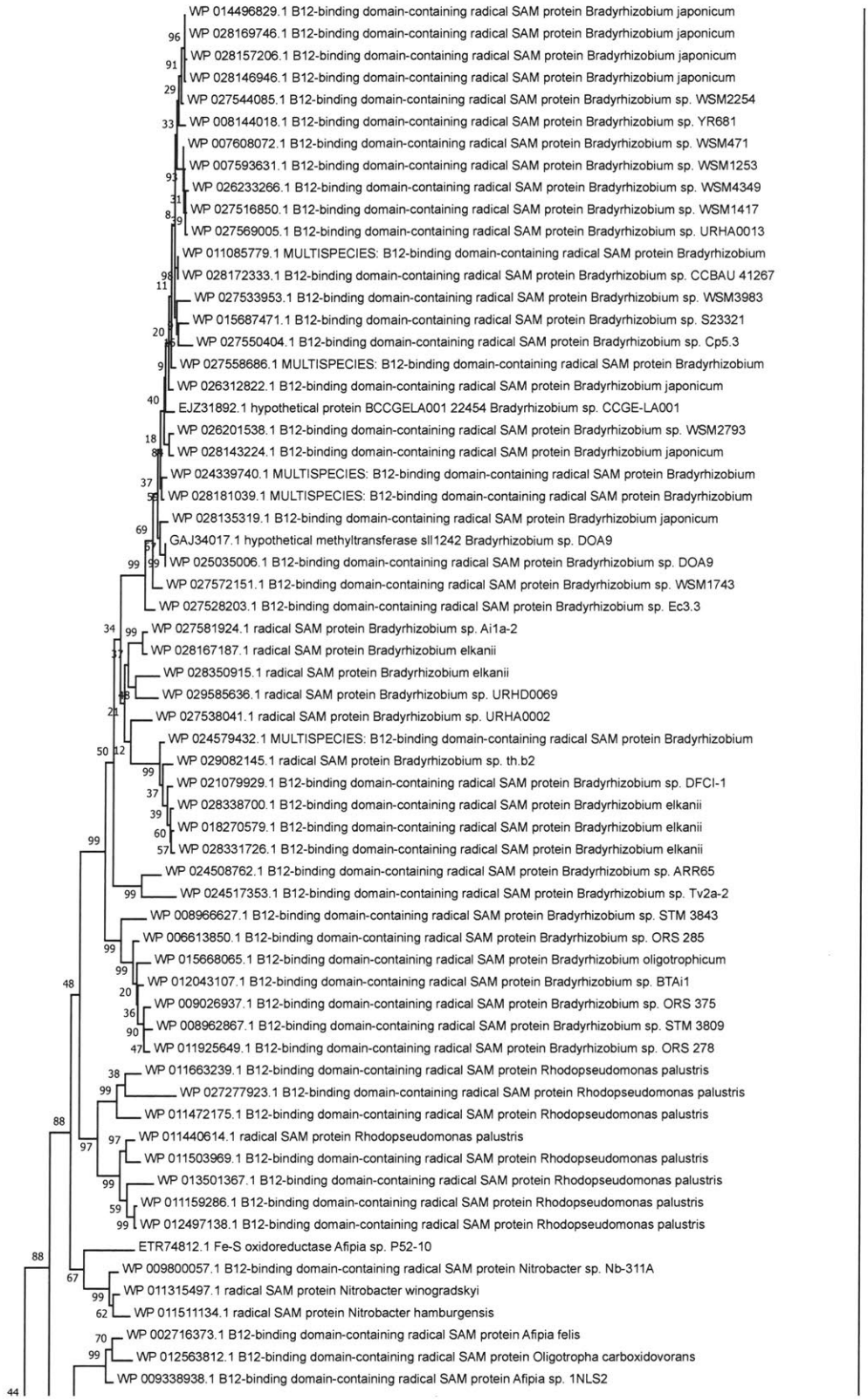
WP 014496829.1 B12-binding domain-containing radical SAM protein Bradyrhizobium japonicum
WP 028169746.1 B12-binding domain-containing radical SAM protein Bradyrhizobium japonicum
WP 028157206.1 B12-binding domain-containing radical SAM protein Bradyrhizobium japonicum
WP 028146946.1 B12-binding domain-containing radical SAM protein Bradyrhizobium japonicum
WP 027544085.1 B12-binding domain-containing radical SAM protein Bradyrhizobium sp. WSM2254
WP 008144018.1 B12-binding domain-containing radical SAM protein Bradyrhizobium sp. YR681
WP 007608072.1 B12-binding domain-containing radical SAM protein Bradyrhizobium sp. WSM471
WP 007593631.1 B12-binding domain-containing radical SAM protein Bradyrhizobium sp. WSM1253
WP 026233266.1 B12-binding domain-containing radical SAM protein Bradyrhizobium sp. WSM4349
WP 027516850.1 B12-binding domain-containing radical SAM protein Bradyrhizobium sp. WSM1417
WP 027569005.1 B12-binding domain-containing radical SAM protein Bradyrhizobium sp. URHA0013
WP 011085779.1 MULTISPECIES: B12-binding domain-containing radical SAM protein Bradyrhizobium
WP 028172333.1 B12-binding domain-containing radical SAM protein Bradyrhizobium sp. CCBAU 41267
WP 027533953.1 B12-binding domain-containing radical SAM protein Bradyrhizobium sp. WSM3983
WP 015687471.1 B12-binding domain-containing radical SAM protein Bradyrhizobium sp. S23321
WP 027550404.1 B12-binding domain-containing radical SAM protein Bradyrhizobium sp. Cp5.3
WP 027558686.1 MULTISPECIES: B12-binding domain-containing radical SAM protein Bradyrhizobium
WP 026312822.1 B12-binding domain-containing radical SAM protein Bradyrhizobium japonicum
EJZ31892.1 hypothetical protein BCCGELA001 22454 Bradyrhizobium sp. CCGE-LA001
WP 026201538.1 B12-binding domain-containing radical SAM protein Bradyrhizobium sp. WSM2793
WP 028143224.1 B12-binding domain-containing radical SAM protein Bradyrhizobium japonicum
WP 024339740.1 MULTISPECIES: B12-binding domain-containing radical SAM protein Bradyrhizobium
WP 028181039.1 MULTISPECIES: B12-binding domain-containing radical SAM protein Bradyrhizobium
WP 028135319.1 B12-binding domain-containing radical SAM protein Bradyrhizobium japonicum
GAJ34017.1 hypothetical methyltransferase sll1242 Bradyrhizobium sp. DOA9
WP 025035006.1 B12-binding domain-containing radical SAM protein Bradyrhizobium sp. DOA9
WP 027572151.1 B12-binding domain-containing radical SAM protein Bradyrhizobium sp. WSM1743
WP 027528203.1 B12-binding domain-containing radical SAM protein Bradyrhizobium sp. Ec3.3
WP 027581924.1 radical SAM protein Bradyrhizobium sp. Ai1a-2
WP 028167187.1 radical SAM protein Bradyrhizobium elkanii
WP 028350915.1 radical SAM protein Bradyrhizobium elkanii
WP 029585636.1 radical SAM protein Bradyrhizobium sp. URHD0069
WP 027538041.1 radical SAM protein Bradyrhizobium sp. URHA0002
WP 024579432.1 MULTISPECIES: B12-binding domain-containing radical SAM protein Bradyrhizobium
WP 029082145.1 radical SAM protein Bradyrhizobium sp. th.b2
WP 021079929.1 B12-binding domain-containing radical SAM protein Bradyrhizobium sp. DFCI-1
WP 028338700.1 B12-binding domain-containing radical SAM protein Bradyrhizobium elkanii
WP 018270579.1 B12-binding domain-containing radical SAM protein Bradyrhizobium elkanii
WP 028331726.1 B12-binding domain-containing radical SAM protein Bradyrhizobium elkanii
WP 024508762.1 B12-binding domain-containing radical SAM protein Bradyrhizobium sp. ARR65
WP 024517353.1 B12-binding domain-containing radical SAM protein Bradyrhizobium sp. Tv2a-2
WP 008966627.1 B12-binding domain-containing radical SAM protein Bradyrhizobium sp. STM 3843
WP 006613850.1 B12-binding domain-containing radical SAM protein Bradyrhizobium sp. ORS 285
WP 015668065.1 B12-binding domain-containing radical SAM protein Bradyrhizobium oligotrophicum
WP 012043107.1 B12-binding domain-containing radical SAM protein Bradyrhizobium sp. BTAi1
WP 009026937.1 B12-binding domain-containing radical SAM protein Bradyrhizobium sp. ORS 375
WP 008962867.1 B12-binding domain-containing radical SAM protein Bradyrhizobium sp. STM 3809
WP 011925649.1 B12-binding domain-containing radical SAM protein Bradyrhizobium sp. ORS 278
WP 011663239.1 B12-binding domain-containing radical SAM protein Rhodopseudomonas palustris
WP 027277923.1 B12-binding domain-containing radical SAM protein Rhodopseudomonas palustris
WP 011472175.1 B12-binding domain-containing radical SAM protein Rhodopseudomonas palustris
WP 011440614.1 radical SAM protein Rhodopseudomonas palustris
WP 011503969.1 B12-binding domain-containing radical SAM protein Rhodopseudomonas palustris
WP 013501367.1 B12-binding domain-containing radical SAM protein Rhodopseudomonas palustris
WP 011159286.1 B12-binding domain-containing radical SAM protein Rhodopseudomonas palustris
WP 012497138.1 B12-binding domain-containing radical SAM protein Rhodopseudomonas palustris
ETR74812.1 Fe-S oxidoreductase Afipia sp. P52-10
WP 009800057.1 B12-binding domain-containing radical SAM protein Nitrobacter sp. Nb-311A
WP 011315497.1 radical SAM protein Nitrobacter winogradskyi
WP 011511134.1 radical SAM protein Nitrobacter hamburgensis
WP 002716373.1 B12-binding domain-containing radical SAM protein Afipia felis
WP 012563812.1 B12-binding domain-containing radical SAM protein Oligotropha carboxidovorans
WP 009338938.1 B12-binding domain-containing radical SAM protein Afipia sp. 1NLS2
Proteobacteria

Supplementary Figure 2. Phylogeny of HpnP protein sequences. Sequences retrieved from the Lake Vanda metagenomic data are indicated in bold.

2.10 Tables

Table 1. Lake Vanda physical and chemical variables measured in January 2014[a]. Depths from which samples were acquired are bold.
[a] DO, dissolved oxygen; DIC, dissolved inorganic carbon; DRP, dissolved reactive phosphorus.
* Data not available.

Depth	Conductivity	DO	Temp	pH	DIC	DRP	NNN	NH4	Irradiance	Irradiance
m	µs/cm	mg/L	C	units	mM	µM	µM	µM	% surface	µmol photon/m^{2}s
9	**904**	**15.78**	**4.53**	**7.96**	*	*	*	*	**13**	**180.79**
10	904	15.89	4.52	8.03	0.8	0.06	1.73	0.23	12.6	170.88
11	**904**	**15.89**	**4.50**	**8.04**	*	*	*	*	**12.2**	**161.91**
12	904	15.89	4.86	8.05	*	*	*	*	11.8	153.73
13	904	15.88	4.46	8.09	*	*	*	*	11.4	146.19
14	904	15.88	4.46	8.09	*	*	*	*	11	139.22
15	**906**	**15.93**	**4.49**	**8.13**	*	*	*	*	**10.6**	**132.73**
16	908	16.04	4.51	8.14	*	*	*	*	10.2	126.66
17	909	15.99	4.51	8.15	*	*	*	*	9.9	120.95
18	911	16.03	4.52	8.17	*	*	*	*	9.5	115.57
19	**911**	**16.05**	**4.50**	**8.19**	*	*	*	*	**9.2**	**110.49**
20	913	16.24	4.51	8.24	0.7	0.07	2.09	0.3	8.9	105.66
21	913	16.25	4.52	8.25	*	*	*	*	8.6	101.07
22	918	16.30	4.67	8.27	*	*	*	*	8.3	96.69
23	**922**	**16.30**	**4.76**	**8.27**	*	*	*	*	**8**	**92.51**
24	924	16.29	4.80	8.28	*	*	*	*	7.7	88.51
25	963	16.22	5.13	8.28	*	*	*	*	7.5	84.67
26	968	16.22	5.16	8.28	*	*	*	*	7.2	80.98
27	**1365**	**17.34**	**5.87**	**8.23**	*	*	*	*	**6.9**	**77.42**
28	1526	18.53	6.54	8.29	*	*	*	*	6.7	74.00
29	1539	18.88	6.56	8.37	*	*	*	*	6.5	70.70
30	1554	19.61	6.62	8.44	0.8	0.07	2.45	0.09	6.2	67.51
31	**1554**	**19.70**	**6.62**	**8.46**	*	*	*	*	**6**	**64.43**
32	1554	19.76	6.62	8.47	*	*	*	*	5.8	61.44
33	1555	19.81	6.62	8.48	*	*	*	*	5.6	58.54

Table 2. Bacteriohopanepolyols in benthic microbial mats from Lake Vanda[a]

[a] TOC, total organic carbon.

* Data not available.

Type	Sample Details	Depth (m)	TOC (%)	Total BHP (ng/mg)	Ribonylhopane *m/z* 627.4625 (ng/mg)	Unsat. BHT *m/z* 653.4781 (ng/mg)	BHT *m/z* 655.4938 (ng/mg)	2-MeBHT *m/z* 669.5094 (ng/mg)	Aminotriol *m/z* 714.5309 (ng/mg)	2-MeBHpentol *m/z* 727.5149 (ng/mg)	3-MeAminotetrol *m/z* 786.5520 (ng/mg)	Unsat. Bhpentol *m/z* 941.5626 (ng/mg)	2-MeBHpentose *m/z* 957.5939 (ng/mg)
Whole Prostrate Mat Samples													
	Homogenized	11	7.32	56.38			41.11	14.50		0.76			
	Homogenized	11	7.37	68.68			49.97	17.90		0.82			
	Homogenized	15	21.69	15.48			11.12	4.10	0.11	0.14			
	Homogenized	15	22.90	9.08			6.45	2.48		0.14			
	Homogenized	19	5.87	34.13			25.05	8.47		0.61			
	Homogenized	19	22.45	61.08	1.04		42.74	16.55		0.74			
	Homogenized	23	36.24	19.72			13.77	4.67	1.01	0.27			
	Homogenized	23	3.88	18.68			11.48	3.72	3.35	0.13			
	Homogenized	27	7.87	48.37			32.96	13.01	1.49	0.92			
	Homogenized	27	24.08	30.99			22.39	7.87		0.73			
Subsampled Pinnacle Structure													
	Surface	19	100.00	98.75	1.06		80.17	11.71	0.08	0.68	3.80		1.26
	Green subsurface	19	41.47	158.62	1.55		94.60	57.67	1.12	1.30	2.39		
	Purple subsurface	19	100.00	81.36	1.59		44.58	33.37	0.78	0.62	0.43		
	Interior	19	93.70	10.87			7.32	3.46	0.00	0.09			
Pinnacle Structures by Size													
	Small pinnacles	19	45.89	83.39			54.07	25.29		1.24	2.79		
	Small pinnacles	19	86.93	53.36	1.27		38.04	13.11		0.93			
	Small pinnacles	19	46.00	57.36	4.23		37.01	12.80	1.70	1.62			
	Medium pinnacles	19	63.89	105.43	7.44		76.02	15.86		0.77	3.27	2.07	
	Medium pinnacles	19	54.76	135.85	8.70		86.13	30.86	3.42	1.90	3.78	1.06	
	Medium pinnacles	19	7.50	113.89	4.97		86.96	15.56	0.00	0.79	4.19	1.42	
Core Samples													
	Top pinnacle	31	14.20	25.32		0.64	17.23	6.76	0.48	0.22			
	Top bulk	31	20.12	26.16		0.95	18.56	6.13	0.30	0.23			
	-0.5-0 cm	31	7.52	11.18		0.12	7.81	2.84	0.30	0.11			
	0-0.5 cm	31	4.89	7.13		0.09	5.12	1.76	0.11	0.06			
	0.5-1 cm	31	2.88	3.43		0.05	2.60	0.71	0.06	0.02			
	1-1.5 cm	31	13.13	1.41		0.04	1.07	0.29	0.01	0.00			
	1.5-2 cm	31	2.58	5.85		0.14	4.05	1.55	0.07	0.03			
	2-2.5 cm	31	2.88	9.33		0.25	6.70	2.20	0.14	0.04			
	2.5-3 cm	31	3.12	7.54		0.30	5.17	1.99	0.06	0.02			

Chapter 3.

2-Methylhopanoids produced in response to limited light exposure by *Phormidium luridum* and *Nostoc punctiforme*

2-Methylhopanoids produced in response to limited light exposure in *Phormidium luridum* and *Nostoc punctiforme*

Emily D. MATYS[1], Lily MOMPER[1], Elliott MUELLER[1], and Roger E. SUMMONS[1]

1. Department of Earth, Atmospheric and Planetary Sciences, Massachusetts Institute of Technology, 77 Massachusetts Avenue, Cambridge, MA 02139, USA

Abstract

2-Methylbacteriohopanepolyols (2-MeBHP) and their diagenetic degradation products, 2-methylhopanes, have been widely applied as molecular biomarkers for cyanobacteria in modern and ancient environments. However, this interpretation has been questioned due to an incomplete understanding of the physiological function of 2-MeBHP in cyanobacteria. Given the abundance 2-MeBHP production by canobacteria in some natural low light environments, we sought to investigate the production of 2-MeBHP by cultured cyanobacteria in response to light limitation. We measured the abundance of 2-MeBHP by two filamentous cyanobacteria, *Nostoc punctiforme* and *Phormidium luridum,* grown at various light exposure periods during a 24-hour cycle. The relative abundance of 2-MeBHP in relation to des-methyl counterparts increases with decreased light duration in both taxa. These results are the first empirical evidence of 2-MeBHP production over des-methyl counterparts in response to photosynthetic stress. Although we have demonstrated a trigger for elevated 2-MeBHP production, a more complete understanding of the physiological function of 2-MeBHP is essential if we are to confidently interpret 2-methylhopanes in sedimentary archives.

Keywords: 2-Methylhopane, 2-Methylhopanoid, Bacteriohopanepolyol, Biomarker, Cyanobacteria

3.1 Introduction

Bacteriohopanepolyols (BHPs) are membrane lipids that are considered sterol surrogates in diverse bacteria (Ourisson et al., 1987). They play a role in membrane integrity (Sáenz et al., 2012, 2015) and stress tolerance (Welander et al., 2009; Ricci et al., 2016). 2-Methylhopanoids (2-MeBHP) are methylated at the C-2 position and have been of great interest for understanding the evolution of life on Earth since the ubiquity of their stable degradation products, 2-methylhopanes, was realized (Ourisson and Albrecht, 1992; Brocks et al., 2005). However, resolving the sources and physiological functions of 2-MeBHP is required in order to confidently interpret 2-methylhopanes in sedimentary archives.

Cyanobacteria have been identified as one of the most significant sources of 2-MeBHP, the basis for the hypothesis that 2-methylhopanes may serve as proxy for cyanobacteria and oxygenic photosynthesis in sedimentary archives (Summons et al., 1999). However, it has since been shown that some α-proteobacteria and an acidobacterium may also produce an abundance 2-MeBHP (Rashby et al., 2007; Welander et al., 2009; Ricci et al., 2015). Furthermore, the physiological function of 2-MeBHP has yet to be determined and no direct link between 2-MeBHP and the oxygenic photosynthesis has been identified. *Nostoc punctiforme* has been used as a model organism to investigate the role of 2-MeBHP in cyanobacteria (Doughty et al., 2009; Garby et al., 2017; Ricci et al., 2016). These studies suggested that 2-MeBHP may be a general stress marker, at least in part due to an abundance of 2-MeBHP in akinete cell types (Doughty et al., 2009) which are produced in response to adverse environmental conditions. However, because a number of cyanobacteria capable of C-2 hopanoid methylation do not differentiate (e.g., heterocysts, akinetes; Talbot et al., 2008) it is of significant interest to identify the role of 2-MeBHP in these organisms.

Several lines of evidence suggest that 2-MeBHP may be associated with photosynthetic stress in the vegetative cells of some cyanobacteria. While 2-MeBHP are most abundant (μg/mg of total lipid fraction extract) in the outer membrane of the *N. punctiforme* akinete cell type, 2-MeBHP were shown to be localized exclusively in the thylakoid membrane of vegetative cell types (Doughty et al., 2009). Thylakoid membranes are the sites of the light-dependent reactions of photosynthesis and the organization and structural dynamics of the thylakoid membrane are essential for cyanobacterial survival and reproduction (Stingaciu et al., 2016). Furthermore, 2-MeBHP are abundant (in some cases >50% total BHP) in some natural low light environments, such as a Little Salt Spring, Florida (Hamilton et al., 2017) and Lake Vanda, Antarctica (Chapter 2; Matys et al., *accepted*). In Lake Vanda, cyanobacteria were

identified as the sole source of 2-MeBHP and the 2-MeBHT ratio (2-MeBHT/total BHT) was found to inversely correlate with relative photosynthetically active radiation (PAR) along a shaded transect where all other environmental conditions remained stable. Here, we test the hypothesis that 2-MeBHP are produced by cyanobacteria over des-methyl counterparts in response to photosynthetic stress associated with short duration of PAR.

We examined the effect of light exposure on 2-MeBHP production by monitoring the growth of filamentous cyanobacteria *N. punctiforme* and *Phormidium luridum* that were exposed to 1-12 hours of light per day. In addition to *N. punctiforme* wild type, we grew an *hpnP* mutant unable to methylate hopanoids at the C-2 position (Welander et al., 2012) in order to characterize the impact of an inability to produce 2-MeBHP on BHP profiles. We present these data in an effort to inform hypotheses regarding the biological function of 2-MeBHP in a more diverse and ecologically relevant set of cyanobacteria.

3.2 Methods

3.2.1 Strains and growth conditions

Nostoc punctiforme is a heterocystous, filamentous cyanobacterium capable of cellular differentiation to heterocyst and akinete cell types following signals of a specific environmental change (Meeks et al., 2002). The strain used for this study was *N. punctiforme* ATCC 29133 (PCC 73102) wild type (WT) and its *hpnP* deletion mutant. These were obtained from Dianne Newman and are described in Ricci et al. (2016). *Phormidium luridum var. olivace* is also a filamentous cyanobacterium that produces BHP (Summons et al., 1999). However, unlike *N. punctiforme*, *P. luridum* does not differentiate into different cell types (Whitton, 2011). Furthermore, *P. luridum* may in fact be more ecologically relevant than *N. punctiforme* as it is widely distributed in various aquatic environments (mainly freshwater) and may proliferate in response to environmental conditions such as increased dissolved inorganic nitrogen concentrations (McAllister et al., 2016). *P. luridum* was obtained from the Culture Collection of Algae at The University of Texas at Austin (UTEX culture collection; B 426). All strains were grown in BG11 broth medium (Sigma-Aldrich 73816) in sterile polycarbonate culture bottles topped with a 0.22 μm to allow for gas exchange. The medium was supplemented with Trace Metal Mix A5 with Co (Sigma-Aldrich 92949) and micronutrient solution (Kuhl and Lorenzen, 1964). The cultures were incubated at 20°C and kept homogeneous by constant stirring under cool white fluorescent lights at 26-32 μmol photon/m^2/s. Cultures receiving 12 hours of light per day were considered to be the control. Periodicity was adjusted in four treatments of varying length with all other conditions consistent and stable. Growth curves

were established for *P. luridum* through optical density measurements in triplicate at 680 nm (chlorophyll *a*) with a Biotek Syntergy 2 spectrophotometer.

3.2.2 Microscopic analysis

The cultures were visually monitored throughout the experiment (Supplementary Fig. 1). Cells were harvested from actively growing cultures by serological pipette and were concentrated by centrifugation at 1000 × *g* for 10 min. Light microscopy was performed on an Axio Imager M1 microscope at 100 ×.

3.2.3 Lipid extraction and analysis

Microbial biomass was placed in combusted glass centrifuge vials. Total lipid extracts (TLEs) were obtained by extracting the samples using a modified Bligh and Dyer method (Bligh and Dyer, 1959) as reported by Matys et al. (2017). Dichloromethane (DCM) was used in place of chloroform. Samples were extracted by ultrasonication (60 mins at room temperature) first (2x) using a mixture of methanol/dichloromethane/phosphate buffer solution (2:1:0.8, v/v/v), and then (1x) using a mixture of methanol/dichloromethane/trichloroacetic acid buffer (2:1:0.8, v/v/v). After each extraction, the supernatants were transferred to different separatory funnels (phosphate vs. trichloroacetic acid buffer). Supernatants were then subjected to liquid-liquid extractions using 5mL of dichloromethane and water (1:1). Extracts were not combined until the TCA was removed from the samples, after the liquid-liquid extraction step. The TLEs were kept at -20 °C until analysis.

The TLE was acetylated with pyridine/acetic anhydride (1:1, v/v) at 70 °C for 1 h and left at room temperature overnight. The acetylated TLEs were analyzed by high-performance liquid chromatography-atmospheric pressure chemical ionization – mass spectrometry (HPLC-APCI-MS) as described in Matys et al. (2017). The LC-MS system comprised a 1200 Series HPLC (Agilent Technologies, Santa Clara, CA, USA) equipped with an auto sampler and a binary pump linked to a Q-TOF 6520 mass spectrometer (Agilent Technologies) via an APCI interface operated in positive ion mode. A Poroshell 120 EC-C18 column (2.1 x 150 mm, 2.7 μm; Agilent Technologies) was chosen to provide fast and high-resolution separations of a wide range of small molecules at lower pressures. The column temperature was set at 30°C. The eluent flow remained constant at 0.19 ml/min. Eluent A contained a mixture of methanol: H_2O 95:5 v/v and eluent B comprised pure isopropyl alcohol (IPA). The HPLC gradient was as follows: isocratic flow of 100% eluent A (0-2 mins), a linear gradient from 0-20% of eluent

B (2-20 mins), isocratic flow of 20% B (20-30 mins), a linear gradient from 20-30% of eluent B (30-40 mins), a linear gradient from 30-0% B (40-45 mins), isocratic flow of 0% B for 5 minutes. The column was conditioned for 5 minutes of post-run time at 100% A. The APCI parameters were as follows: gas temperature 325 °C, vaporizer temperature 350 °C, drying gas (N_2) flow 6 l/min, nebulizer (N_2) flow 30 l/min, capillary voltage 1200 V, corona needle 4 μA, and fragmentor 150 V.

BHPs were identified on the basis of accurate mass measurements of their protonated molecular ions, fragmentation patterns in MS-MS mode, and by comparison of relative retention times of BHP in previously characterized samples (Talbot et al., 2003, 2007; Welander et al., 2012). Quantification was achieved through an internal standard of 3α,12α-Dihydroxy-5β-pregnan-20-one,3,12-diacetate (PD) and external standard calibration curves of PD, BHT, and 2-MeBHT. PD was chosen as an internal standard because of its structural similarity to hopanoids and because it has a retention time that does not overlap with the range of BHPs of interest. Calibrations with authentic BHP standards were necessary to account for variations in ionization efficiencies of different BHPs (Wu et al., 2015).

3.3 Results

3.3.1 Growth of cyanobacteria under a range of diel cycles

Phormidium luridum var. olivace was grown under 5 different light treatments for 41 days: 1, 2, 4, 6, and 12 h of irradiance per day (denoted 1-12L). Culture growth rate increased with the duration of light cycle (Fig. 1). Precise growth curves for *N. punctiforme* WT and *hpnP* mutant could not be established due to variance in the production of chlorophyll *a* (Chl *a*) in different cell types. However, growth was visible under all light treatments, with the most turbidity and biomass in the 12L treatment. It is possible that low light treatments (<12L) prompted the differentiation of vegetative cells into akinete cell types in the *N. punctiforme* cultures. The medium contained an abundance of nitrogen (nitrate and ammonium) to impede the development of heterocysts, specialized nitrogen-fixing cells formed during nitrogen starvation. Light microscopy indicated that a small number of heterocysts and no akinetes were present in the 12L treatment.

3.3.2 Expression of bacteriohopanepolyols

P. luridum produced bacteriohopanetetrol (BHT) and 2-methylbacteriohopanetetrol (2-MeBHT; Table 1). In addition to BHT and 2-MeBHT, *N. punctiforme* WT produced 2 isomers of bacteriohopanepentol (denoted BHpentol-I and BHpentol-II) and 2-

methylbacteriohopanepentol (denoted 2-MeBHpentol-I and 2-MeBHpentol-II; Table 2). *N. punctiforme hpnP* mutant did not produce 2-MeBHP (Table 2). Instead, the relative abundance of BHpentol-I and BHpentol-II increases from 9.5% of the total BHP in the WT strain to 42.8% of the total BHP in the *hpnP* mutant grown under control conditions (12/12 h L/D cycle). The relative abundance of BHT remained ~60% in *Nostoc punctiforme* WT and *hpnP* mutant grown under control conditions (12/12 h L/D cycle).

3.3.3 Effects of diel cycle length on hopanoid production

Phormidium luridum var. olivace produced only BHT and 2-MeBHT. As a result, changes in the BHP profiles of the strain grown under 1-12 hours of light per day (1-12L) were monitored by the relative abundance (%) of 2-MeBHT on days 17, 24, 31, and 41 of the experiment (Fig. 2). The 12L treatment was considered the control. The relative abundance of 2-MeBHT in the control incubation remained stable (*mean*= 4.8%; *SD*= 0.47; *n*=4) during the entire experiment (41 days). The relative abundance of 2-MeBHT in experimental incubations (<12L) generally increased with decreasing light exposure as follows: From 4.3-7.7% in 6L incubations (*mean*= 5.6; *SD*= 1.5; *n*= 4); From 4.2-7.3% in 4L incubations (*mean*= 5.4; *SD*= 1.4; *n*= 4); From 5.4-9.8% in 2L incubations (*mean*= 7.2; *SD*= 1.9; *n*= 4); From 7.6-14.8% in 1L incubations (*mean*= 10.2; *SD*= 3.2; *n*= 4).

The BHP profiles (relative abundance) of *N. punctiforme* WT cultures were analyzed on day 35 of incubation (Fig. 3) to assess the relative abundance of 2-MeBHT in strains grown under 1-12 hours of light per day. The 12L incubation was considered the control. The relative abundance of 2-MeBHT was linearly correlated with duration of light exposure ($y = -3.607\ln(x) + 34.237$; $R^2 = 0.93$), from 25.9% at 12L to 33.9% at 1L. The relative abundances of 2-MeBHpentol (-I and -II) show no particular trend (*mean*= 12.5%; *SD*= 4.4; *n*= 5), with a maximum (19.9%) in 6L incubations. However, the relative abundance of 2-MeBHpentol-II exceeds 2-MeBHpentol-I in 6L and 12L incubations and 2-MeBHpentol-I exceeds 2-MeBHpentol-II in 1, 2, and 4L incubations. Total BHpentol (BHpentol-I + BHpentol-II) is linearly correlated with duration of light treatment ($y = 0.8511x - 1.1107$; $R^2 = 0.9647$). BHpentol-II exceeds BHpentol-I in all incubations.

The BHP profiles (relative abundance) of *N. punctiforme hpnP* mutant cultures were analyzed on day 35 of incubation (Fig. 3). The 12L incubation was considered the control. The relative abundance of BHT was approximately 55% in *N. punctiforme* WT and *hpnP* mutant control. However, although the relative abundance of BHT remained relatively consistent, from 50.9-57.4% of total BHP in all *N. punctiforme* WT treatments, the relative abundance of BHT

in the *hpnP* mutant strain ranged from 29.5-57.2% of the total BHP. The relative abundance of total BHpentol was considerably higher in the *hpnP* mutant treatments, ranging from 42.8-70.5% of the total BHP, as compared to 0.3-9.5% of the total BHP in the *N. punctiforme* WT. BHpentol-I was consistently more abundant than BHpentol-II in the *hpnP* mutant, as compared to the WT where BHpentol-II exceeded BHpentol-I in all treatments.

3.4 Discussion

Hopanoid methylation has been shown to enhance membrane rigidity (Wu et al., 2015), which may be why hopanoid methylation is increased in response to environmental conditions in the anoxygenic phototroph *Rhodopseudomonas palustris* (Welander et al., 2009; Wu et al., 2015) and the cyanobacterium *Nostoc punctiforme* (Doughty et al., 2009; Ricci et al., 2016; Garby et al., 2017). 2-MeBHPs localize in the akinete cell types of *N. punctiforme* in response to low light conditions (Doughty et al., 2009). However, many filamentous cyanobacteria that are capable of hopanoid C-2 methylation no not differentiate into akinete cell types and 2-MeBHP are abundant and diverse in low light environments dominated by shade-adapted cyanobacteria (Matys et al., submitted; Hamilton et al., 2017) that do not produce akinetes. As such, we extend observations of 2-MeBHP production and localization in response to photosynthetic stress in the filamentous cyanobacterium *Phormidium luridum* and complement these studies with the analysis of *N. punctiforme* wild type (WT) and *hpnP* mutant strain unable to methylate BHP at the C-2 position. We find that 2-MeBHP are produced in abundance in response to reduced (<12 L) light period in *Phormidium luridum* and *N. punctiforme* and discuss our findings and implications for 2-MeBHP as molecular biomarkers.

3.4.1 *Phormidium luridum*

Within 17 days of incubation, BHP profiles of *P. luridum* cultures grown under 1-2L exhibited an increase in the relative abundance of 2-MeBHT, as compared to the control (12L; Fig. 2). The relative abundance of 2-MeBHT increases with decreased light exposure from 4.41% in the control to 9.58% in the 1L culture, a difference of 5.17% 2-MeBHT. However, growth curves of 1L and 2L treatments indicate that very little growth has occurred within that same time period (17 days; Fig. 1). Rather than investing in cellular growth and division, we hypothesize that the cells are energetically restricted and therefore are directing available resources to repair and maintenance of cellular components. One such response is the modification of preexisting membrane lipids, such as BHT, to produce a membrane lipid profile that is better suited for the low PAR environment. The methylation of BHT at C-2, for

instance, may change the packing of the hopanoid with other lipids and proteins and affect membrane biophysical properties such as rigidity (Wu et al., 2015). These data suggest that changes in 2-MeBHP signatures of some cyanobacteria may reflect a response to environmental conditions on very short timescales. In fact, increased 2-MeBHP membrane lipid composition was likely achieved within the first 17 days of the incubation according to our measurements. During exponential growth (approximately 17-41 days), the relative abundance of 2-MeBHT in all incubations was likely maintained through a combination of the modification of preexisting membrane lipid structures (the methylation of BHT at C-2 to produce 2-MeBHT) and *de novo* synthesis of new membrane lipids (2-MeBHT).

The change in membrane lipid composition between days 31 and 41 of incubation in all treatments <12L cannot be explained by cellular growth alone, due to insignificant changes in chl *a*. We hypothesize that upon approaching stationary phase of growth, cells no longer allocate resources to cellular division but apportion resources to cellular maintenance and reconfigure membrane lipids accordingly. Welander et al. (2009) also noted an increase in the abundance of 2-MeBHT in stationary phase of *R. palustris* TIE-1 cultures. Nutrient deficiency, resulting from cellular growth, is unlikely to prompt the production of 2-MeBHP. If this were the case, the treatments with the highest growth rates (12L) would exhibit the greatest increase in % 2-MeBHP which is not seen here. In conclusion, we suggest that the BHP profiles described here reflect the duration of light exposure and phase of growth rather than other peripheral environmental conditions.

3.4.2 *Nostoc punctiforme*

Unlike *P. luridum*, *N. punctiforme* may differentiate into hormogonia, akinete and heterocyst cell types (Meeks et al., 2002), which contain distinct BHP profiles (Doughty et al., 2009). Based on light microscopy and the relative abundance of BHT, 2-MeBHT, and 2-MeBHpentol measured here and the previously reported hopanoid compositions of *N. punctiforme* cell types (Doughty et al., 2009), the cellular composition of 1-12L incubations appear to be dominated by vegetative cell types. Vegetative cell types have been shown to contain an abundance of BHT as well as 2-MeBHT and 2-MeBHpentol (thylakoid membrane 1.7:1.7:1; outer membrane 1.2:0:0; Doughty et al., 2009). Akinetes contain three times more 2-MeBHpentol than BHT in the outer membrane. If present, they would increase in the relative abundance of 2-MeBHpentol. However, only a small increase in 2-MeBHpentol exists in <12L treatments, suggesting that while akinetes may be present they are not abundant and do not

make a significant impact on the BHP profile of *N. punctiforme* cultures exposed to 35 days of <12 L. We interpret the BHP profiles of *N. punctiforme* incubations accordingly.

The relative abundance of 2-MeBHT, in relation to BHT (denoted % 2-MeBHT), produced by *N. punctiforme* WT increased with decreasing light exposure (Fig. 2). This reiterates the relationship between light duration and 2-MeBHT production identified with *P. luridium*. In addition to BHT and 2-MeBHT, *N. punctiforme* WT also produced abundant 2-MeBHpentol (2-MeBHpentol-I and 2-MeBHpenol-II). The relative abundance of 2-MeBHpentol, in relation to des-methyl counterpart BHpentol (BHpentol-I and BHpentol-II; denoted % 2-MeBHpentol), also increased with decreasing light duration (Fig. 2), with a notable difference of 47.6%. We suggest that 2-MeBHPs are being produced over des-methyl counterparts in *N. punctiforme* vegetative cells as seen in *P. luridum*. It is possible that the increase % 2-MeBHpentol may reflect the production of akinete cells (Doughty et al., 2009) rather than membrane lipid reconfiguration hypothesized for 2-MeBHT. However, this would cause a decrease in 2-MeBHT ratio values due to an increase in the presence of BHT in akinete cell types.

When unable to produce 2-MeBHP (2-MeBHT, 2-MeBHpentol-I, and 2-MeBHpentol-II), *N. punctiforme hpnP* mutants exposed to <12 L produced an abundance of BHpentol-I and BHpenol-II. It seems unlikely that *N. punctiforme hpnP* mutants would differentiate while WT would not, given identical growth conditions. As a result, these results suggest that while not optimal, BHpentol may compensate for a lack of 2-MeBHP in *N. punctiforme* vegetative cell types, serving a rigidifying function. Similar membrane lipid modifications were identified by Garby et al. (2017). The ability of bacteria to synthesize other lipids (i.e. BHpentol) that functionally complement the inability to produce C-2 methylated hopanoids may be one of the reasons why no clear phenotype for 2-MeBHP has been identified to date.

3.5 Conclusions

We describe the production of C-2 methylated bacteriohopanepolyols (2-MeBHP) over des-methyl counterparts in response to photosynthetic stress (limited light duration) in two types of filamentous cyanobacteria, *Phormidium luridum* and *Nostoc punctiforme*. *P. luridum* likely employed 2 strategies for adjusting membrane lipid composition in response to photosynthetic stress, including the modification of preexisting lipid structures and *de novo* synthesis of new lipids, throughout the growth cycle. While the *N. punctiforme* growth cycle was not monitored, we find that within 35 days of incubation the majority of vegetative cells did not differentiate into akinete cell types, known to produce an abundance of 2-MeBHP. As

a result, we conclude that decreased light cycles result in the modification of vegetative cell membrane lipids to include a higher abundance of C-2 methylated hopanoids in relation to their des-methyl counterparts. When unable to produce 2-MeBHP, *N. punctiforme hpnP* mutants produce an abundance of two isomers of bacteriohopanepentol. While structurally dissimilar, 2-MeBHPs and bacteriohopanepentols may perform a similar function in adapting to environmental stressors, such as photosynthetic stress. Although 2-MeBHP localization has been addressed in vegetative cells of *Nostoc punctiforme*, we suggest that future studies which isolate and characterize the hopanoid contents of cytoplasmic, thylakoid, and outer membrane fractions of *Phormidium luridum* are essential to identifying the role of 2-MeBHP in a comprehensive suite of cyanobacteria.

3.6 Acknowledgements

We would like to acknowledge Prof. Tanja Bosak for use of laboratory equipment, including spectrophotometer and microscope. Without this logistical support this work would not have been possible. We also thank Prof. Dianne Newman for *N. punctiforme* WT and *hpnP* mutants.

3.7 Funding

This research was supported by the NASA Astrobiology Institute (Award NNA13AA90A) to RES.

3.8 References

Bligh, E.G., Dyer, W.J., 1959. A rapid method of total lipid extraction and purification. Canadian Journal of Biochemistry and Physiology 37, 911–917.

Brocks, J.J., Love, G.D., Summons, R.E., Knoll, A.H., Logan, G.A., Bowden, S.A., 2005. Biomarker evidence for green and purple sulphur bacteria in a stratified Palaeoproterozoic sea. Nature 437, 866-70.

Doughty, D.M., Hunter, R.C., Summons, R.E., Newman, D.K., 2009. 2-Methylhopanoids are maximally produced in akinetes of Nostoc punctiforme: geobiological implications. Geobiology 7, 524–32.

Garby, T.J., Matys, E.D., Ongley, S.E., Salih, A., Larkum, A.W.D., Walter, M.R., ... Neilan, B.A., 2017. Lack of methylated hopanoids renders the cyanobacterium Nostoc punctiforme sensitive to osmotic and pH Stress. Applied Environmental Microbiology, 83, e00777-17.

Hamilton, T.L., Welander, P.V., Albrecht, H.L., Fulton, J.M., Schaperdoth, I., Bird, L.R., ... Macalady, J.L., 2017. Microbial communities and organic biomarkers in a Proterozoic-analog sinkhole. Geobiology 15, 784–797.

Kuhl, A., Lorenzen, H., 1964. Handling and culturing of Chlorella. In: D.M. Prescott, ed., Methods in cell physiology. Vol.1, pp. 152-187, Academic Press, New York and London.

Matys, E.D., Sepúlveda, J., Pantoja, S., Lange, C.B., Caniupan, M., Lamy, F., Summons, R.E., 2017. Bacteriohopanepolyols along redox gradients in the Humboldt Current System off northern Chile. Geobiology 15, 844-857.

Matys, E.D., Mackey, T., Sumner D.Y., Hawes, I., Grettenberger, C., Mueller, E., Summons, R.E., *accepted.* Bacteriohopanepolyols in benthic microbial mats across environmental gradients in Lake Vanda, Antarctica. Geobiology.

McAllister, T.G., Wood, S.A., Hawes, I., 2016. The rise of toxic benthic Phormidium proliferations: A review of their taxonomy, distribution, toxin conent and factors regulating prevalence and increased severity. Harmful Algae 55, 282-294.

Meeks, J.C., Campbell, E.L., Summers, M.L., Wong, F.C., 2002. Cellular differentiation in the cyanobacterium Nostoc punctiforme. Archives of Microbiology 178, 395-403.

Ourisson, G., Albrecht, P., 1992. Geohopanoids: The most abundant natural products on Earth? Accounts of Chemical Research 25, 398-402.

Ourisson, G., Rohmer, M., Poralla, K., 1987. Prokaryotic hopanoids and other polyterpenoid sterol surrogates. Annual Review of Microbiology 41, 301–333.

Rashby, S.E., Sessions, A.L., Summons, R.E., Newman, D.K., 2007. Biosynthesis of 2-methylbacteriohopanepolyols by an anoxygenic phototroph. PNAS 104, 15099-15104.

Ricci, J.N, Michel, A.J., Newman, D.K., 2015. Phylogenetic analysis of HpnP reveals the origin of 2-methylhopanoid production in Alphaproteobacteria. Geobiology 13, 267–77.

Ricci, J.N., Morton, R., Kulkarni, G., Summers, M.L., Newman, D.K., 2016. Hopanoids play a role in stress tolerance and nutrient storage in the cyanobacterium *Nostoc punctiforme*. Geobiology 15, 173-183.

Sáenz, J.P., Grosser, D., Bradley, A.S., Lagny, T.J., Lavrynenko, O., Broda, M., Simons, K., 2015. Hopanoids as functional analogues of cholesterol in bacterial membranes. PNAS 112, 11971–76.

Sáenz, J.P., Sezgin, E., Schwille, P., Simons, K., 2012. Functional convergence of hopanoids and sterols in membrane ordering. PNAS 109, 14236-14240.

Stingaciu, L.-R., O'Neill, H., Liberton, M., Urban, V.S., Pakrasi, H., Ohl, M., 2016. Revealing the Dynamics of Thylakoid Membranes in Living Cyanobacterial Cells. Scientific Reports 6, 19627.

Summons, R.E., Jahnke, L.L., Hope, J.M., Logan, G.A., 1999. 2-Methylhopanoids as biomarkers for cyanobacterial oxygenic photosynthesis. Nature 400, 554-556.

Talbot, H.M., Summons, R.E., Jahnke, L., Farrimond, P., 2003. Characteristic fragmentation of bacteriohopanepolyols during atmospheric pressure chemical ionisation liquid chromatography/ion trap mass spectrometry. Rapid Communications in Mass Spectrometry 17, 2788-2796.

Talbot, H.M., Rohmer, M., Farrimond, P., 2007. Structural characterization of unsaturated bacterial hopanoids by atmospheric pressure chemical ionization liquid chromatography/ion trap mass spectrometry. Rapid Communications in Mass Spectrometry 21, 1613-1622.

Talbot, H.M., Summons, R.E., Jahnke, L.L., Cockell, C.S., Rohmer, M., Farrimond, P., 2008. Cyanobacterial bacteriohopanepolyol signatures from cultures and natural environmental settings. Organic Geochemistry 39, 232-263.

Welander, P.V., Doughty, D.M., Wu, C.-H., Mehay, S., Summons, R.E., Newman, D.K., 2012. Identification and characterization of Rhodopseudomonas palustris TIE-1 hopanoid biosynthesis mutants. Geobiology 10, 163-177.

Welander, P.V., Hunter, R.C., Zhang, L., Sessions, A.L., Summons, R.E., Newman, D.K., 2009. Hopanoids play a role in membrane integrity and pH homeostasis in Rhodopseudomonas palustris TIE-1. Journal of Bacteriology 191, 6145-6156.

Whitton, B.A., 2011. Cyanobacteria (Cyanophyta). In: The freshwater algal flora of the British Isles. An identification guide to freshwater and terrestrial algae. Second edition. (John, D.M., Whitton, B.A. & Brook, A.J. Eds), pp. 31-158.

Wu, C.-H., Kong, L., Bialecka-Fornal, M., Park, S., Thompson, A.L., Kulkarni, G., ... Newman, D.K., 2015. Quantitative hopanoid analysis enables robust pattern detection and comparison between laboratories. Geobiology 13, 391–407.

3.9 Figures

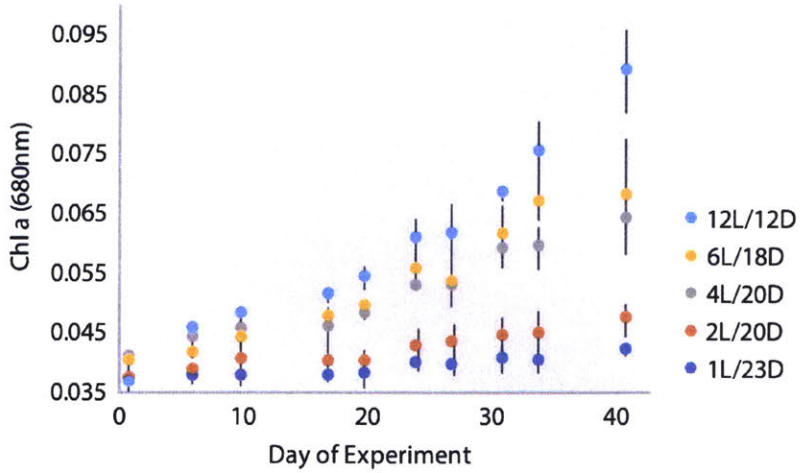

Figure 1. *Phormidium luridum* growth curves established through the measurement of chlorophyll *a* (Chl *a*) absorbance. Error bars indicate ± 1 standard deviation.

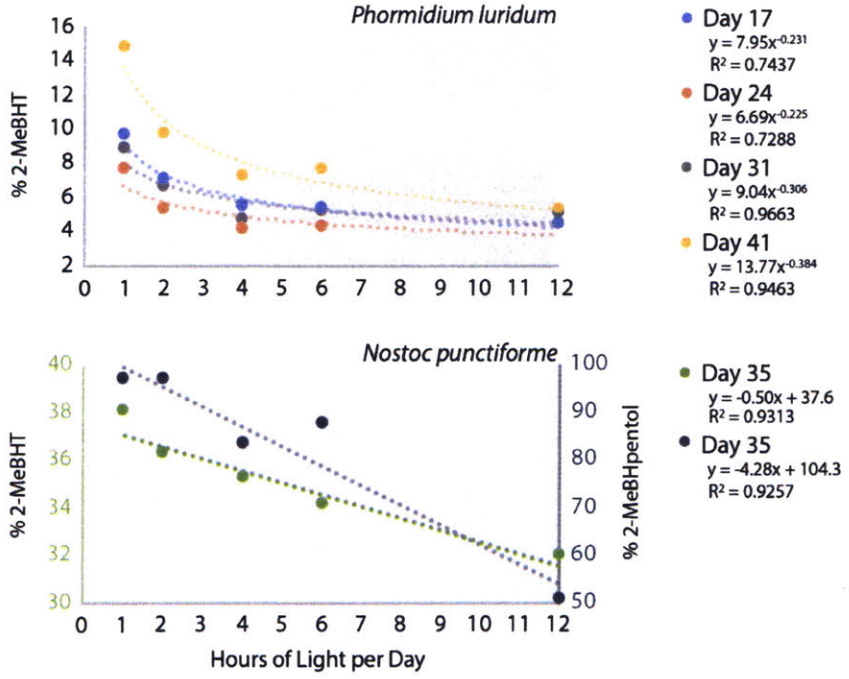

Figure 2. The relative abundance of 2-methylbacteriohopanepolyols in relation to des-methyl counterparts in *Phormidium luridum* and *Nostoc punctiforme* wild type. The % 2-MeBHT was measured on days 17, 24, 31, and 41 of *P. luridium* incubations exposed to 1, 2, 4, 6, and 12 hours of light per day. The % 2-MeBHT and % 2-MeBHpentol was measured after 35 days of growth of *N. punctiforme* cultures exposed to 1, 2, 4, 6, and 12 hours of light per day.
% 2-MeBHT: 2-MeBHT/ (2-MeBHT + BHT)
% 2-MeBHpentol: 2-MeBHpentol-I + 2-MeBHpentol-II/ (2-MeBHpentol-I + 2-MeBHpentol-II + BHpentol-I + BHpentol-II)

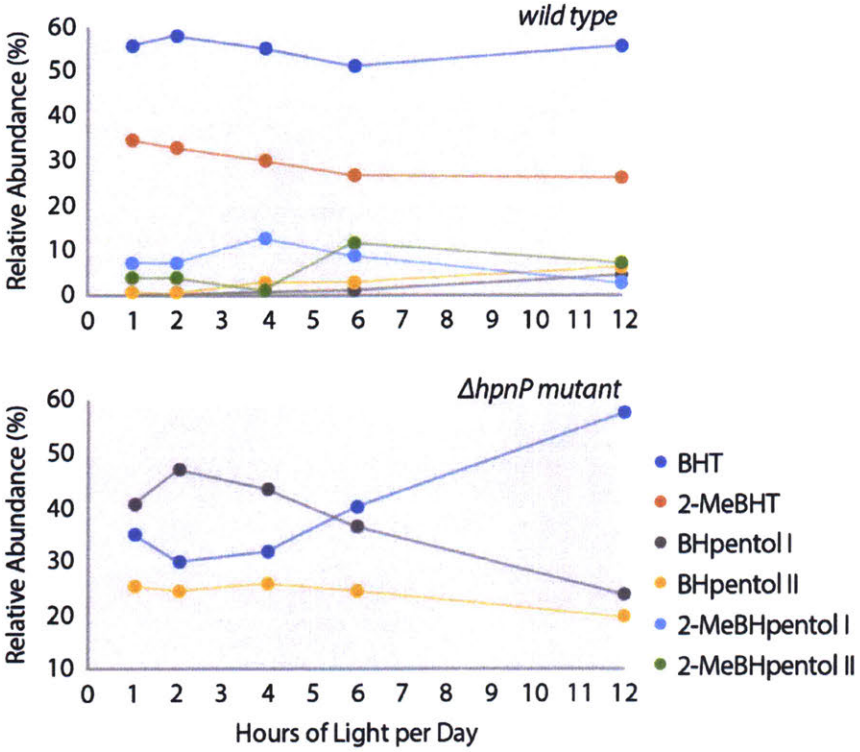

Figure 3. Relative abundance of BHPs identified in *Nostoc punctiforme* wild type and *hpnP* mutants grown under 1, 2, 4, 6, and 12 hours of light per day for 35 days.

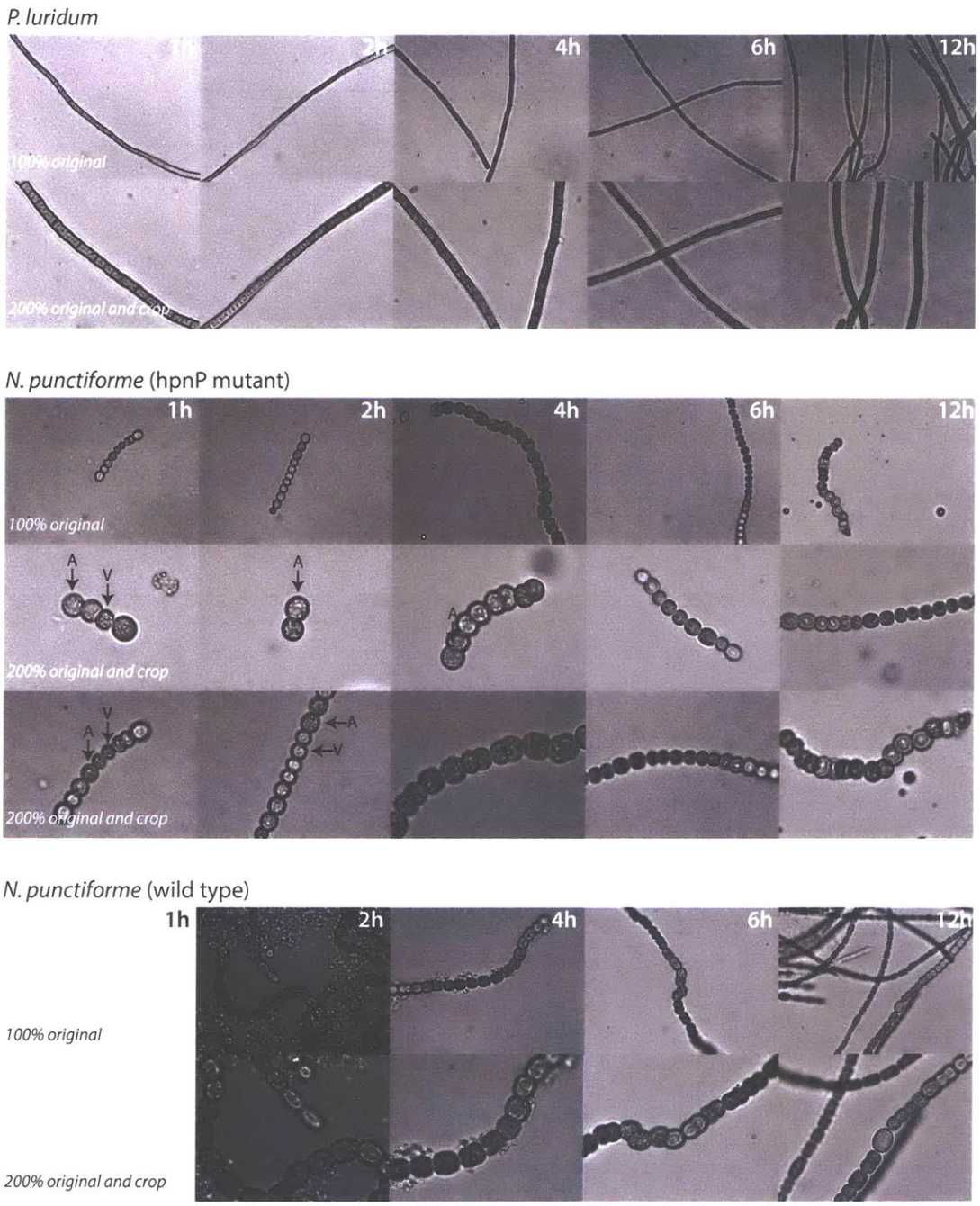

Supplementary Figure 1. Light micrographs of *Phormidium luridum* and *Nostoc punctiforme*. *P. luridum* micrographs were taken on day 41. *N. punctiforme* micrographs were taken on day 35. Micrographs were not available for *N. punctiforme* wild type 1h.

3.10 Tables

Table 1. *Phormidium luridum* bacteriohopanepolyol profiles measured on days 17, 24, 31, and 41 of incubation.

	Relative Abundance (%)	
Day	BHT	2-MeBHT
12 hours of light per day		
17	95.59	4.41
24	95.58	4.42
31	94.92	5.08
41	94.67	5.33
6 hours of light per day		
17	94.72	5.28
24	95.76	4.24
31	94.82	5.18
41	92.33	7.67
4 hours of light per day		
17	94.49	5.51
24	95.81	4.19
31	95.29	4.71
41	92.70	7.30
2 hours of light per day		
17	92.99	7.01
24	94.65	5.35
31	93.32	6.68
41	90.19	9.81
1 hour of light per day		
17	90.42	9.58
24	92.36	7.64
31	91.19	8.81
41	85.23	14.77

Table 2. *Nostoc punctiforme* bacteriohopanepolyol profiles measured on day 35 of incubation.

			Relative Abundance (%)			
Treatment	BHT	2-MeBHT	Bhpentol-I	Bhpentol-II	2-MeBHpentol-I	2-MeBHpentol-II
Nostoc punctiforme wild type						
12	55.22	25.91	3.69	5.84	2.48	6.87
6	50.95	26.30	0.63	2.24	8.53	11.35
4	54.38	29.57	0.68	2.03	12.48	0.86
2	57.37	32.59	0.10	0.21	6.62	3.11
1	55.40	33.88	0.10	0.21	6.94	3.46
Nostoc punctiforme hpnP mutant						
12	57.22	-	23.33	19.46	-	-
6	39.75	-	36.17	24.08	-	-
4	31.55	-	43.07	25.37	-	-
2	29.52	-	46.57	23.91	-	-
1	34.45	-	40.43	25.12	-	-

Chapter 4:

Bacteriohopanepolyols along redox gradients in the Humboldt Current System off northern Chile

This chapter was published in Geobiology by Wiley-Blackwell in 2017 and is reprinted here with their permission as granted in the original copyright agreement.

Matys EM, Sépulveda J, Pantoja S, Lange CB, Caniupán M, Lamy F, Summons RE (2017) Bacteriohopanepolyols along redox gradients in the Humboldt Current System off northern Chile. *Geobiology* 15:844-857.

Bacteriohopanepolyols along redox gradients in the Humboldt Current System off northern Chile

Emily MATYS[1*], Julio SEPÚLVEDA[2*], Silvio PANTOJA[3], Carina B. LANGE[3], Magaly CANIUPÁN[3], Frank LAMY[4], and Roger E. SUMMONS[1]

1. Department of Earth, Atmospheric and Planetary Sciences, Massachusetts Institute of Technology, 77 Massachusetts Avenue, Cambridge, MA 02139, USA
2. Department of Geological Sciences, Institute of Arctic and Alpine Research (INSTAAR), University of Colorado Boulder, Boulder, CO, USA
3. Department of Oceanography and COPAS Sur-Austral, University of Concepción, Concepción, Chile
4. Alfred Wegener Institute for Polar and Marine Research (AWI), Bremerhaven, Germany

* Corresponding author:

Email Address: ematys@mit.edu (E. D. Matys)

Telephone: +01 617-324-3952

Abstract

Marine oxygen minimum zones (OMZs) are characterized by the presence of subsurface suboxic or anoxic layers where diverse microbial processes are responsible for the removal of fixed nitrogen. OMZs have expanded over past decades and are expected to continue expanding in response to the changing climate. The implications for marine biogeochemistry, particularly nitrogen cycling, are uncertain. Cell membrane lipids (biomarkers), such as bacterial bacteriohopanepolyols (BHPs) and their degradation products (hopanoids), have distinctive structural attributes that convey information about their biological sources. Since the discovery of fossil hopanoids in ancient sediments, the study of BHPs has been of great biogeochemical interest due to their potential to serve as proxies for bacteria in the geological record. A stereoisomer of bacteriohopanetetrol (BHT), BHT II, has been previously identified in OMZ waters, and has since been unequivocally identified in culture enrichments of anammox bacteria, a key group contributing to nitrogen loss in marine OMZs. We tested BHT II as a proxy for suboxia/anoxia and anammox bacteria in suspended organic matter across OMZ waters of the Humboldt Current System off northern Chile, as well as in surface and deeply buried sediments (125-150 ky). The BHT II ratio (BHT II/total BHT) increases as oxygen

content decreases through the water column, consistent with previous results from Perú, the Cariaco Basin and the Arabian Sea, and in line with microbiological evidence indicating intense anammox activity in the Chilean OMZ. Notably, BHT II is transported from the water column to surface sediments, and preserved in deeply buried sediments, where the BHT II ratio correlates with changes in $\delta^{15}N$ sediment values during glacial-interglacial transitions. This study suggests that BHT II offers a proxy for past changes in the relative importance of anammox, and fluctuations in nitrogen cycling in response to ocean redox changes through the geological record.

Keywords: bacteriohopanepolyol, bacteriohopanetetrol isomer, anammox, oxygen minimum zone, Chile

4.1 Introduction

The consequences of a reduction in dissolved oxygen on the structure of marine ecosystems, biological and biogeochemical processes, ocean management, and sustainable fisheries remain uncertain (Capone and Hutchins, 2013). Thus, the study of microbial processes in oxygen minimum zones (OMZs) — dynamic regions of the modern ocean characterized by the presence of subsurface suboxic to anoxic waters, such as in the Eastern Tropical South Pacific (ETSP) off northern Chile — is critical to better understand how they may respond to future scenarios of environmental change. OMZs are operationally defined as water masses with <20 μmol O_2/kg water (Paulmier and Ruiz-Pino, 2009). This is the maximum O_2 level at which the use of alternate electron acceptors has been reported (Smethie, 1987). OMZs comprise ~1–7% (v/v) of the global ocean, occurring in the Pacific Ocean, the Atlantic Ocean, and the Arabian Sea, particularly along continental margins where the wind-driven upwelling of nutrient-rich waters sustains enhanced marine productivity and microbial respiration (Paulmier and Ruiz-Pino, 2009; Wright et al., 2012). In poorly ventilated regions, respiratory O_2 demand during degradation of organic matter exceeds O_2 availability leading to the development of suboxic (1–20 μmol O_2/kg water) to essentially anoxic (<1 μmol O_2/kg water) regions at mid-water depths (Wright et al., 2012).

OMZs are inhospitable to most metazoans but are instead dominated by prokaryotes and microaerobic unicellular eukaryotes (Ulloa et al., 2012; Wright et al., 2012; Capone and Hutchins, 2013). In fact, these areas support thriving microbial communities that cycle organic and inorganic nutrients such as nitrogen through aerobic and anaerobic processes, making a significant contribution to the productivity and microbial biogeochemistry of the modern global ocean (Stevens and Ulloa 2008; Capone and Hutchins, 2013). Nitrogen can be a limiting nutrient for biological production and shapes the biogeochemistry and microbial ecology of OMZs. Nitrate is actively reduced to nitrite, which is further converted to N_2 gas through heterotrophic denitrification and the autotrophic anaerobic oxidation of ammonium (anammox) process, or to ammonium through dissimilatory nitrate reduction (Lam and Kuypers, 2011; Thamdrup, 2012). Pelagic and coastal OMZs have expanded over the last five decades and are expected to continue expanding under global warming conditions (Stramma et al., 2008), which includes an increase in sea surface temperature and thermal stratification, further reducing O_2 solubility and ocean ventilation (Bograd et al., 2008; Stramma et al., 2008; Keeling et al., 2010). However, the effect of OMZ expansion on nitrogen cycling remains unclear.

Present-day and past changes in marine oxygenation (e.g., OMZ extension and intensity) and nitrogen cycling may be studied using molecular biomarkers such as lipids found

in oxygen-depleted waters and preserved in the geological record. Molecular biomarkers are natural products that may serve as proxies for biological sources, biogeochemical processes, microbial metabolisms, and environmental conditions (Summons and Lincoln, 2012; Newman et al., 2016). Bacteriohopanepolyols (BHPs) comprise a structurally diverse group of bacterial pentacyclic triterpenoids and a biomarker class that is widely used for environmental, paleoceanographic and paleo-reconstruction studies (Talbot and Farrimond, 2007; Wakeham et al., 2012; Blumenberg et al., 2013). Since the discovery of their fossil counterparts in ancient sediments (Ourisson et al., 1979), hopanoids and their biological precursors (BHPs) have been of great interest for their potential to serve as proxies for bacteria in the geological record (Brocks and Summons, 2003). Interpreting the significance of particular sedimentary hopanoids, however, is presently hampered by an incomplete understanding of their phylogenetic associations, biological functions, and spatial and temporal disposition of BHPs within the environment (e.g., Newman et al., 2016).

BHPs are biosynthesized by a wide variety of aerobic aquatic and soil bacteria including heterotrophs, methanotrophs, methylotrophs, cyanobacteria and purple non-sulfur bacteria (Rohmer et al., 1984; Farrimond et al., 1998; Summons et al., 1999; Talbot and Farrimond, 2007). They are also produced by diverse anaerobes, both obligate and facultative, that include anaerobic ammonium oxidizing bacteria, sulfate-reducing bacteria, Planctomycetes and *Geobacter* sp. (Sinninghe Damsté et al., 2004; Fischer et al., 2005; Hartner et al., 2005; Blumenberg et al., 2006; Rattray et al., 2008; Eickhoff et al., 2013, Rush et al., 2014). BHPs may serve a variety of physiological functions, including the regulation of membrane permeability and fluidity, lipid ordering, and membrane compartmentalization (Doughty et al., 2009: Welander et al., 2009; Sáenz et al., 2012, 2015). Environmental conditions appear to be a significant factor affecting BHP diversity (Rashby et al., 2007; Talbot and Farrimond 2007; Cooke et al., 2008; Pearson et al., 2009; Ricci et al., 2014), with changes in temperature, salinity, pH, light intensity, redox potential, nutrients, and oxygen concentrations prompting the production of particular BHP structures in different bacterial groups (Talbot et al., 2003). However, the exact environmental mechanisms controlling the chemical diversity and composition of BHPs, as well as their role in cellular physiology are topics of continuing study.

Marine environments are of particular interest for the study of BHPs given the prevalence of hopanoid hydrocarbons in ancient marine sediments and petroleum, and the paucity of studies that have directly measured intact BHPs in the marine water column and sediments (Blumenberg et al., 2007; Pearson et al., 2007; Wakeham et al., 2007; Sáenz et al.,

2011; Kharbush et al., 2013). BHPs previously identified in marine waters include bacteriohopanetetrol (BHT), a putative BHT stereoisomer (BHT II), a C-2 methylated homologue of BHT (2-MeBHT), aminobacteriohopanetriol (aminotriol), Δ6/11 unsaturated aminotriol, aminobacteriohopanetetrol (aminotetrol), aminobacteriohopanepentol (aminopentol), Δ6/11 unsaturated aminopentol, bacteriohopanepentol (BHpentol), hopane ribonolactone (lactone), anhydrobacteriohopanetetrol (anhydroBHT), ribonyl hopane, and adenosylhopane.

So far, BHT II has been identified exclusively in OMZ waters of the Eastern Tropical Pacific, Cariaco Basin, and the Arabian and Baltic Seas (Sáenz et al., 2011; Wakeham et al., 2012; Kharbush et al., 2013; Berndmeyer et al., 2014), which suggests that this isomer may be one of the few marine BHP structures with a unique environmental pattern and the potential to be developed as a biomarker for modern and ancient water column hypoxia/anoxia (Sáenz et al., 2011; Kharbush et al., 2013). Although its phylogenetic association was unknown at that time, it was suggested that a 'BHT II ratio' (BHT II/total BHT) could serve as a useful proxy for suboxic to anoxic conditions (Sáenz et al., 2011). More recently, BHT II was unequivocally identified in culture enrichments of the anammox bacterium '*Candidatus* Scalindua profunda' and in sediments from Golfo Dulce, an anoxic marine fjord-like enclosure, at depths where anammox bacteria proliferate (Rush et al., 2014). Notably, the distribution of BHT II in Gulfo Dulce sediment cores closely tracks the distribution of ladderane fatty acids (Rush et al., 2014), unique biomarkers for anammox bacteria (Sinninghe Damsté et al., 2002; Kuypers et al., 2003; Jaeschke et al., 2009). This is consistent with a study of the water column of the anoxic and sulfidic Cariaco Basin, which revealed that the greatest concentrations of ladderane fatty acids and BHT II co-occurred at the chemocline (Wakeham et al., 2012). Although ladderane lipids have been detected in Pleistocene (~140 ka) marine sediments (Jaeschke et al., 2009), these lipids are thermally unstable (Jaeschke et al., 2008) and their degradation products have not yet been reported in ancient sediments. Unlike ladderane lipids, intact BHPs have been reported in sediments as old as the Jurassic (Bednarczyk et al., 2005) and their recalcitrant carbon skeletons are stable in sedimentary records over timescales of up to 1.64 Ga (e.g., Summons et al., 1988). In fact, BHT II has been detected in ancient sapropel sediments (2.97 Ma; Rush et al., 2017), which suggests that BHT II may serve as a proxy for anammox bacteria over much longer time scales than is currently possible using ladderane lipids.

In this study, we analyzed the distribution and diversity of BHPs in water column samples, surface sediments, and deeply buried sediments from the Humboldt Current System off the coast of northern Chile. We particularly focused on the distribution of BHT and BHT

II, with depth and along a latitudinal gradient of oxygenation within the OMZ of the ETSP to validate its use as a biomarker for anammox activity in the water column and in paleoceanographic archives. Our results suggest that the production, transport, and preservation of BHT II affords a window into past changes in the relative abundance of anammox and, thus, fluctuations in nitrogen cycling during periods of ocean redox variability.

4.2 Methods

4.2.1 Study area

The Eastern Tropical South Pacific (ETSP) contains one of the three major permanent OMZs in the modern global ocean. The OMZ persists within the Humboldt Current System, a major upwelling system that extends from northern Peru and Ecuador (~4° S) to southern Chile (~45° S; Montecino and Lange, 2009), accounting for approximately 11% (v/v) of the global OMZ volume (Fuenzalida et al., 2009). The water column in this OMZ system is characterized by steep O_2 gradients (oxyclines) from dysoxic (20–90 μmol O_2/kg water) to suboxic conditions above and below the anoxic core. The OMZ is strong and more persistent off Perú and northern Chile, more dynamic in the central-south, and more pronounced near the coast than further offshore (Paulmier et al., 2006). Low oxygen levels in this area are maintained through the combination of high primary productivity (9 gC/m^2/day; Daneri et al., 2000), decomposition of sinking organic material (Pantoja et al., 2004; Chavez and Messie, 2009), and weak circulation (Bettencourt et al., 2015). Suboxic to anoxic conditions within the OMZ core (Canfield et al., 2010; Ulloa et al., 2012) prompt the development of a dynamic nitrogen cycle (Thamdrup, 2012). Previous studies have identified anammox as a significant pathway of nitrogen (N) loss in OMZs and the dominant pathway in the ETSP, considerably outpacing denitrification at the top of the OMZ core (Lam et al., 2009; Canfield et al., 2010; Thamdrup, 2012).

4.2.2 Sample Collection

Water column, surface sediment, and subsurface sediment samples were collected during three oceanographic cruises carried out during austral winter (MOOMZ-2 in 2009) and spring (ChiMeBo and BiG RAPA in 2010) in the Humboldt Current System, off the coast of northern Chile between 20.1° S and 30.2° S (Table 1; Fig. 1), following a bathymetrical and latitudinal gradient of oxygenation.

ChiMeBo Cruise

The R/V SONNE University of Bremen expedition ChiMeBo (Cruise SO-211) collected samples along the Chilean continental slope between the cities of Valparaíso (~33° S) and Antofagasta (~23.5° S) during austral spring (November 2-29) in 2010 (Hebbeln et al., 2011). Three water column profiles along the Chilean continental slope were examined in this study, off Taltal (25° S), off Copiapó (27.5° S), and off Coquimbo (30.2° S; Table 1). At the time of the cruise, the OMZ core in the studied region spanned ~80-350 m in depth. About 40-100 L of seawater was collected from 3-4 water depths at each station covering oxic surface waters (~10 m), anoxic subsurface waters (~60-240 m), and oxic deep waters (~850-1200 m) using a rosette equipped with Niskin bottles. Seawater was transferred to darkened carboys, and particulate organic mater (POM) was filtered onboard through pre-combusted glass fiber filters (47 mm, 0.7 μm, Millipore) using a peristaltic pump, and kept frozen at -20 °C until extraction in the laboratory.

Surface sediments (top 0-1 cm of sediment core) along the Chilean continental margin were sampled at a total of 7 stations between ~23.5° S and ~27.5° S, off the coast of the cities of Antofagasta and Copiapó, respectively (Table 1; Hebbeln et al., 2011). A multi-corer (MUC) equipped with eight large (10 cm diameter) and four small (6 cm diameter) acrylic glass-coring tubes of 60 cm in length was used to obtain sediment samples with an undisturbed surface layer. Cores were extruded and subsampled onboard at 1-cm resolution and kept frozen at -20 °C until extraction in the laboratory. Two sites were sampled along the Antofagasta transect (~23.5° S), characterized by a steep upper slope and shallow-water plateaus with no recent sedimentation (15012 and 15011). Two sites were sampled on the Taltal transect (~25° S). The site at 920 m (GeoB 15007) is related to a sediment drift body. The site at 539 m (GeoB 15008) was located in a depression on a SE-NW trending ridge. Three sites were sampled along the Copiapó transect (~27.5° S). The slope angle in this area is lower than in the other sampling areas. Therefore, the probability for sediment deposition is significantly higher in sites 15004, 15005, and 15022.

In addition to surface sediments, subsurface sediments were collected using the seafloor drill rig MARUM-MeBo from the University of Bremen (Table 1). This study describes a small subset of samples from site GeoB15016 (27°29' S, 71°08' W; 971 m water depth), which correspond to Glacial Termination II, or the transition from Marine Isotope Stages 6 to 5 (~120-150 ky; Martínez-Méndez et al., 2013).

BiG RAPA Cruise

The R/V Melville C-MORE expedition BiG RAPA (Biogeochemical Gradients: Role in Arranging Planktonic Assemblages) collected samples between Iquique (20.2° S, 70.1° W) and Rapa Nui (Easter Island; 27.1° S, 109.3° W), Chile during austral spring (November 18-December 14) in 2010 (Table 1). This study describes samples from a water column profile collected at Station 1, which spanned the OMZ structure off the coast of Iquique (20.3° S). At the time of the cruise, the OMZ core in the studied region spanned ~50-530 m in depth. POM was collected from six water depths (0, 30, 40, 65, 200, and 1900 m) extending from the photic zone, across the oxycline, through the OMZ core and below using a rosette equipped with Niskin bottles. Samples of ~200 L were transferred to darkened carboys, filtered onboard through pre-combusted glass fiber filters (0.7 μm, Millipore) using a peristaltic pump, and kept frozen at -20 °C until extraction in the laboratory. No sediment samples were collected during this cruise.

MOOMZ-2 Cruise

The R/V AGOR Vidal Gormáz Agouron expedition MOOMZ-2 collected samples off the coast of Iquique, Chile (20.2° S, 70.1° W) during austral winter (August) in 2009 (Alarcón and Ulloa, 2009; Table 1). This study describes samples from a water column profile collected at Station 3, which spanned the OMZ structure off the coast of Iquique (20.3° S). At the time of the cruise, the OMZ core in the studied region spanned ~58-480 m in depth. Two WTS-LV08 McLane Laboratories *in situ* pumps were used in tandem to provide a continuous stream of seawater to be filtered along a high-resolution profile. POM was collected from 9 depths (10, 25, 50, 70, 110, 200, 300, 450 and 600 m) extending from the photic zone, across the oxycline, through the OMZ core and below. Seawater was filtered into two size classes (0.3–3 μm and >3 μm) using a 3.0 μm, 142 mm diameter glass fiber filter (Pall) as a pre-filter, and a 0.3 μm, 142 mm diameter glass fiber filter (Sterlitech). This approach allows us to characterize the biomarker composition of POM >3.0 μm, assumed to represent particle-associated microorganisms and marine aggregates, and of a fine fraction of 0.3–3.0 μm assumed to mostly represent free-living microorganisms and small suspended particles (Karl et al., 1988). Filters were kept frozen at -20 °C until extraction in the laboratory. No sediment samples were collected during this cruise.

4.2.3 Lipid extraction and analysis

Frozen surface sediment and water column filters were placed in combusted glass centrifuge vials and spiked with 40 ng of C_{16}PAF as a recovery standard. Total lipid extracts

(TLEs) were obtained by extracting the samples using a modified Bligh and Dyer method (Bligh and Dyer, 1959) as reported by Sturt et al. (2004). Dichloromethane (DCM) was used in place of chloroform. Filters and surface sediments were extracted by ultrasonication (30 mins at room temperature) first (2x) using a mixture of methanol/DCM/phosphate buffer solution (2:1:0.8, v/v/v), and then (2x) using a mixture of methanol/DCM/trichloroacetic acid (TCA) buffer solution (2:1:0.8, v/v/v). After each extraction the vials were centrifuged at 3000 rpm for 15 mins, and the supernatants were transferred to different separatory funnels (phosphate buffer vs. trichloroacetic acid buffer). Supernatants were then subjected to liquid-liquid extractions using DCM/water (1:1, v/v). The organic layers were collected as separated TLEs, dried under a gentle stream of N_2, and then combined into one final TLE. The extraction with a phosphate buffer solution was used to maximize the extraction of bacterial membrane lipids, while the extraction with TCA buffer was used to maximize the extraction of more recalcitrant cellular structures (i.e. archaeal membrane lipids; Nishihara and Koga, 1987). However, since it has been shown that TCA can accelerate the degradation of BHPs (Sáenz, 2010), the extracts were not combined until the TCA was removed from the samples, after the liquid-liquid extraction step. The TLEs were kept frozen at -20 °C until analysis. Subsurface, ancient sediment samples preserve core lipids that do not require the use of buffers essential to the Bligh and Dyer extraction, which are used to disrupt viable cells. Accordingly, freeze-dried subsurface sediment samples from core GeoB15016 were extracted (3x) using an Accelerated Solvent extraction system (DIONEX ASE 200) and a solvent mixture of DCM/methanol (9:1, v/v; static time of 5 min at 100 °C).

A fraction of each TLE was acetylated with pyridine/acetic anhydride (1:1, v/v) at 70 °C for 1 h and left at room temperature overnight. The acetylated TLEs were analyzed by high-performance liquid chromatography- atmospheric pressure chemical ionization – mass spectrometry (HPLC-APCI-MS). The LC-MS system comprised a 1200 Series HPLC (Agilent Technologies, Santa Clara, CA, USA) equipped with an auto sampler and a binary pump linked to a Q-TOF 6520 mass spectrometer (Agilent Technologies) via an APCI interface operated in positive ion mode (Welander et al., 2012). A Poroshell 120 EC-C_{18} column (2.1 x 150 mm, 2.7 µm; Agilent Technologies) was chosen to provide fast and high-resolution separations of a wide range of small molecules at lower pressures. The column temperature was set at 30 °C. The eluent flow remained constant at 0.19 ml/min throughout the analysis. Eluent A contained a mixture of methanol/H_2O (95:5, v/v) and eluent B comprised pure isopropyl alcohol (IPA). The HPLC gradient was as follow: isocratic flow of 100% eluent A (0-2 mins), a linear gradient from 0-20% of eluent B (2-20 mins), isocratic flow of 20% B (20-30 mins), a linear gradient

from 20-30% of eluent B (30-40 mins), a linear gradient from 30-0% B (40-45 mins), isocratic flow of 0% B for 5 minutes. The column was conditioned for 5 mins of post-run time at 0% B. The APCI parameters were as follows: gas temperature 325 °C, vaporizer temperature 350 °C, drying gas (N_2) flow 6 l/min, nebulizer (N_2) flow 30 l/min, capillary voltage 1200V, corona needle 4μA, and fragmentor 150V. BHPs were identified on the basis of accurate mass measurements of their protonated molecular ions, fragmentation patterns in MS-MS mode, and by comparison of relative retention times (Talbot et al., 2003, 2007; Welander et al., 2012). Quantification was achieved through an external standard curve of 3α,12α-Dihydroxy-5β-pregnan-20-one,3,12-diacetate. This compound was chosen as an internal standard because of its structural similarity to hopanoids and because it has a retention time that does not overlap with the range of BHPs of interest.

4.2.4 Metagenomic search

Metagenomes from the MOOMZ-2 cruise at Station 3 are publicly available (accession numbers SRR304671-3 and SRR070081). Files were uploaded to the metagenomics RAST (Rapid Annotation using Subsystem Technology) server (MG-RAST) for automated phylogenetic classification.

4.2.5 Stable nitrogen isotope analysis of bulk sediment

The stable nitrogen isotope composition ($\delta^{15}N$) of bulk sediment (~25 mg) was determined through triplicate samples using a Fisons (Carlo Erba) NA 1500 elemental analyzer fitted with a Costech Zero Blank Autosampler and coupled to a Thermo Finnigan Delta Plus XP isotope ratio mass spectrometer. Analytical reproducibility (1σ) was calculated as better than 0.5‰. Acetanilide and urea (Arndt Schimmelmann, Indiana University), and IAEA-NO_3 (Potassium nitrate) and IAEA-N-2 (ammonium sulfate) of known isotopic composition were used as standards.

4.3 Results

4.3.1 Biogeochemical structure of the Humboldt Current System off northern Chile

Cross sections for the Humboldt Current System are shown in Fig. 2. Temperature, salinity, and dissolved oxygen concentrations were measured at all five stations, located along the Chilean coast between 20.1° S and 30.2° S. Note that the hydrographic profiles were obtained during three different cruises and different dates.

Dissolved oxygen concentrations in surface waters (10 m) ranged from 150 μmol O_2/kg water at 30.2° S to 260 μmol O_2/kg water at 20.1° S (Fig. 2). The underlying OMZ structure consists of an upper oxycline (transition from oxygenated surface waters to the upper OMZ region), an OMZ core (O_2 concentrations <20 μmol/kg water), and a deep oxycline (transition from the bottom of the OMZ to abyssal waters; Wright et al., 2012; Bettencourt et al., 2015). The OMZ core extended from approximately 50 to 500 m at 20.1° S and from 50 to 400 m at 30.2° S. The minimum dissolved oxygen concentrations measured throughout the OMZ core ranged from 3.2 μmol O_2/kg water at 30.2° S to 0.9 μmol O_2/kg water at 20.1° S. Generally, the depth of the upper OMZ limit remained constant at ~50 to 60 m. However, the minimum dissolved oxygen concentration and width of the OMZ core are related to latitude, with lower dissolved oxygen concentrations, and a more expansive and persistent OMZ structure existing in the northernmost portion of the sampling region. These measurements parallel previous studies of the ETSP (Pantoja et al., 2004; Farías et al., 2007; Canfield et al., 2010).

Nutrient measurements were obtained throughout the water column at 20.3° S, 70.8° W during expedition BiG RAPA and are freely available online on the C-MORE website (http://hahana.soest.hawaii.edu/cmorebigrapa/bigrapa.html; Fig. 3). Nitrate (NO_3^-), the predominant form of bioavailable inorganic nitrogen in the ocean, was measured in highest concentration throughout the OMZ structure, reaching a maximum (39.6 μmol NO_3^-/kg water) at 60 m, followed by a decrease (to 15 μmol NO_3^-/kg water), and a secondary maximum at 350 m (>40 μmol NO_3^-/kg water). Nitrite oxidation by autotrophic and heterotrophic bacteria is a primary source of oceanic NO_3^- and the likely source of NO_3^- in the ETSP (Lam and Kuypers, 2011). Ammonium (NH_4^+) was present between 5-65 m depth, reaching a maximum of 1.96 μmol/kg water at 24 m. Likely sources of NH_4^+ include the dissimilatory nitrate reduction to ammonium (DNRA) and the remineralization of organic matter. With depth, NH_4^+ reached very low values (0.02 μmol/kg water; >65 m). It is likely that NH_4^+ is being produced, but consumed by active anammox processes in the upper OMZ, as suggested by Thamdrup (2012). Nitrite (NO_2^-) was present in low concentrations (~0.5 μmol/kg water) in the surface ocean and through the chemocline, and is attributed to nitrate reduction. Further into the OMZ core (65–300 m), NO_2^- concentrations increased to a maximum of 7.28 μmol/kg water at 120 m depth. It has been proposed that this maximum is largely the result of shelf production and horizontal advection (Lam et al., 2009). In general, these trends agree with previous studies in the ETSP including those reported for the MOOMZ-2 cruise (Canfield et al., 2010).

4.3.2 Distribution and abundance of BHPs in the water column

The total BHP concentration was low in the surface waters (10 m; 0.06-3.09 ng/L) and generally increased with depth through the upper oxycline before decreasing toward surface sediments (Fig. 4). A BHP maximum occurred between 65 and 240 m (4.79-23.99 ng/L). Concentrations decreased below the OMZ core to <10 ng/L below 1000 m depth. Three BHPs were identified (Fig. 4). Bacteriohopanetetrol (BHT; Supplementary Fig. 1 **Ia**) and its putative isomer (BHT II; **Ib**) were the most abundant compounds in all profiles. Bacteriohopanepentol (BHpentol; **Ic**) was detected exclusively in the MOOMZ-2 profile, though in relatively low concentrations (0.003-0.097 ng/L). BHT was present in all water column samples described here. BHT concentrations were low (<3 ng/L) in surface waters (10 m), reached maximum values (3.39–10.26 ng/L) in the OMZ core (65-240 m), and decreased to lowest values (0.06-0.59 ng/L) with depth (>280 m; Fig. 4). BHT II was absent in all surface water samples (10 m) where oxygen levels were high (>200 μmol O_2/kg water). The concentration of BHT II reached a maximum (1.78-13.72 ng/L) within the upper and core OMZ around 70-240 m (0.9-8.3 μmol/kg water), and then decreased in abundance (<3 ng/L) with depth below the OMZ core (>1000 m).

The BHT II ratio (expressed as BHT II/total BHT) is used to normalize BHT II and to determine its relative abundance (Sáenz et al., 2011). The BHT II ratio was zero at the sea surface (0-10 m) due to the absence of BHT II. The ratio increased through the chemocline (~50 m) where BHT II was first detected, then peaked at 50-240 m (0.45-0.73), and decreased only slightly to 0.37-0.57 with depth (>1000 m; Fig. 4). Notably, BHT II exceeded BHT at ~200 m in three out of five profiles.

Size fractionated samples (0.3–3.0 μm and >3.0 μm) were collected during the MOOMZ-2 cruise off Iquique (20.1° S). The distribution and abundance of BHPs throughout the water column in the small (0.3–3.0 μm) and large (>3.0 μm) size fraction follow trends that are similar to profiles previously described (>0.7 μm). BHP concentrations in the small and large size fractions are low in surface waters, increase toward a maximum at the oxycline, and then decrease with depth (Fig. 5). However, the large size fraction typically shows higher BHP concentrations than the small size fraction at any particular depth, amounting to >2 ng/L at the concentration maximum (70 m) as compared to 1.7 ng/L in the small size fraction. The BHT II ratio is also higher in the large size fraction (0.41) than in the small size fraction (0.36) at 70 m depth (Fig. 5). Notably, BHT II exceeds BHT (BHT II ratio >0.5) at five of the nine water

column depths in the large size fraction; at 50 m and ≥110 m. BHT II exceeds BHT at one depth (200 m) in the small size fraction.

4.3.3 Distribution and abundance of BHPs in surface and deeply buried sediments

Seven BHP structures were identified in surface sediment samples from a total of seven localities between 23 and 27° S (Fig. 6). In decreasing order of abundance, these structures include BHT, BHT II, 2-methylbacteriohopanetetrol (2-MeBHT; **IIa**), bacteriohopanepentol (BHpentol), aminobacteriohopanetriol (aminotriol; **Id**), anhydrobacteriohopanetetrol (anhydroBHT; **Ie**), and adenosylhopane (**If**). Total BHP concentrations in surface sediments ranged from 0.55 to 3.29 ng/g. As in the overlying water column, BHT and BHT II were the most abundant BHPs in surface sediments, accounting for 30-42% and 51-66% of total BHP, respectively. In combination, BHT and BHT II accounted for >95% of the total BHP pool. BHT II concentrations exceeded BHT concentrations in all samples, with BHT II ratio values ranging from 0.55 to 0.69. Minor BHPs accounted for 3.2-6.1% of the total BHP at each locality. 2-MeBHT (1.8-2.7%), BHpentol (0.6-1.1%), and aminotriol (0.7-1.7%) were identified in all samples. Adenosylhopane (0.6 and 2.2%) and anhydroBHT (0.6 and 0.8%) were limited to two samples each.

BHT and BHT II were identified throughout deeply buried sediments from core GeoB15016 corresponding to the Glacial Termination II leading to the Eemian interglacial period (Marine Isotope Stages 6 to 5, 150-125 ky BP; Martínez-Méndez et al., 2013). The BHT II ratio increased during Termination II to values of >0.8 during the interglacial period along with a marked isotopic enrichment in the $\delta^{15}N$ of bulk sediment (Fig. 7).

4.4 Discussion

The diversity and distribution of BHPs in the ETSP OMZ system off northern Chile are in agreement with previous studies of anoxic marine environments in the OMZ systems off Perú, Cariaco Basin and the Arabian Sea (Sáenz et al., 2011), and the Black Sea (Wakeham et al., 2007). Generally, BHP abundances throughout the water column parallel vertical trends in hopanoid producers, as evidenced by the relative abundance of the squalene hopene cyclase (*sqhC*) gene at MOOMZ-2 Station 3 (Kharbush et al., 2016). Variability in BHP concentrations at any particular depth, particularly in the area of maximum abundance (4.79-23.99 ng/L), are not correlated with any particular environmental parameters (i.e. oxygenation) but instead may be attributed to the dynamic nature of these systems (e.g., Ulloa et al., 2012). BHP concentrations and the relative abundance of *sqhC* are low in surface waters (10 m), reach a

maximum between 70-200 m in suboxic to anoxic subsurface waters, and decrease with depth toward underlying sediments (Fig. 5). The analysis of the metagenomic data from the same profile indicates that the primary hopanoid producers identified include the anammox planctomycete *Candidatus Scalindua brodae* and nitrite oxidizing bacteria *Nitrospina sp.* (Kharbush et al., 2016). These results suggest that hopanoid-producing bacteria within the OMZ waters play a key role in nitrogen cycling.

BHT and BHT II were the most abundant compounds identified. The detection of BHpentol, produced broadly by cyanbacteria (e.g. Talbot et al., 2008; Sáenz et al., 2012), exclusively in the MOOMZ-2 profile is likely due to the high volumes of seawater that were filtered at this site (781-2133 L) compared to the more modest volumes (40-240 L) filtered in all other profiles (Table 1). For this reason, and since BHpentol has been identified in other OMZ systems (Sáenz et al., 2011), it is likely that BHpentol is present as a minor compound in other areas of the Chilean OMZ here studied. Indeed, we cannot rule out the presence of other BHPs in this region, though they are likely below detection limit in our samples. For instance, in addition to BHT, BHT II, and BHpentol, Sáenz et al., (2011) also identified (in order of decreasing abundance) aminotriol, lactoneBHP, and anhydroBHT as minor components of the total BHP pool. However, we note that since this study is primarily concerned with the distribution and abundance of BHT and BHT II, the detection limit for other BHPs has no impact on the scope of our work.

BHT is ubiquitous as a bacterial membrane lipid in marine water column samples, and not surprisingly, was identified in all samples described here. BHT II was identified in all samples below the surface waters (>40 m), exhibiting a strong relationship with suboxic to anoxic conditions (Fig. 4, 5), consistent with the fact that anammox bacteria are obligate anaerobes and their metabolism is reversibly inhibited above 2 μM O_2 (Strous et al., 1997). BHT II maxima (1.78-13.72 ng/L) within the upper portion and core of the OMZ at 70-240 m parallel the presence of anammox, as evidenced by maxima of two taxa known to conduct anammox (*Candidatus Kuenenia* and *Candidatus Scalindua*) at 110 m (BiG RAPA Station 1; Supplementary Fig. 2), and a planctomycetes maximum at 70 m (MOOMZ-2 Station 3; Fig. 5). *Candidatus Kuenenia* and *Candidatus Scalindua* make up 73.6% of protein-coding reads matching planctomycetes from BiG RAPA Station 1 (Ganesh et al., 2014) and are likely the sources of BHT II at MOOMZ-2 Station 3. Our results are also consistent with studies from previous cruises off Iquique (~20° S) reporting an anammox bacteria maxima at ~50 m (Galán et al., 2009) and ~200 m (Ulloa et al., 2012). The decrease in BHT II below the OMZ is

consistent with previous reports indicating a decline in the abundance of anammox bacteria (Galán et al., 2009; Ulloa et al., 2012; Ganesh et al., 2014).

Figure 8 shows the relationship between the BHT II ratio and dissolved oxygen concentration in the Chilean OMZ, in comparison to the OMZ systems of Perú, Cariaco Basin, and the Arabian Sea (Sáenz et al., 2011). The highest BHT II ratio values were detected in water masses with <3 μmol O_2/kg water, concurrent with the highest anammox concentrations (Ganesh et al., 2014; Kharbush et al., 2016). Samples from oxygenated waters below the OMZ were excluded as their elevated BHT II ratio values likely reflect the signal of organic matter exported from within the OMZ region, and possibly active bacteria in anoxic microniches within sinking particles, not free-living bacteria. Unfortunately, the limited number of samples where both biomarker and genetic data exists precludes us from developing a similar relationship between the BHT II ratio and anammox bacteria as done for oxygen. To the best of our knowledge, our study provides the first report of BHT II substantially exceeding BHT in OMZ waters. Such elevated contribution reflects the preferential production of BHT II over BHT reported by the marine anammox bacterium *Candidatus Scalindua profunda* (Rush et al., 2014) and perhaps, enhanced activity of anammox bacteria in this region compared to other OMZ systems.

Size-fractionated particle analysis (0.3–3.0 and >3 μm) in samples from MOOMZ-2 Station 3 allows for further query of the source and transport of BHPs through OMZ waters of the ETSP. The small (0.3–3.0 μm) and large (>3 μm) size fractions likely represent free-living microorganisms and small aggregates, and particle-associated microorganisms and larger aggregates, respectively (e.g. Rieck et al., 2015). Genomic studies suggest that anammox bacteria, the putative source of BHT II, are most abundant in small size fractions. In fact, coding sequences of anammox planctomycetes (BiG RAPA Station 3; Ganesh et al., 2014) and anammox-associated transcripts (Eastern Tropical North Pacific OMZ; Ganesh et al., 2015) were enriched up to 3- and 15-fold, respectively, in free-living fractions (0.2-1.6 μm) as compared to larger size fractions (>1.6 μm). However, BHT II concentrations in our study are consistently higher (0.1-77.5%) at any depth in the large size fraction, which could be interpreted as a larger standing stock of anammox bacteria biomass in large particles as compared to the smaller size fraction. This likely accounts for elevated BHT II ratios in the large size fraction (0.73) as compared to the small size fraction (0.36) at 70 m. Differences between our study and that by Ganesh et al. (2014) may be the result of inherent uncertainties in the interpretation of biomarker and genetic approaches. For instance, the role of BHT II in bacteria, as well as its relationship with anammox activity remains unknown, while

metagenomic data is not indicative of metabolic activity per se. BHT II is likely produced within the free-living size fraction and through the process of aggregation, is accumulated in the larger size fraction. Also, we cannot rule out *in situ* production of BHPs within particles, especially in the large size fraction, which may result in enhanced preservation of BHT II. In fact, hopanoid producers have been identified in a range of size fractions throughout the ETSP (Ganesh et al., 2014, 2015; Kharbush et al., 2016).

The larger diversity of BHPs in surface sediments as compared to the overlying water column is likely due to the integrated deposition and accumulation of POM from the water column over time. Additionally, it is possible that *in situ* microbial activity may contribute to the BHP signature in surface sediments. Adenosylhopane is often associated with soil bacteria and consequently used as a marker for terrestrial input (Talbot and Farrimond, 2007; Cooke et al., 2008). Thus, while the presence of adenosylhopane in two samples suggests the influence of terrestrial input, its absence from the other five sites suggests a lack of it. Also, anhydroBHT was identified in sediments that contained the highest concentration of total BHP (1.1-3.3 μg/g). AnhydroBHT is a diagenetic degradation product of BHT and composite BHPs under acidic and marine sedimentary conditions (Bednarczyk et al., 2005; Schaeffer et al., 2008, 2010; Sessions et al., 2013). Finally, 2-MeBHT was present in all surface sediments (10.6-78.6 ng/g). The abundance of this compound is particularly significant because 2-MeBHT has been interpreted as a biomarker for cyanobacteria (e.g. Summons et al., 1999). However, 2-methylhopanoids are also produced by other bacteria, particularly taxa within the alphaproteobacteria (e.g. Rashby et al., 2007; Welander et al., 2010; Ricci et al., 2014; Newman et al., 2016), and are rarely reported from the marine environment. 2-MeBHT did not coincide with adenosylhopane in surface sediments, so it is likely that it was produced locally and does not represent a transported signal from the terrestrial environment. Notably, no apparent correlation was found between any BHP and latitude, water depth, or distance from the coast.

BHT II ratio values (0.55–0.69) in surface sediments greatly exceeded those reported in surface sediments off Perú (0.22-0.29; Sáenz et al., 2011). Our BHT II ratio values are comparable with those measured within the OMZ core in the overlying water column (0.46–0.64), suggesting that the BHT II signal from the OMZ off the coast of northern Chile is transferred to, and preserved in, surface sediments. However, since anammox is a common bacterial metabolism in anoxic marine sediments, and a likely additional source of BHT II in this environment, we cannot rule out *in situ* production in surface sediments. Such contribution could be possibly addressed using genomic approaches not available for this study.

Long-term changes in anammox activity may be studied in the geological record using the BHT II ratio, which provides an opportunity to characterize the relative intensity, spatial and temporal scales of anammox activity and, by extension, OMZ change. The BHT II ratio increased during Termination II to values of >0.8 during the interglacial period, possibly reflecting a decrease in oxygenation and enhanced anammox abundance accompanying the transition to the warmer-than-present climate of the Eemian (Fig. 7). Notably, the $\delta^{15}N$ of bulk sediment, a proxy commonly used to trace the intensity of bacterial denitrification in overlying waters (e.g., Altabet et al., 1995; Ganeshram et al., 1995; Galbraith et al., 2013), showed a marked enrichment during Termination II that paralleled the increase in the BHT II ratio. This result indicates that both bacterial denitrification and anammox were increasingly enhanced during Termination II and deglacial times, consistent with the proposed overall decrease in dissolved oxygen of the global ocean (Jaccard and Galbraith, 2012), and with changes in the global N inventory due to enhanced denitrification (Altabet et al., 1995; Ganeshram et al., 1995; Galbraith et al., 2013). Our finding confirms that BHT II is well preserved in deeply buried sediments over hundreds of thousands of years which may allow for the reconstruction of anammox activity, at least in relative terms, during time periods of warm transitions leading to the expansion of marine oxygen-depleted waters. Also, the absolute concentration, or the accumulation rate of BHT II could be used to assess temporal changes in anammox bacteria biomass. A recent report of BHT II in Pliocene sapropels indicates that this biomarker can be stable even for millions of years (Rush et al., 2017). We caution, however, that further work is needed to fully understand the relationship between the BHT II ratio and anammox activity, and between the BHT II ratio and $\delta^{15}N$ in sedimentary records to draw more conclusive observations about nitrogen cycling in the past. Future research is needed to understand why anammox bacteria produce BHT II, how its production may relate to anammox activity, and what physiological role this biomarker plays in planctomycetes.

4.5 Conclusions

We report on the distribution of BHPs in suspended organic matter across the OMZ of the Humboldt Current System off northern Chile between 20.1° S and 30.2° S, as well as in surface and deeply buried marine sediments (125-150 ky). BHT and BHT II were the most abundant compounds in water column samples, particularly where OMZ waters were most persistent, and where intrusions of oxygenated water were less common. Water column samples were characterized by a low diversity of BHPs that also included a minor contribution of BHpentol. The BHT II ratio (expressed as BHT II/total BHT) increased as oxygen content

decreased in the water column, consistent with previous results from Perú, the Cariaco Basin and the Arabian Sea, and in line with previous microbiological evidence which indicates intense anammox activity in OMZ waters of this region.

The diversity of BHPs in surface sediments was greater than water column samples and comprised 7 compounds. We highlight that the signature of the BHT II signature is transported from the water column to surface sediments, and preserved in older sediments, where the BHT II ratio correlates with $\delta^{15}N$ values of bulk sediment during a glacial-interglacial transition. This study suggests that the production, transport, and preservation of BHT II in oxygen-deficient marine settings offers a proxy for past changes in the relative importance of anammox, and fluctuations in nitrogen cycling in response to ocean redox changes through the geological record.

4.6 Acknowledgements

We are thankful to the captains, crews and scientists of the German R/V Sonne cruise SO-211 (ChiMeBo), The Chilean R/V Vidal Gormaz cruise MOOMZ-2, and the US R/V Melville cruise BiG RAPA. In particular, we thank the chief scientists D. Hebbeln, O. Ulloa and D. Repeta, respectively. We also wish to thank L. Nuñez, J. Vera, B. Srain, R. Castro, A. Ávila, M. Mohtadi, R. De Pol-Holz, G. Martínez-Méndez, G. Alarcón, S. Lincoln, F. Stewart, and C. Colonero for sample collection and/or laboratory assistance. The ChiMeBo project was funded by the Bundesministerium für Bildung & Forschung (BMBF), the MOOMZ-2 cruise was funded by the Agouron Institute, and the BiG RAPA cruise was funded by the Center for Microbial Oceanography: Research and Education (C-MORE). Research at MIT was supported by the NASA Astrobiology Institute. J. Sepúlveda and R. Summons also thank the MIT-Chile MISTI Global Seed Funds grant program for funding. S. Pantoja and C. Lange thank the COPAS Sur-Austral CONICYT PIA PFB31 for partial funding. M. Caniupán thanks the CONICYT/PAI Concurso Nacional Apoyo al Retorno de Investigadores desde el Extranjero, Convocatoria 2013 (Grant 821320066) for funding. We thank three anonymous reviewers for their constructive comments that helped improving this manuscript.

4.7 References

Alldredge, A.L., Silver, M.W., 1988. Characteristics, dynamics and significance of marine snow. Progress in Oceanography 20, 41–82.

Altabet, M.A., Francois, R., Murray, D.W., Prell, W.L., 1995. Climate-related variations in denitrification in the Arabian Sea from sediment $^{15}N/^{14}N$ ratios. Nature 373, 506–509.

Armstrong, R.A., Lee, C., Hedges, J.I., Honjo, S., Wakeham, S.G., 2002. A new, mechanistic model for organic carbon fluxes in the ocean based on the quantitative association of POC with ballast minerals. Deep-Sea Research II, 49, 219-236.

Bednarczyk, A., Hernandez, T.C., Schaeffer, P., Adam, P., Talbot, H.M., Farrimond, P., Riboulleau, A., Largeau, C., Derenne, S., Rohmer, M., Albrecht, P., 2005. 32,35-Anhydrobacteriohopanetetrol: an unusual bacteriohopanepolyol widespread in recent and past environments. Organic Geochemistry 36, 673–677.

Berndmeyer, C., Thiel, V., Schmale, O., Wasmund, N., Blumenberg, M., 2014. Biomarkers in the stratified water column of the Landsort Deep (Baltic Sea). Biogeosciences 11, 7009-7023.

Bettencourt, J.H., López, C., Hernández-García, E., Montes, I., Sudre, J., Dewitte, B., Paulmier, A., Garçon, V., 2015. Boundaries of the Peruvian oxygen minimum zone shaped by coherent meoscale dynamics. Nature Geoscience Letters 8, 937-941.

Bligh, E.G., Dyer, W.J., 1959. A rapid method of total lipid extraction and purification. Canadian Journal of Biochemistry and Physiology 37, 911–917.

Blumenberg, M., Kruger, M., Nauhaus, K., Talbot, H.M., Oppermann, B.I., Seifert, R., Pape, T., Michaelis, W., 2006. Biosynthesis of hopanoids by sulfate-reducing bacteria (genus Desulfovibrio). Environmental Microbiology 8, 1220–1227.

Blumenberg, M., Seifert, R., Michaelis, W., 2007. Aerobic methanotrophy in the oxic– anoxic transition zone of the Black Sea water column. Organic Geochemistry 38, 84–91.

Blumenberg, M., Berndmeyer, C., Moros, M., Muschalla, M., Schmale, O., Thiel, V., 2013. Bacteriohopanepolyols record stratification, nitrogen fixation and other biogeochemical perturbations in Holocene sediments of the central Baltic Sea. Biogeosciences 10, 2725–2735.

Bograd, S.J., Castro, C.G., Di Lorenzo, E., Palacios, D.M., Bailey, H., Gilly, W., Chavez, F.P., 2008. Oxygen declines and the shoaling of the hypoxic boundary in the California Current. Geophysical Research Letters 35, L12607.

Brocks, J.J., Summons, R.E., 2003. Biomarkers of Early Life. Biogeochemistry 8, 63-115.

Canfield, D.E., Stewart, F.J., Thamdrup, B., De Brabandere, L., Dalsgaard, T., DeLong, E. F., et al. 2010. A Cryptic Sulfur Cycle in Oxygen-Minimum-Zone Waters off the Chilean Coast. Science 330, 1375–1378.

Capone, D.G., Hutchins, D.A., 2013. Microbial biogeochemistry of coastal upwelling regimes in a changing ocean. Nature Geosciences 6, 711–717.

Chavez, F., Messie, M., 2009. A comparison of eastern boundary upwelling ecosystems. Progress in Oceanography 83, 80–96.

Cooke, M.P., Talbot, H.M., Farrimond, P., 2008. Bacterial populations recorded in bacteriohopanepolyol distributions in soils from Northern England. Organic Geochemistry 39, 1347–1358.

Dalsgaard, T., Thamdrup, B., Farías, L., Revsbech, N.P., 2012. Anammox and denitrification in the oxygen minimum zone of the eastern South Pacific. Limnology and Oceanography 57, 1331-1346.

Daneri, G., Dellarossa, V., Quiñones, R., Jacob, B., Montero, P., Ulloa, O., 2000. Primary production and community respiration in the Humboldt Current System off Chile and associated oceanic areas. Marine Ecology Progress Series 197, 41-49.

Doughty, D.M., Hunter, R.C., Summons, R.E., Newman, D.K., 2009. 2-Methylhopanoids are maximally produced in akinetes of Nostoc punctiforme: geobiological implications. Geobiology 7, 524–532.

Eickhoff, M., Talbot, H.M., Peckmann, J., Kappler, A., 2013. Oxidation of Fe(II) leads to increased C-2 methylation of pentacyclic triterpenoids in the anoxygenic phototrophic bacterium *Rhodopseudomonas palustris* strain TIE-1. Geobiology 11, 268-278.

Farías, L., Paulmier, A., Gallegos, M., 2007. Nitrous oxide and N-nutrient cycling in the oxygen minimum zone off northern Chile. Deep-Sea Research I 54, 164–180.

Farrimond, P., Fox, P.A., Innes, H.E., Miskin, I.P., Head, I.M., 1998. Bacterial sources of hopanoids in recent sediments: improving our understanding of ancient hopane biomarkers. Ancient Biomolecules 2, 147–166.

Fischer, W.W., Summons, R.E., Pearson, A., 2005. Targeted genomic detection of biosynthetic pathways: anaerobic production of hopanoid biomarkers by a common sedimentary microbe. Geobiology 3, 33–40.

Fuenzalida, R., Schneider, W., Garces-Vargas, J., Bravo, L., Lange, C., 2009. Vertical and horizontal extension of the oxygen minimum zone in the Eastern South Pacific Ocean. Deep-Sea Research II 56, 1027–1038.

Galán, A., Molina, V., Thamdrup, B., Woebken, D., Lavik, G., Kuypers, M.M.M., Ulloa, O., 2009. Anammox bacteria and anaerobic oxidation of ammonium in the oxygen minimum zone off northern Chile. Deep-Sea Research II 56, 1021-1031.

Ganesh, S., Parris, D.J., DeLong, E.F., Stewart, F.J., 2014. Metagenomic analysis of size-fractioned picoplankton in marine oxygen minimum zone. The ISME Journal, 8, 187-211.

Ganesh, S., Bristow, L.A., Larsen, M., Sarode, N., Thamdrup, B, Stewart, F., 2015. Size-fraction partitioning of community gene transcription and nitrogen metabolism in a marine oxygen minimum zone. The ISME Journal 9, 2682-2696.

Galbraith, E.D., Kienast, M., et al., 2013. The acceleration of ocean denitrification during deglacial warming. Nature Geoscience Articles 6, 579-584.

Ganeshram, R.S., Pedersen, T.F., Calvert, S.E., Murray, J.W., 1995. Large changes in oceanic nutrient inventories from glacial to interglacial periods. Nature 376, 755–758.

Hartner, T., Straub, K.L., Kannenberg, E., 2005. Occurrence of hopanoid lipids in anaerobic Geobacter species. FEMS Microbiology Letters 243, 59–64.

Hebbeln, D. and cruise participants, 2011. Report and preliminary results of R/V Sonne cruise SO211, Valparaiso-Valparaiso, 2 November - 29 November, 2010, ChiMeBo, Berichte aus dem Fachbereich Geowissenschaften der Universität Bremen ; 279.

Hedges, J.I., Baldock, J.A., Géllinas, Y., Lee, C., Peterson, M., Wakeham, S.G., 2001. Evidence for non-selective preservation of organic matter in sinking marine particles. Letters to Nature 409, 801-804.

Jaccard, S.L., Galbraith, E.D., 2012. Large climate-driven changes of oceanic oxygen concentrations during the last deglaciation. Nature Geoscience 5, 151-156.

Jaeschke, A., Lewan, M.D., Hopmans, E.C., Schouten, S., Sinninghe Damsté, J.S., 2008. Thermal stability of ladderane lipids as determined by hydrous pyrolysis. Organic Geochemistry 39, 1735–1741.

Jaeschke, A., Ziegler, M., Hopmans, E.C., Reichart, G.J., Lourens, L.J., Schouten, S., Sinninghe Damsté, J.S., 2009. Molecular fossil evidence for anaerobic ammonium oxidation in the Arabian Sea over the last glacial cycle. Paleoceanography 24, PA2202.

Karl, D.M., Knauer, G.A., Martin, J.H., 1988. Downward flux of particulate organic matter in the ocean: A particle decomposition paradox. Nature 332, 438-441.

Keeling, R. F., Kortzinger, A., Gruber, N., 2010. Ocean deoxygenation in a warming world. Annual Reviews in Marine Science 2, 199–229.

Kharbush, J.J., Ugalde, J.A., Hogle, S.L., Allen, E.E., Aluwiharea, L.I., 2013. Composite bacterial hopanoids and their microbial producers across oxygen gradients in the water column of the California Current. Applied and Environmental Microbiology 79, 7491-7501.

Kharbush, J.J., Kejriwal, K., Aluwihare, L.I., 2016. Distribution and abundance of hopanoid producers in low-oxygen environments of the Eastern Pacific Ocean. Microbial Ecology 71, 401-408.

Kuypers, M.M.M., Sliekers, A.O., Lavik, G., Schmid, M., Jorgensen, B.B., Kuenen, J.G., Sinninghe Damsté, J.S., Strous, M., Jetten, M.S.M., 2003. Anaerobic ammonium oxidation by anammox bacteria in the Black Sea. Nature 422, 608–611.

Lam, P., Kuypers, M.M.M., 2011. Microbial Nitrogen Cycling Processes in Oxygen Minimum Zones. Annual Review of Marine Science 3, 317–345.

Lam, P., Lavik, G., Jensen, M. M., van de Vossenberg, J., Schmid, M., Woebken, D., et al., 2009. Revising the nitrogen cycle in the Peruvian oxygen minimum zone. PNAS 106, 4752–4757.

Lisiecki, L.E., Raymo, M.E., 2005. A Pliocene-Pleistocene stack of 57 globally distributed benthic $\delta^{18}O$ records. Paleoceanography 20, PA1003.

Martínez-Méndez, G., Hebbeln, D., Mohtadi, M., Lamy, F., De Pol-Holz, R., Reyes-Macaya, D., Freudenthal, T., 2013. Changes in the advection of Antarctic Intermediate Water to the northern Chilean coast during the last 970 kyr. Paleooceanography 28, 607-618.

Montecino, V., Lange, C.B., 2009. The Humboldt Current System: Ecosystem components and processes, fisheries, and sediment studies. Progress in Oceanography 83, 65-79.

Newman, D.K., Neubauer, C., Ricci, J., Wu, C-H., Pearson, A., 2016. Cellular and molecular biological approaches to interpreting ancient biomarkers. Annual Reviews Earth Planetary Sciences 44, 493–522.

Nishihara, M., Koga, Y., 1987. Extraction and composition of polar lipids from the archaebacterium, Methanobacterium thermoautotrophicum: effective extraction of tetraether lipids by an acidified solvent. Journal of Biochemistry 101, 997-1005.

Ourisson, G., Albrecht, P., Rohmer, M., 1979. Hopanoids: palaeochemistry and biochemistry of a group of natural products. Pure and Applied Chemistry 51, 709–729.

Pantoja, S., Sepúlveda, J. and González, H.E., 2004. Decomposition of sinking proteinaceous material during fall in the oxygen minimum zone off northern Chile. Deep Sea Research Part I: Oceanographic Research Papers 51, 55-70.

Paulmier, A., Ruiz-Pino, D., Garçon, V., Farías, L., 2006. Maintaining of the East South Pacific Oxygen Minimum Zone (OMZ) off Chile. Geophysical Research Letters 33, L20601.

Paulmier, A., Ruiz-Pino, D., 2009. Oxygen minimum zones (OMZs) in the modern ocean. Progress in Oceanography 80, 113-128.

Pearson, A., Flood Page, S.R., Jorgenson, T.L., Fischer, W.W., Higgins, M.B., 2007. Novel hopanoid cyclases from the environment. Environmental Microbiology 9, 2175-2188.

Pearson, A., Leavitt, W.D., Sáenz, J.P., Summons, R.E., Tam, M.C.-M., Close, H.G., 2009. Diversity of hopanoids and squalene-hopene cyclases across a tropical land-sea gradient. Environmental Micorbiology 11, 1208-1223.

Rashby, S.E., Sessions, A.L., Summons, R.E., Newman, D.K., 2007. Biosynthesis of 2-methylbacteriohopanepolyols by an anoxygenic phototroph. PNAS 104, 15099–15104.

Rattray, J.E., van de Vossenberg, J., Hopmans, E.C., Kartal, B., van Niftrik, L., Rijpstra, W.I.C., Strous, M., Jetten, M.S.M., Schouten, S., Sinninghe Damsté, J.S., 2008. Ladderane lipid distribution in four genera of anammox bacteria. Archives of Microbiology 190, 51–66.

Ricci, J.N., Coleman, M.L., Welander, P.V., Sessions, A.L., Summons, R.E., Spear, J.R., Newman, D.K., 2014. Diverse capacity for 2-methylhopanoid production correlates with a specific ecological niche. The ISME Journal 8, 675-684.

Rieck, A., Herlemann, D.P.R., Jürgens, K., Grossart, H.-P., 2015. Particle-Associated Differ from Free-Living Bacteria in Surface Waters of the Baltic Sea. Frontiers in Microbiology 6, 1297.

Rohmer, M., Bouvier-Nave, P., Ourisson, G., 1984. Distribution of hopanoid triterpenes in prokaryotes. Journal of General Microbiology 130, 1137–1150.

Rush, D., Sinninghe Damsté, J.S., Poulton, S.W., Thamdrup, B., Garside, A.L., González, J. A., Schouten, S., Jetten, M.S.M., Talbot, H.M., 2014. Anaerobic ammonium-oxidising bacteria: A biological source of the bacteriohopanetetrol stereoisomer in marine sediments. Geochimica Et Cosmochimica Acta 140, 50–64.

Rush, D., Talbot, H.M., Schwartz-Narbonne, R., Wagner, T., Sinninghe Damsté, J.S. Anaerobic ammonium oxidation is an important nitrogen cycle process during Mediterranean sapropel deposition. Abstract #, 28th International Meeting on Organic Geochemistry, 17-22 September 2017, Florence, Italy.

Sáenz, J.P., 2010. Exploring the Distribution and Physiological Roles of Bacterial Membrane Lipids in the Marine Environment (Doctoral dissertation).

Sáenz, J.P., Wakeham, S.G., Eglinton, T.I., Summons, R.E., 2011. New constraints on the provenance of hopanoids in the marine geologic record: Bacteriohopanepolyols in marine suboxic and anoxic environments. Organic Geochemistry 42, 1351–1362.

Sáenz, J.P., Sezgin, E., Schwille, P., Simons, K., 2012. Functional convergence of hopanoids and sterols in membrane ordering. PNAS 109, 14236–14240.

Sáenz, J.P., Grosser, D., Bradley, A.S., Lagny, T.J., Lavrynenko, O., Broda, M., Simons, K., 2015. Hopanoids as functional analogues of cholesterol in bacterial membranes. PNAS 112, 11971-11976.

Schaeffer, P., Schmitt, G., Adam, P., Rohmer, M., 2008. Acid-catalyzed formation of 32,35-anhydrobacteriohopanetetrol from bacteriohopanetetrol. Organic Geochemistry 39, 1479–1482.

Schaeffer, P., Schmitt, G., Adam, P., Rohmer, M., 2010. Abiotic formation of 32,35-anhydrobacteriohopanetetrol: a geomimetic approach. Organic Geochemistry 41, 1005–1008.

Sessions, A.L., Zhang, L., Welander, P.V., Doughty, D., Summons, R.E. and Newman, D.K. 2013 Identification and quantification of polyfunctionalized hopanoids by high temperature gas chromatography–mass spectrometry. Organic Geochemistry 56, 120-130.

Sinninghe Damsté, J.S., Strous, M., Rijpstra, W.I.C, Hopmans, E., Geenevasen, J.A.J, van Duin, A.C.T., van Niftrik, L.A., Jetten, M.S.M., 2002. Linearly concatenated cyclobutane lipids form a dense bacterial membrane. Nature 419, 708-712.

Sinninghe Damsté, J.S, Rijpstra, W.I.C., Schouten, S., Fuerst, J.A., Jetten, M.S.M., Strous, M., 2004. The occurrence of hopanoids in planctomycetes: implications for the sedimentary biomarker record. Organic Geochemistry 35, 561–566.

Smethie, W.M., 1987. Nutrient regeneration and denitrification in low oxygen fjords. Deep-Sea Research 34, 983–1006.

Stevens, H., Ulloa, O., 2008. Bacterial diversity in the oxygen minimum zone of the eastern tropical South Pacific. Environmental Microbiology 10, 1244–1259.

Stewart, F.J., Ulloa, S., DeLong, E.F., 2012. Microbial metatranscriptomics in a permanent marine oxygen minimum zone. Environmental Microbiology 14, 23-40.

Stramma, L., Johnson, G.C., Sprintall, J., Mohrholz, V., 2008. Expanding oxygen-minimum zones in the tropical oceans. Science 320, 655–658.

Sturt, H.F., Summons, R.E., Smith, K., Elvert, M., Hinrichs, K.-U., 2004. Intact polar membrane lipids in prokaryotes and sediments deciphered by high-performance liquid chromatography/electrospray ionization multistage mass spectrometry—new biomarkers for biogeochemistry and microbial ecology. Rapid Communications in Mass Spectrometry 18, 617–628.

Summons, R.E., Lincoln, S.A., 2012. Biomarkers: Informative molecules for studies in geobiology. In: Knoll, A.H., Canfield, D.E., and Konhauser, K.O. (Eds.), Fundamentals of Geobiology.

Summons R.E., Brassell, S.C., Eglinton, G., Evans, E., Horodyski, R.J., Robinson, N., Ward, D.M., 1988. Distinctive hydrocarbon biomarkers from fossiliferous sediments of the Late Proterozoic Walcott Member, Chuar Group, Grand Canyon, Arizona. Geochimica et Cosmochimica Acta 52, 2625–2637.

Summons, R.E., Jahnke, L.L., Hope, J.M., Logan, G.A., 1999. 2-Methylhopanoids as biomarkers for cyanobacterial oxygenic photosynthesis. Nature 400, 554–557.

Talbot, H.M., Squier, A.H., Keely, B.J., Farrimond, P., 2003. Atmospheric pressure chemical ionisation reversed-phase liquid chromatography/ion trap mass spectrometry of intact bacteriohopanepolyols. Rapid Communications in Mass Spectrometry 17, 728 –737.

Talbot, H.M., Farrimond, P., 2007. Bacterial populations recorded in diverse sedimentary biohopanoid distributions. Organic Geochemistry 38, 1212–1225.

Talbot, H.M., Rohmer, M., Farrimond, P., 2007. Rapid structural elucidation of composite bacterial hopanoids by atmospheric pressure chemical ionisation liquid chromatography/ion trap mass spectrometry. Rapid Communications in Mass Spectrometry 21, 880 – 892.

Thamdrup, B., 2012. New pathways and processes in the global nitrogen cycle. Annual Review of Ecology, Evolution, and Systematics 43, 407-428.

Ulloa, O., Canfield, D.E., DeLong, E.F., Letelier, R.M., Stewart, F.J., 2012. Microbial oceanography of anoxic oxygen minimum zones. PNAS 109, 15996–16003.

Wakeham, S.G., Amann, R., Freeman, K.H., Hopmans, E.C., Jorgensen, B.B., Putnam, I.F., Schouten, S., Sinninghe Damsté, J.S., Talbot, H.M., Woebken, D., 2007. Microbial ecology of the stratified water column of the Black Sea as revealed by a comprehensive biomarker study. Organic Geochemistry 38, 2070–2097.

Wakeham, S.G., Turich, C., Schubotz, F., Podlaska, A., Li, X.N.N., Varela, R., Astor, Y., Sáenz, J.P., Rush, D., Sinninghe Damsté, J.S., Summons, R.E., Scranton, M.I., Taylor, G.T., Hinrichs, K.-U., 2012. Biomarkers, chemistry and microbiology show chemoautotrophy in a multilayer chemocline in the Cariaco Basin. Deep-Sea Research I 63, 133–156.

Welander, P.V., Hunter, R.C., Zhang, L.C., Sessions, A.L., Summons, R.E., Newman, D.K., 2009. Hopanoids play a role in membrane integrity and pH homeostasis in Rhodopseudomonas palustris TIE-1. Journal of Bacteriology 191, 6145–6156.

Welander, P.V., Coleman, M.L., Sessions, A.L., Summons, R.E., Newman, D.K., 2010. Identification of a methylase required for 2-methylhopanoid production and implications for the interpretation of sedimentary hopanes. PNAS 107, 8537–8542.

Welander, P.V., Doughty, D.M., Wu, C.H., Mehay, S., Summons, R.E., Newman, D.K., 2012. Identification and characterization of Rhodopseudomonas palustris TIE-1 hopanoid biosynthesis mutants. Geobiology 10, 163–177.

Wright, J.J., Konwar, K.M., Hallam, S.J., 2012. Microbial ecology of expanding oxygen minimum zones. Nature Reviews Microbiology 10, 381-394.

4.8 Figures

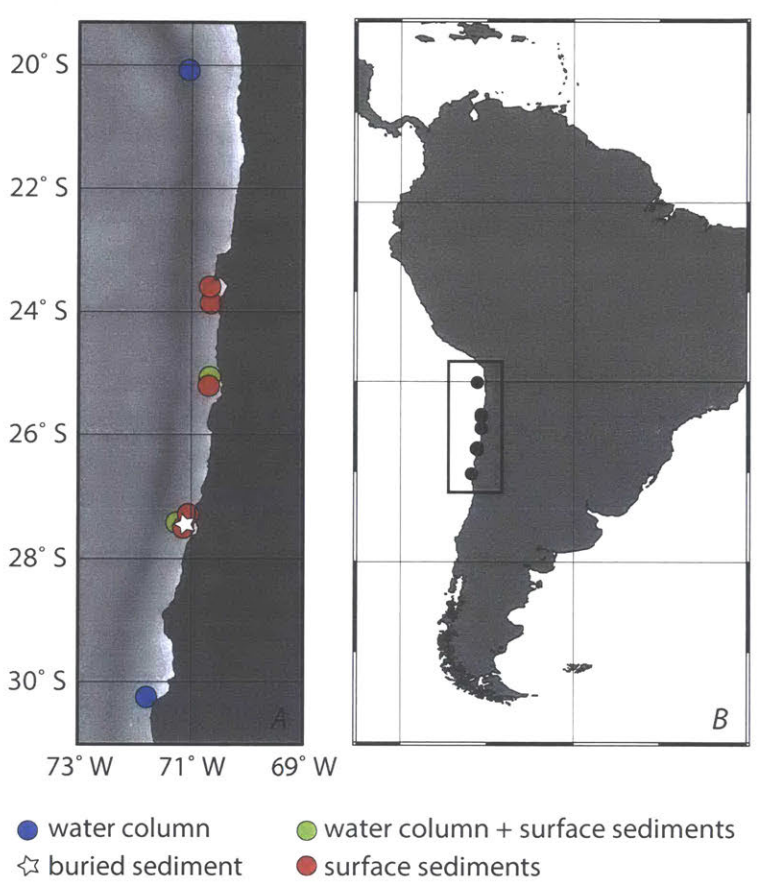

Figure 1. (A) Map of northern Chile showing the locations of sampling stations where water column, surface sediment, and deeply buried sediment samples were collected. (B) Map of South America showing the study area in the OMZ system off the coast of northern Chile.

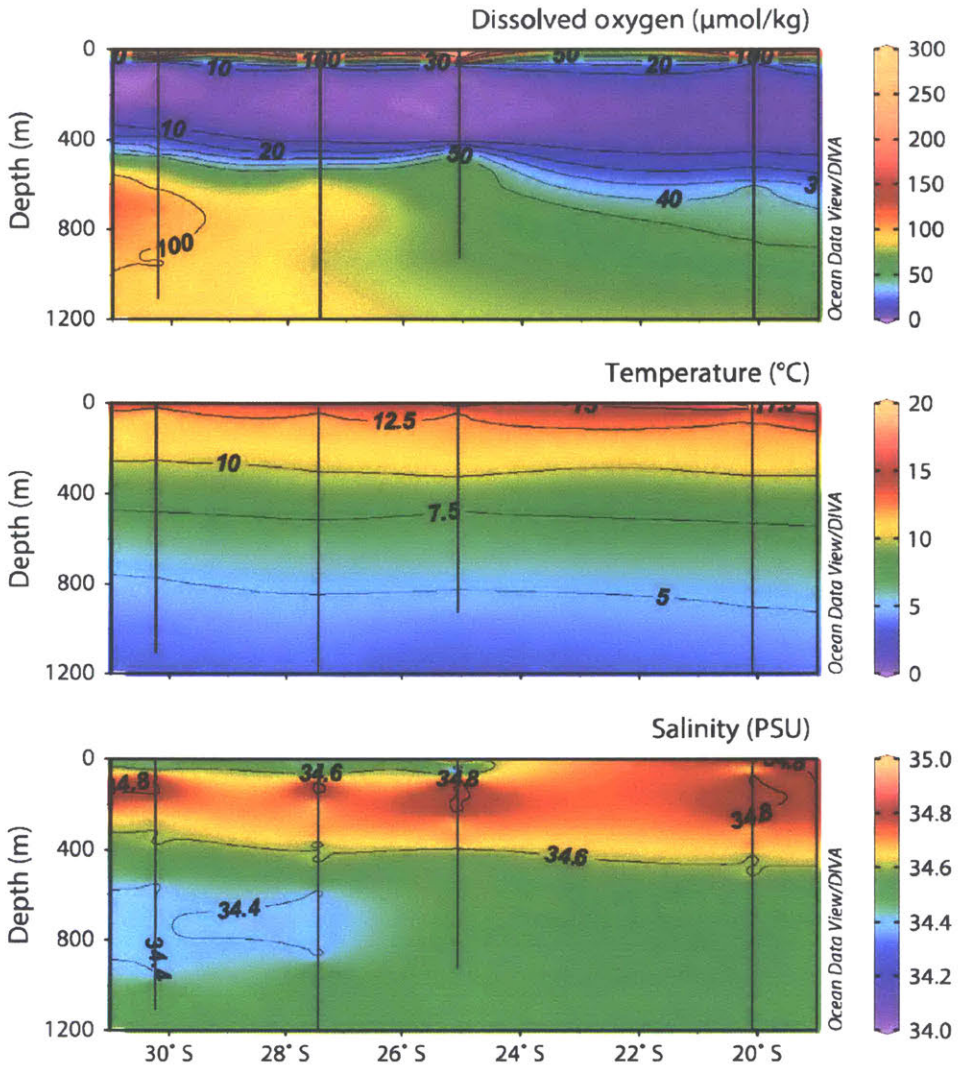

Figure 2. Cross sections of physical-chemical parameters from the ETSP OMZ off northern Chile between ~19° S and 31° S: dissolved oxygen (µmol/kg), temperature (°C), and salinity (PSU) as recorded during the ChiMeBo, MOOMZ-2 and BiG RAPA cruises (Table 1). Note that the cruise measurements, indicated as grey vertical markers, were obtained at different times.

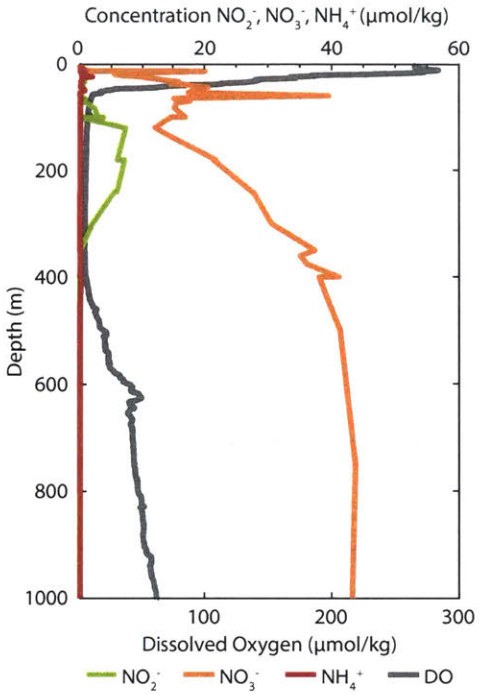

Figure 3. Representative depth profiles of nutrients (NO_2^-, NO_3^-, and NH_4^+; µg/kg) and dissolved oxygen (µmol/kg) from the OMZ off the coast of northern Chile during the BiG RAPA cruise in November 2010 (20.3° S).

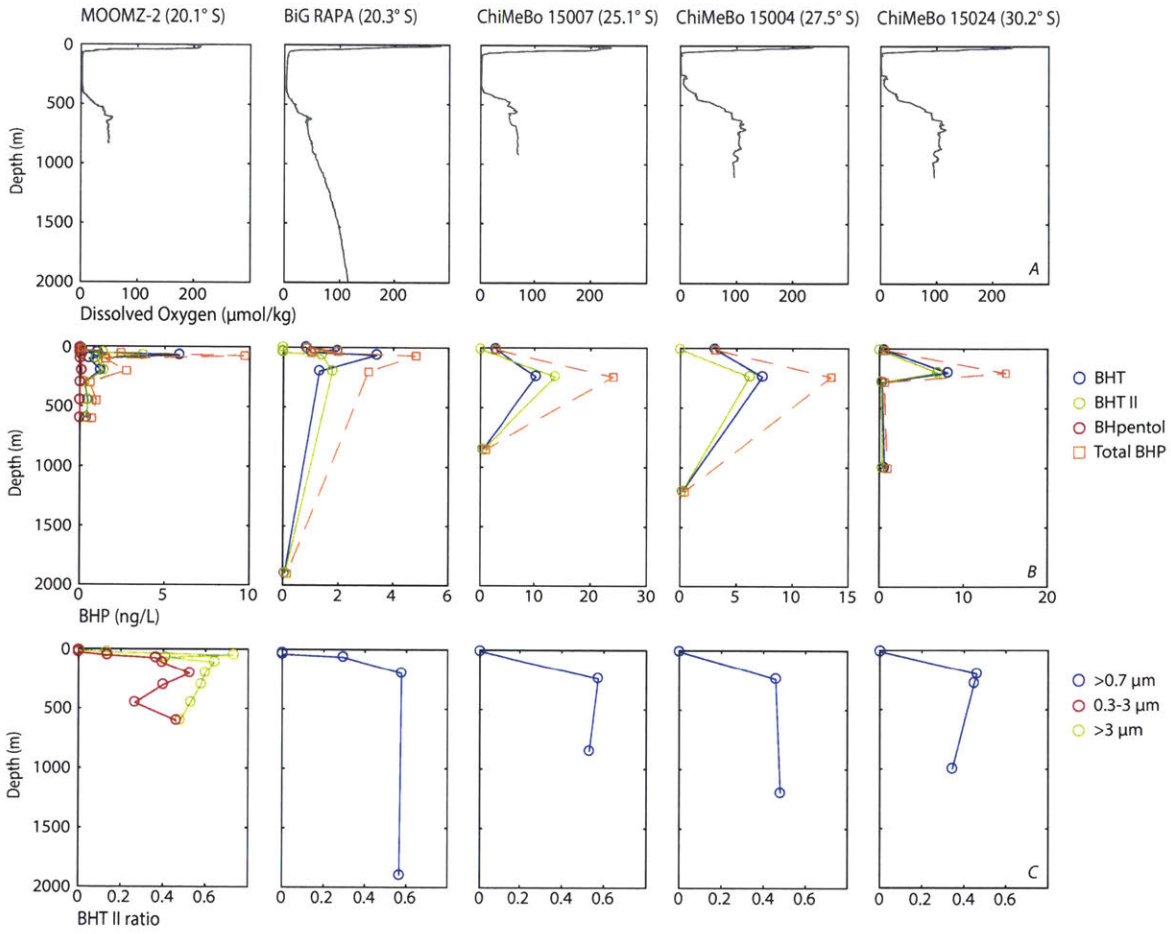

Figure 4. Depth profiles of dissolved oxygen (A; µmol/kg), individual BHPs (B; ng/L), and the BHT II ratio (C; BHT II/total BHT) in samples collected from MOOMZ-2 Station 3 (20.1° S), BiG RAPA Station 1 (20.3° S), and ChiMeBo Stations 15007 (25.1° S), 15004 (27.5° S), and 15024 (30.2° S). Note that BHP concentrations from MOOMZ-2 (B) correspond to the sum of single measurements from two size fractions (>3.0 µm and 0.3-3 µm). All other BHP concentrations are single measurements from >0.7 µm size fractions.

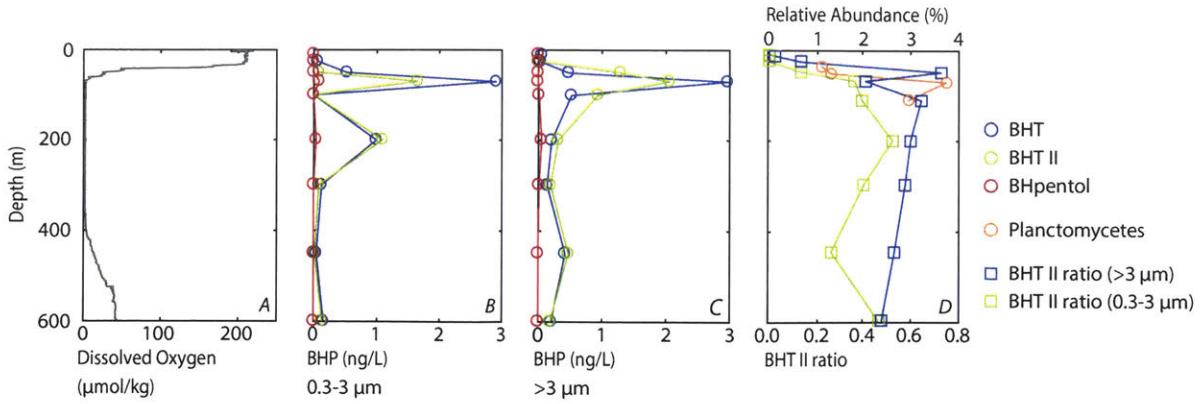

Figure 5. Dissolved oxygen (A; µmol/kg) compared to BHP concentrations from 0.3-3 µm (B) and >3 µm (C) size fractions, BHT II ratio values from both size fractions (D) and the relative abundance of planctomycetes (D) at MOOMZ-2 Station 3 (20.1° S).

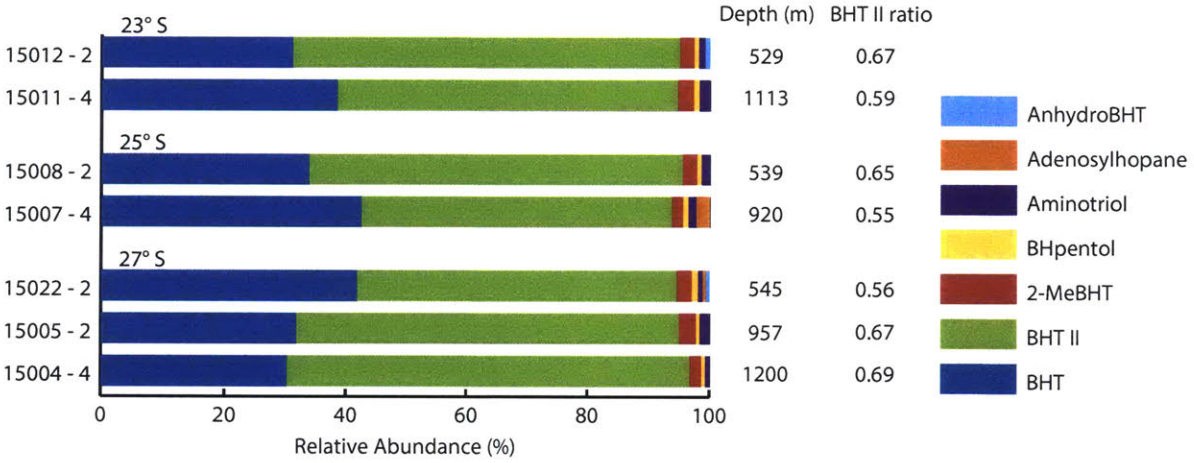

Figure 6. Relative abundance (%) of BHPs and BHT II ratio values in surface sediments along a latitudinal transect from 23° S to 27° S. Within each location, samples are organized by increasing water depth from top to bottom.

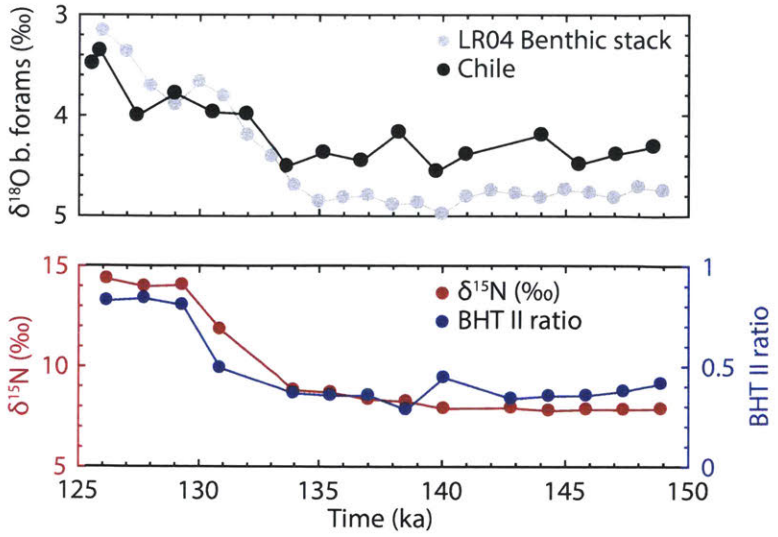

Figure 7. Stable isotope and geochemical signatures in core GeoB15016 at 27° S off the coast of northern Chile during Glacial Termination II (transition from MIS-6 to MIS-5). Top panel: LR04 Benthic stack $\delta^{18}O$ data (grey) from Lisiecki and Raymo (2005), and $\delta^{18}O$ from benthic foraminifera (black) in core GeoB15016 from Martínez-Méndez et al. (2013). Lower panel: $\delta^{15}N$ of bulk sediment (red) and BHT II ratio (blue) in core GeoB15016.

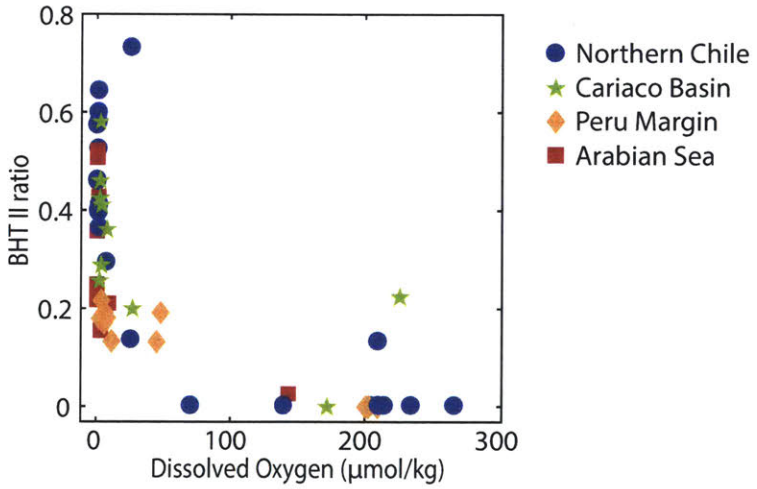

Figure 8. The relationship between the BHT II ratio and dissolved oxygen (µmol/kg) in samples from this study (Northern Chile; blue squares) and other OMZ systems as described by Sáenz et al. (2011). Note that samples from oxygenated waters below the OMZ were not included because they represent organic matter exported from within the OMZ. See main text for further details.

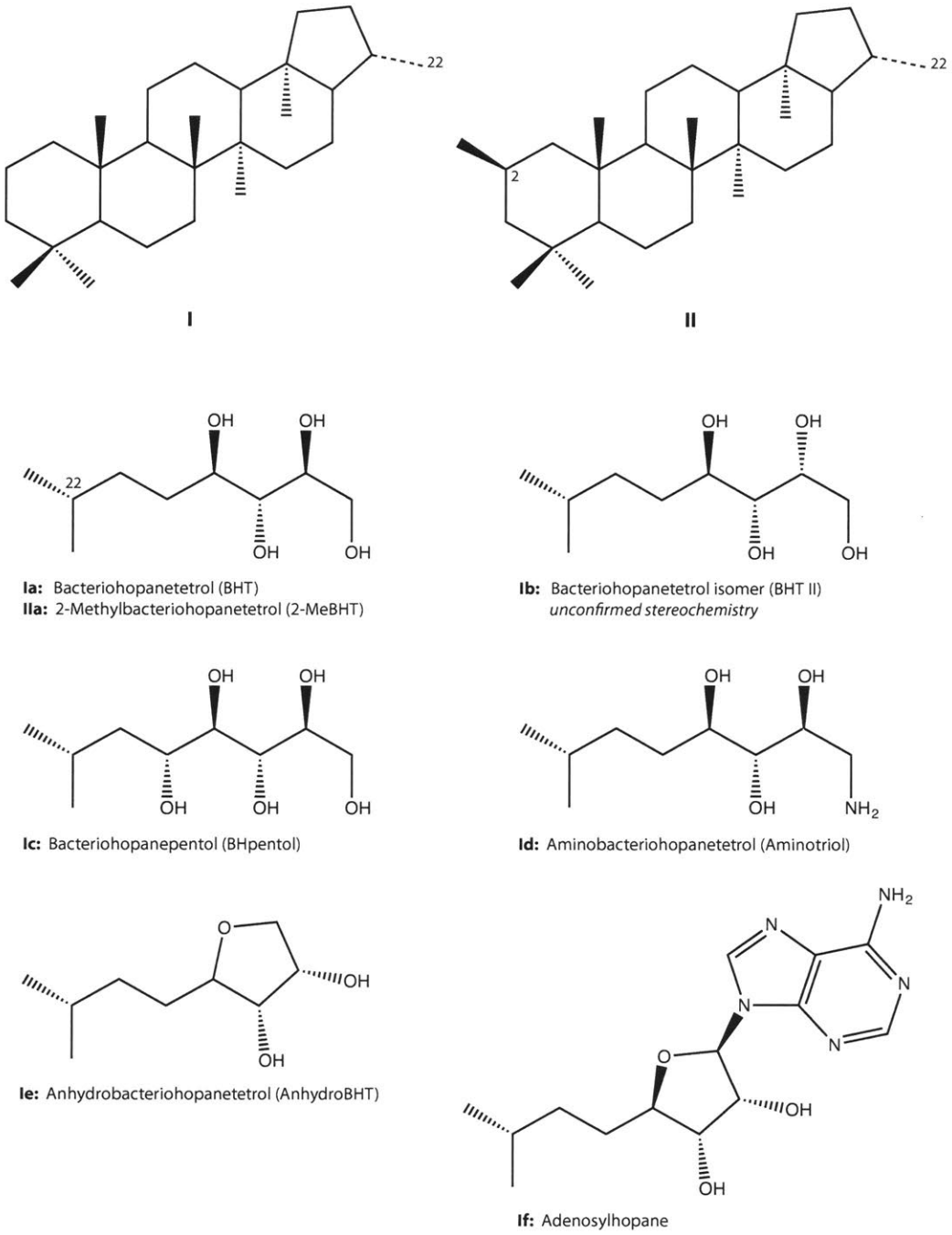

Supplementary Figure 1. Structures of BHP compounds identified in the ETSP OMZ off northern Chile.

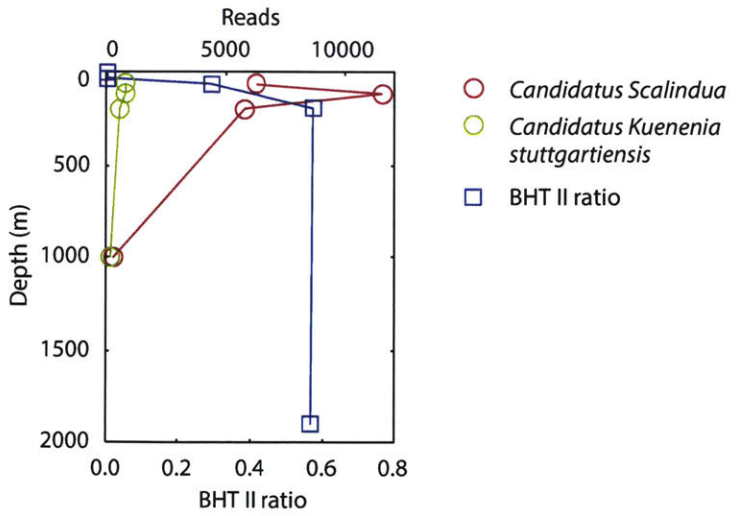

Supplementary Figure 2. Reads of phyla known to conduct anammox (Ganesh et al., 2014) and BHT II ratio values at BiG RAPA Station 1 (20.3°S).

4.9 Tables

Table 1. Summary of sampling types and locations during the three independent oceanographic cruises described here.

Cruise		Station	Date Collected (MM/YY)	Latitude (°S)	Longitude (°W)	Water Depth (m)	Water Filtered (L)	Sediment Extracted (g)
Water Column								
MOOMZ-2	08-18/08/2009	3	08/09	20.12	70.42	10-600	781-2133	-
BiG RAPA	18/11 to 14/12/2010	1	11/10	20.33	70.81	0-1900	200-240	-
ChiMeBo	02-29/11/2010	15-007	11/10	25.07	70.67	10-850	40-100	-
ChiMeBo	02-29/11/2010	15-004	11/10	27.45	71.16	10-1200	40-100	-
ChiMeBo	02-29/11/2010	15-024	11/10	30.24	71.78	10-1000	40-100	-
Surface Sediments								
ChiMeBo	02-29/11/2010	15-012	11/10	23.59	70.67	529	-	5
ChiMeBo	02-29/11/2010	15-011	11/10	23.85	70.65	1113	-	5
ChiMeBo	02-29/11/2010	15-007	11/10	25.07	70.66	920	-	5
ChiMeBo	02-29/11/2010	15-008	11/10	25.20	70.68	539	-	5
ChiMeBo	02-29/11/2010	15-022	11/10	27.29	71.05	545	-	5
ChiMeBo	02-29/11/2010	15-004	11/10	27.45	71.16	1200	-	5
ChiMeBo	02-29/11/2010	15-005	11/10	27.50	71.13	957	-	5
Buried Sediments								
ChiMeBo	02-29/11/2010	15-016	11/10	27.50	71.13	971	-	2

Chapter 5:

Environmental controls on bacteriohopanepolyol profiles of benthic microbial mats from Lake Fryxell, Antarctica

Environmental controls on bacteriohopanepolyol profiles of benthic microbial mats from Lake Fryxell, Antarctica

Emily D. MATYS[1*], Tyler MACKEY[1], Elliott MUELLER[1], Anne JUNGBLUT[2], Dawn Y. SUMNER[3], Ian HAWES[4], and Roger E. SUMMONS[1]

1. Department of Earth, Atmospheric and Planetary Sciences, Massachusetts Institute of Technology, Cambridge, MA
2. Department of Life Sciences, The Natural History Museum, London UK
3. Department of Earth and Planetary Sciences, University of California, Davis, CA
4. University of Waikato, Tauranga, New Zealand

Abstract

Bacteriohopanepolyols (BHPs) are pentacyclic triterpenoid lipids that contribute to the structural integrity and physiology of some bacteria. Some BHPs have potential as taxonomically and environmentally diagnostic biomarkers. For example, a stereoisomer of bacteriohopanetetrol (informally BHT II) has been associated with anaerobic ammonium oxidation (anammox) bacteria and suboxic to anoxic marine environments where anammox is active. Its recognition in the sedimentary record may inform reconstructions of nitrogen cycling in response to ocean redox changes through the geological record. However, it is unclear whether additional sources of BHT II exist, if it is produced in abundance in non-marine environments, and what the implications such findings would have on interpretations of the rock record. We investigate the BHP composition of benthic microbial mats from Lake Fryxell, Antarctica. Lake Fryxell is a perennially ice-covered lake with a sharp oxycline in a density stabilized water column. We describe the diversity and abundance of BHPs in benthic microbial mats across a transect from oxic to anoxic conditions. Generally, BHP abundances and diversity vary with the morphologies of microbial mats, which reflect local environmental conditions, such as irradiance and oxygen and sulfide concentrations. BHT II was identified in mats that exist within oxic to anoxic portions of the lake. Our results suggest that BHT II is produced at least in part by anammox bacteria, which populate anoxic mats and may exploit anaerobic microenvironments in otherwise oxygenated mats. We examine our results in the context of BHPs as biomarkers in modern and ancient environments.

Keywords: Anammox, Bacteriohopanepolyol, Bacteriohopanetetrol isomer, Biomarker, McMurdo Dry Valleys

5.1 Introduction

Stable lipid biomarkers such as hopanes preserve evidence of ancient biological activity in the geological record (Brocks and Pearson, 2005; Peters et al., 2005). Hopane parent molecules, bacteriohopanepolyols (BHPs) are pentacyclic triterpenoid lipids that contribute to membrane structural integrity and physiology in some α-, ß-, and γ-Proteobacteria, cyanobacteria and planctomycetes. A large diversity of BHPs that mainly differ in the side chain structures, has been described (e.g. Talbot et al., 2007). Side chain structures may be specific to particular organisms or be formed in response to particular environmental conditions. As such, BHPs have great potential as taxonomically and environmentally diagnostic biomarkers. However, an incomplete understanding of BHP diversity and source organisms in modern environments precludes the interpretation of hopanes in the rock record.

In recent years to develop some BHPs as biomarkers, with the goal of improving confidence in interpretations of geohopane patterns in sedimentary archives. Analytical advances, such as the development of high precision liquid chromatography mass spectrometry (HPLC-MS) methods for the analysis of intact BHPs, (Talbot et al., 2001, 2003) and compound-specific response factors (Wu et al., 2015) have allowed for robust identification and semi-quantification of BHPs in complex samples from a range of modern environments. For example, it is now possible to separate, identify, and quantify composite BHPs and stereoisomers. Furthermore, the development of culture-independent techniques to predict the capacity for hopanoid biosynthesis through the identification of biosynthetic genes (e.g. Pearson and Rusch, 2009; Welander et al., 2010; Ricci et al., 2014; Ricci et al., 2015) has greatly increased our understanding of hopanoid source organisms and limits the necessity of culture-dependent techniques (Rashby et al., 2007). However, relatively few environments have been screened for BHPs. Moreover, the complete biosynthetic pathway for some BHPs are not yet fully understood. It is therefore important to characterize BHP diversity, possible source organisms, and associated environmental conditions in a wide range of previously unexplored environments to constrain geobiological interpretations of hopanes in the rock record.

To date, environmental studies of BHPs have focused predominantly on low- to mid-latitude marine, lacustrine (Castañeda and Schouten, 2011), and terrestrial (Cook et al., 2008) environments. For example, a stereoisomer of bacteriohopanetetrol (BHT), BHT II, has been identified in marine oxygen minimum zones (e.g. Sáenz et al., 2011; Wakeham et al., 2012; Kharbush et al., 2013; Matys et al., 2017), sediments from an anoxic marine fjord-like

enclosure (Rush et al., 2014), and in enrichment cultures of anaerobic ammonium-oxidizing (anammox) bacteria (Rush et al., 2014). As a result, the "BHT II ratio" (BHT II/total BHT) has been proposed as a proxy for past changes in the relative importance of anammox and fluctuations in nitrogen cycling in response to ocean redox changes through the geological record. The development of this biomarker has significant implications for tracing past changes in the marine nitrogen cycle, as anammox bacteria are a major sink for fixed nitrogen in the ocean (Dalsgaard et al., 2003). However, it is unclear if additional sources of BHT II exist. A unique biosynthetic pathway of BHT II has yet to be elucidated, precluding the investigation of the capacity for BHT II production through genomic approaches. Until then, environmental screening for BHT II and possible source organisms may be the best way to realize its scope and identify additional sources of BHT II or confirm its specificity to anammox bacteria.

Few studies have described BHPs in polar environments and in particular, Antarctica, despite the high diversity of BHPs identified relative to low-latitude settings, including tetra and penta-functionalized methylated, non-methylated and unsaturated compounds (Talbot et al., 2008; Cooke et al., 2009). Here, we describe BHP diversity and abundance in benthic microbial mats from Lake Fryxell, Antarctica. The benthic microbial communities are structured by local environmental conditions, such as irradiance and oxygenation (Jungblut et al., 2016). BHP profiles vary with mat morphotype and local environmental conditions, with the most substantial change in BHP diversity occurring at the oxycline. Of particular interest is the abundance of BHT II and shifts in penta-functionalized hopanoids across the oxic-anoxic transition. These results develop the known distribution and diversity of BHPs in Polar Regions and present insights for interpreting the distribution of BHPs, including BHT II, in modern environments and sedimentary archives.

5.2 Methods

5.2.1 Site Description

Lake Fryxell (77°36'S 162°6'E) is a closed-basin, perennially ice-covered lake in the McMurdo Dry Valleys, Antarctica (Fig. 1). The ice cover (approximately 4-5 m thick; Vincent, 1981) minimizes wind-induced mixing. In addition, the balance between ablation of the ice cover and inflowing melt water determines annual changes in lake level (Dugan et al., 2013). Ice ablates from the top of the ice cover and freezes on the bottom; as a result, stable or falling lake levels are associated with increasing salinity as solutes are excluded from the ice cover. Excess inflowing melt water can lead to development of a freshwater lens beneath the ice cover. The lake level history at Lake Fryxell has led to a strong salinity gradient and density stratified

water column (Lyons et al., 2005). The ice cover also limits the transport and diffusion of solutes and gasses into and out of the lake. As a result, oxygen is present at high concentrations (137-622 μmol kg^{-1}) in the upper water column. Net photosynthesis transitions to net respiration with declining irradiance with depth into the lake, and this transition enables the development of an oxycline between 9-10 m depth and complete anoxia (O_2 limit) below 10 m depth (Sumner et al., 2015). The oxycline also coincides with an increase in sulfide, dissolved reactive phosphorus (DRP), and ammonium (NH_4N) concentrations into the anoxic zone, from low concentrations in overlying oxic waters. Nitrate as nitrogen (NO_3N) remained at low concentrations at all depths described here (Jungblut et al., 2016; Table 1).

Benthic microbial mats colonize the Lake Fryxell floor. The microbial communities are structured according to local environmental conditions, such as irradiance and oxygenation (Jungblut et al., 2016). While geochemical gradients are steep vertically throughout the water column, the transition from an oxic to anoxic water column intersects the gently sloping lake floor over a relatively long in horizontal distance. Across the lake bottom, phototrophic communities are present at depths of at least 10.5 m (Wharton et al., 1983), with a change in dominant metabolism from oxygenic to anoxygenic photosynthesis occurring below the oxycline. Microbial mat morphologies change considerably across the oxycline: (i) cuspate pinnacle mats are present in the upper hyperoxic zone from approximately 8.8–9.4 m depth, (ii) ridge-pit mats are present immediately above the oxic-anoxic transition from approximately 8.8–9.7 m, and (iii) prostrate mats are present in the upper anoxic zone from approximately 9.6–10.3 m. Flocculent biomass is present below (10.1–11 m) and is defined by a non-cohesive accumulation of dark gray-brown organic material (Jungblut et al., 2016).

Benthic microbial mats typically consist of well-defined zones, shaped by local environmental conditions and microorganisms performing distinct metabolisms. For example, in Lake Vanda, another ice-covered lake in the McMurdo Dry Valleys, the benthic microbial mats contain characteristic pigmented zones that reflect acclimation of cyanobacteria to changing spectral characteristics through the synthesis of particular pigments. As a result, pigmented zones range from orange (carotenoids) to green (phycocyanin) and pink (phycoerythrin; Hawes et al., 2013). The photosynthetic communities may also produce transient microenvironments with O_2 concentrations of ~50 μmol O_2 L^{-1} s^{-1} (Sumner et al., 2015). It is possible that transient suboxic to anoxic environments may also exist within individual mats.

5.2.2 Sample collection

Sampling at Lake Fryxell was conducted in November 2012 (Table 2), as described by Jungblut et al. (2016). Biomass was collected by SCUBA divers, who operated through a single dive hole melted through the ice cover at 77°36.4'S, 163°09.1'E. Benthic microbial mats were sampled at six stations along a benthic transect between 8.9 and 11 m depth (Table 1). Due to the gradual slope of the lake bottom, the horizontal distance sampled was approximately 50 m.

Samples for lipid biomarker analysis were taken with a 38-mm-diameter corer. Individual cores were placed into a 60-ml wide-mouthed bottle underwater, sealed, and returned to the surface. On-site processing involved draining excess water and freezing (-20° C). Upon return to New Zealand, samples were freeze-dried and ground to a fine powder.

Benthic microbial mats of ridge-pit morphology from 9.4 and 9.5 m depth were subsampled immediately following collection and dissected using flame-sterilized blades and forceps. Mats from 9.4 m depth were subsampled according to their distinctively pigmented horizontal top (brown-purple), middle (green), and bottom (beige) layers. Ridge-pit mats from 9.5 m depth were dissected according to mat features: photosynthetic surface (brown-purple), middle (beige), and pit base (dark). Dissected subsamples were rinsed in sterile deionized water, transferred into sterile plastic tubes, and frozen at -20°C until further analysis. Samples were freeze-dried in New Zealand prior to transport for lipid extraction and analysis at MIT.

5.2.3 Lipid extraction and analysis

Microbial biomass was placed in combusted glass centrifuge vials, homogenized and spiked with 40 ng of C16PAF as a recovery standard. Total lipid extracts (TLEs) were obtained by extracting the samples using a modified Bligh and Dyer method (Bligh and Dyer, 1959) as reported by Matys et al. (2017). Dichloromethane (DCM) was used in place of chloroform. Samples were extracted by ultrasonication (30 mins at room temperature) first (2x) using a mixture of methanol/dichloromethane/phosphate buffer solution (2:1:0.8, v/v/v), and then (2x) using a mixture of methanol/dichloromethane/trichloroacetic acid buffer (2:1:0.8, v/v/v). After each extraction, the supernatants were transferred to different separatory funnels (phosphate vs. trichloroacetic acid buffer). Supernatants were then subjected to liquid-liquid extractions using 5mL of dichloromethane and water (1:1). Extracts were not combined until the TCA was removed from the samples, after the liquid-liquid extraction step. The TLEs were kept at -20 °C until analysis.

A fraction of each TLE was acetylated with pyridine/acetic anhydride (1:1, v/v) at 70 °C for 1 h and left at room temperature overnight. The acetylated TLEs were analyzed by high-performance liquid chromatography-atmospheric pressure chemical ionization – mass

spectrometry (HPLC-APCI-MS) as described in Matys et al. (2017). The LC-MS system comprised a 1200 Series HPLC (Agilent Technologies, Santa Clara, CA, USA) equipped with an auto sampler and a binary pump linked to a Q-TOF 6520 mass spectrometer (Agilent Technologies) via an APCI interface operated in positive ion mode. A Poroshell 120 EC-C18 column (2.1 x 150 mm, 2.7 μm; Agilent Technologies) was chosen to provide fast and high-resolution separations of a wide range of small molecules at lower pressures. The column temperature was set at 30°C. The eluent flow remained constant at 0.19 ml/min. Eluent A contained a mixture of methanol: H_2O 95:5 v/v and eluent B comprised pure isopropyl alcohol (IPA). The HPLC gradient was as follows: isocratic flow of 100% eluent A (0-2 mins), a linear gradient from 0-20% of eluent B (2-20 mins), isocratic flow of 20% B (20-30 mins), a linear gradient from 20-30% of eluent B (30-40 mins), a linear gradient from 30-0% B (40-45 mins), isocratic flow of 0% B for 5 minutes. The column was conditioned for 5 minutes of post-run time at 100% A. The APCI parameters were as follows: gas temperature 325 °C, vaporizer temperature 350 °C, drying gas (N_2) flow 6 l/min, nebulizer (N_2) flow 30 l/min, capillary voltage 1200 V, corona needle 4 μA, and fragmentor 150 V.

BHPs were identified on the basis of accurate mass measurements of their protonated molecular ions, fragmentation patterns in MS-MS mode, and by comparison of relative retention times (Talbot et al., 2003, 2007; Welander et al., 2012). Quantification was achieved through an internal standard of 3α,12α-Dihydroxy-5β-pregnan-20-one,3,12-diacetate (PD) and external standard calibration curves of PD and authentic BHT, 2-MeBHT, Diplopterol, 2-MeDiplopterol, and aminotetrol. PD was chosen as an internal standard because of its structural similarity to hopanoids and because it has a retention time that does not overlap with the range of BHPs of interest. Calibrations with authentic BHP standards were necessary to account for variations in ionization efficiencies of different BHPs (Wu et al., 2017).

5.2.4 Loss on ignition

Benthic mat samples from McMurdo Dry Valley lakes have been shown to vary in supplementary constituents, including carbonates and silicates (Mackey et al., 2017), which bias bulk weight. Therefore, all quantitative BHP analysis was normalized to total organic carbon (TOC) measured for each sample. All extracted material was dried, weighed, and combusted at 450 °C for 4 hours in accordance with Mackey et al. (2017).

5.3 Results

5.3.1 Total organic carbon

Bacteriohopanepolyol (BHP) abundances were normalized to total organic carbon (TOC), which was measured for each sample analyzed (Table 2). Mat samples (whole, subsampled, and dissected) from Lake Fryxell were composed of 2.8-25.2% TOC. Generally, TOC in whole mat samples decreased from an average of 20.5% at 9 m depth to 6.6% at 11 m depth. TOC in ridge-pit mat subsamples from 9.4 m depth was high (*mean*= 21%) in top and middle samples and was relatively low in the bottom sample (12.5%). In dissected ridge-pit mat subsamples (surface, middle, and pit base) from 9.5 m, TOC was consistently low, with an average of 4.5% (*SD*= 1.1, *n*= 9).

5.3.2 Bacteriohopanepolyols

Bacteriohopanepolyol abundance

Total BHP, the summed concentration of all BHPs identified, ranged from 21–89 ng BHP/mg TOC in whole mat samples (Fig. 2). Generally, total BHP increased with depth into Lake Fryxell from an average of 24.7 ng/mg (*SD*= 2.7; *n*= 3) at 9 m depth to 74.4 ng/mg (*SD*= 20.1; *n*=2) at 11 m depth. Total BHP in ridge-pit subsamples from 9.4 m depth decreased with depth into the mat structure, from 90.7 ng/mg in the top mat subsample to 48 ng/mg in the middle and bottom subsamples. Total BHP in dissected ridge-pit mat samples from 9.5 m depth also generally decreased with depth into the mat structure, from an average of 31.7 ng/mg (*SD*= 5.9; *n*= 3) in the surface to 14.8 ng/mg (*SD*= 2.8; *n*= 3) in the middle and 18.8 ng/mg (*SD*= 2.5; *n*= 3) in the pit base samples.

Bacteriohopanepolyol diversity

Bacteriohopanepolyol (BHP) diversity in whole benthic mat samples collected between 9.7 and 11 m depth varies with mat morphology (Fig. 2). Five BHP compounds were identified in cuspate pinnacle mats, collected from 9-9.3 m depth in the upper hyperoxic zone. Bacteriohopanetetrol (BHT, **1a;** numbers refer to the structures in Supplementary Fig. 1) and aminobacteriohopanetriol (aminotriol, **1d**) comprised an average of 59% (*SD*= 16.7; *n*=4) and 32.7% (*SD*= 19.4; *n*=4) of total BHPs respectively. Three minor BHP compounds were identified, including a later eluting BHT stereoisomer (BHT II, **1b**), 2-methylbacteriohopanetetrol (2-MeBHT, **2a**), and 3-methylbacteriohopanetetrol (3-MeBHT, **3a**). The BHP profile of one sample from 9 m depth included low relative abundance of two penta-functionalized compounds, as seen in the deeper ridge-pit morphology. The highest diversity of BHP compounds (8) was identified in mats of the ridge-pit morphology at 9.7 m depth, at the oxic-anoxic transition. BHT was the most abundant compound and comprised

68.4% (*SD*= 2.5; *n*= 3) of total BHP. Minor BHP compounds identified included those BHPs identified in pinnacle mats in addition to three penta-functionalized BHP including bacteriohopanepentol (BHpentol, **1c**) and a later eluting isomer (BHpentol II; unknown stereochemistry) and a C-2 methylated variant (2-MeBHpentol, **2c**). BHP diversity decreased below the oxycline (9.8 m), in prostrate and flocculent mat morphologies, which lie in the anoxic zone. Six BHP compounds were identified in prostrate and flocculent mats, including BHT (*mean*= 76.8%; *SD*= 8%; *n*= 4), BHT II, 2-MeBHT, BHpentol, aminotriol, 2-MeBHpentol.

The subsampled ridge-pit mat from 9.4 m depth exhibited the same BHP diversity as whole mat samples from 9.7 m depth, the closest whole mat sample of similar mat morphology (ridge-pit). Compounds identified include BHT, BHT II, 2-MeBHT, 3-MeBHT, BHpentol, BHpentol II, 2-MeBHpentol, and aminotriol (Fig. 3). 3-MeBHT and BHpentol II were not present in the top mat sample, but were present in both the middle and bottom mat samples, accounting for an increase in diversity with depth into the mat structure. BHT accounted for an average of 76.5% of the total BHP (*SD*= 4.2%; *n*=3). BHT II was abundant (17.8% of the total BHP) in the top mat sample and decreased toward the base of the mat (*mean*= 5%; *SD*= 0.7; *n*=2). The relative abundance of 2-MeBHT also decreased with depth into the mat structure, from 5% of the total BHP in the top mat sample to 3.8% and 3.3% in the middle and bottom mat samples, respectively. The relative abundances of 3-MeBHT, BHpentol, BHpentol II, and 2-MeBHpentol all increased with depth into the mat structure, accounting for 0.6% of the total BHP in the top, 2.6% in the middle, and 5.4% in the bottom mat sample. Aminotriol was abundant (11.3% total BHP) in the middle mat sample and averaged 5.3% of the total BHP (*SD*= 0.9%; *n*=2) in the top and bottom mat samples.

The dissected ridge-pit mat from 9.5 m depth contained 7 BHPs, including BHT, BHT II, 2-MeBHT, BHpentol, BHpentol II, and aminotriol (Fig. 4). Unlike whole ridge-pit mat samples from 9.7 m depth, 3-MeBHT was not detected and 2-MeBHpentol was only identified in one middle mat sample. BHP diversity did not vary substantially between dissected ridge-pit subsamples (top, middle, and pit).

5.4 Discussion

5.4.1 Distribution of BHPs in whole mat samples that span the oxic/anoxic transition

BHP profiles (abundance and diversity) of whole benthic microbial mat samples vary with mat morphology and local environmental conditions, which range from oxic (9-9.3 m) to suboxic/anoxic (9.7-11 m) and vary in nutrients available (Table 1). Unlike neighboring Lake

Vanda (Matys et al., *accepted;* Chapter 2), organic matter preserved in benthic microbial mats may not only be produced *in situ*, but may contain some contribution of organic matter from the overlying water column. The Lake Fryxell water column is productive with bacterial concentrations ranging from 1.0-3.8 × 10^8 l^{-1} in the oxic portion of the water column to 20 × 10^8 l^{-1} in anoxic bottom waters (Laybourn-Parry et al., 1996). However, $\delta^{13}C$ compositions of benthic organic matter and particulate organic matter indicate that benthic productivity dominates in in Lake Fryxell at the depths described here (Lawson et al., 2004). As a result, BHP abundance and diversity were generally interpreted as markers of active microbial communities that reflect and respond to local environmental conditions. Still, contributions by particulate organic matter input were considered throughout this study.

We observed an increase in BHP abundance (total BHP) and diversity in whole benthic microbial mat samples with depth into Lake Fryxell, from oxic to suboxic/anoxic environments. Similar trends have been noted in the marine water column through oxygen minimum zones (OMZ; Sáenz et al., 2011; Kharbush et al., 2016; Matys et al., 2017). While BHPs have traditionally been considered most abundant in aerobic bacteria, these results support the current hypothesis that hopanoid producers may be more diverse and abundant in low-oxygen environments than previously thought, and possibly even more abundant than in environments that are well-oxygenated. In fact, this may account for the high diversity of BHPs in the low oxygen depths of Lake Fryxell, as compared to nearby Lake Vanda (Matys et al., *accepted*), which remains well oxygenated throughout the region described. As a result, it is of considerable interest to further investigate the abundance, diversity, distribution, possible biological sources and physiological functions of hopanoids in suboxic/anoxic environments.

It should be noted that organic matter is preferentially preserved in hypoxic environments as a result of decreased rates of remineralization (Jessen et al., 2017), which may account for the increase in BHP abundance in anoxic portions of Lake Fryxell. However, the increase in BHP diversity suggests that additional hopanoid sources also exist within this region.

5.4.2 C-2 methylated hopanoids

2-MeBHPs have been widely applied as biomarkers for cyanobacteria (Summons et al., 1999), although alternative sources have been identified, including diverse α-proteobacteria (Welander et al., 2010; Ricci et al., 2013).

2-MeBHPs have been described as both diverse and abundant in Polar Regions (Talbot et al., 2008; Matys et al., *accepted*). In Lake Vanda, another ice-covered lake in the McMurdo Dry Valleys, 2-MeBHPs amount to >40% of the total BHP (Matys et al., *accepted*). Cyanobacteria were identified as the singular source of 2-MeBHP in Lake Vanda and it was hypothesized that 2-MeBHP were being produced in abundance in response to the low light environment. However, 2-MeBHPs (2-MeBHT and 2-MeBHpentol) account for only 1.5-12.6% of the total BHP in whole mat samples in Lake Fryxell. The relatively low diversity and abundance of 2-MeBHP in Lake Fryxell as compared to Lake Vanda may be due to differences in cyanobacteria abundance or an abundance of other BHPs. Approximately 3% of surface irradiance is transmitted through the ice cover in Lake Fryxell (Jungblut et al., 2016) as compared to 15-20% transmittance in Lake Vanda (Howard-Williams, 1998; Hawes and Schwarz, 2000), creating a very different habitat for photosynthetic communities. However, cyanobacteria such as *Leptolyngbya* and *Phormidium* are abundant in Lake Fryxell and are known hopanoid-producers. For example, the surfaces of ridge-pit mats contain high abundances (absolute and relative) of 2-MeBHP and are dominated by *Leptolyngbya.* The decrease in 2-MeBHP with depth into the mat follows changes in the relative abundance of cyanobacteria (Dillon, 2018).

Alphaproteobacteria are also potential contributors to 2-MeBHP inventories in Lake Fryxell. For instance, 2-MeBHPs are abundant in flocculent mat samples (10.6 and 11 m depth), which do not contain cyanobacteria as a result of irradiance limitation (Sumner et al., 2015; Jungblut et al., 2016). Alternatively, a pelagic source of 2-MeBHP cannot be ruled out.

5.4.3 C-3 methylated hopanoids

3-MeBHT was the only C-3 methylated hopanoid identified in Lake Fryxell. 3-MeBHT has been used as a biomarker for aerobic methanotrophs and aerobic acetic acid bacteria (Zundel and Rohmer 1985), although alternative sources have been identified (Welander and Summons, 2012), including diverse Proteobacteria (α-, β-, and γ-Proteobacteria), which are abundant throughout Lake Fryxell (Dillon, 2018).

Aerobic methanotrophs (*Methylococcus calpsulatus* and *Methylomicrobium alcaliphilum* and *album*) and aerobic acetic acid bacteria (*Acetobacter aceti, tropicalis, pomorum,* and *pasteurianus*) known to contain the gene required for C-3 methylation of hopanoids (*hpnR*; Welander and Summons, 2012) have not been identified in Lake Fryxell (Dillon, 2018). However, HpnR sequences have been identified in *Frankia* (2 sp.) and

Burkholderia (3 sp.; Welander and Summons, 2012). Frankia have been identified in mat subsamples (top, middle, and bottom) collected from 9.0 and 9.3 m depth and Burkholderia have been identified in mat subsamples (top, middle, and bottom) collected from 9.0 m depth in Lake Fryxell (Dillon, 2018). The relative abundance of *Frankia*, *Burkholderia* and 3-MeBHT increase with depth into mats analyzed. This relationship suggests that 3-MeBHT is produced at least in part by *Frankia* and *Burkholderia* in oxic portions of Lake Fryxell. However, neither *Frankia* nor *Burkholderia* were identified in anoxic portions of Lake Fryxell (9.8 m sample; Dillon, 2018), which implies that other sources of 3-MeBHT are likely in anoxic samples described here.

5.4.4 Penta-functionalized hopanoids

Penta-functionalized BHPs (BHpentol, BHpentol II, and 2-MeBHpentol) vary significantly among mat morphologies with clear differences between mats in the oxic and anoxic portion of Lake Fryxell. BHpentol and 2-MeBHpentol are typically associated with cyanobacteria (Bisseret et al., 1985; Zhao et al., 1996) and as a result, should decrease with depth into Lake Fryxell as the abundance of cyanobacteria decreases (Dillon, 2018). BHpentol II is only present in oxic portions of Lake Fryxell. However, BHpentol and its C-2 methylated counterpart, 2-MeBHpentol, are most abundant in the suboxic to anoxic portion of the lake. The relative abundances of BHpentol and 2-MeBHpentol also increase with depth into the subsampled mat structure from 9.4 m, to greatest concentrations where cyanobacteria and O_2 would be lowest. Similar trends in penta-functionalized BHP have been noted in marine oxygen minimum zones (Sáenz et al., 2011), where BHpentol is most abundant below the oxic-anoxic transition. It is possible that penta-functionalized BHPs have a greater diversity of source organisms than previously thought, or are produced in response to environmental conditions, such as low light (as described in Chapter 3) and oxygen. However, studies that further examine the physiological role of penta-functionalized BHP must be performed in order to test this hypothesis.

5.4.5 BHT stereoisomer (BHT II)

BHT II has been proposed as a biomarker for anaerobic ammonium oxidation (anammox) bacteria (Rush et al., 2014). Additionally, the BHT II ratio (BHT II/total BHT) has been used as a proxy for suboxic to anoxic conditions, such as those associated with marine oxygen minimum zones (OMZs; Sáenz et al., 2011). In characterizing the relative contribution of BHT II in respect to the earlier eluting isomer (BHT), it is possible to compare a wide range

of environments with variable productivity and preservation potential. We describe the abundance of BHT II and local environmental conditions in order to consider BHT II source organisms in Lake Fryxell. We also compare BHT II ratio values from Lake Fryxell and marine OMZ systems to investigate implications of .

The greatest abundance of BHT II was detected in whole mat samples from the oxycline, where O_2 is <10 μmol/kg and NH_4^+ is present (8 μg/L). This result agrees with previous studies that describe the highest abundances of anammox bacteria and BHT II at marine oxygen minimum zones (e.g. Matys et al., 2017). The presence of BHT II in benthic microbial mats underlying an oxic water column (9.0 and 9.3 m) may be due to the formation of seasonally suboxic to anoxic microenvironments within the mats. However, the detailed oxygen structures of individual Lake Fryxell microbial mat environments not been investigated although a previous study described pervasive oxygenation (Sumner et al., 2015), especially at the mat surface, where BHT is most abundant in mats from 9.4 m depth. If suboxic microenvironments were present below the mat surface, anammox could persist albeit limited by nitrogen (NO_2^- and NH_4^+), if present in very low concentrations due to nutrient recycling. As a result, BHT II would be present but in very low abundance (0.5-1.0ng/mg), as seen in whole mat samples from 9.0 and 9.3 m.

It is not possible to rule out alternative sources of BHT II. Isomers of BHT have also been reported in non-marine environments. For example, an isomer of BHT was detected in a stratified mat from a hypersaline lake and tentative sources of α-Proteobacteria or acetic acid bacteria were reported (Blumenberg et al., 2013). Proteobacteria are abundant in Lake Fryxell (Dillon, 2018). However, the putative sources which include the purple non-sulfur bacterium *Rhodopseudomonas acidophila* (Neunlist et al., 1988) and acetic acid bacteria (Peiseler and Rohmer, 1992; e.g. *Acetobacter* spp.) have not been identified in the lake. An isomer of BHT has also been reported in *Frankia* sp. a terrestrial nitrogen-fixing plant symbiont (Rosa-Putra et al., 2001) and an aerobic Type II methanotrophic bacteria (*Methylocella palustris*; van Winden et al., 2012). *Frankia* sp. has been identified in Lake Fryxell (Dillon, 2018) at 9.0 and 9.3 m. However, the relative abundance of *Frankia* sp. increases with depth into the mats as compared to the relative abundance of BHT II, which decreases with depth into mats from 9.4 m.

It is also not possible to exclude seasonal anammox activity in the water column and subsequent deposition of BHT II to benthic microbial mats. However, the abundance of BHT II measured below the O_2 limit in flocculent mats (*mean*= 2.6 ng/mg) would likely be similar

to higher values measured near the O_2 limit in ridge-pit and prostrate mats (*mean*= 3.8 ng/mg) due to the production and export of the same signature to depth. While in marine OMZ systems BHT II abundance decreases below the oxycline due to the recycling of sinking organic matter (Matys et al., 2017), this is not likely over short (1.1 m) distances described here.

These results, which identify the highest BHT II concentrations at depths where anammox bacteria are likely to persist (low O_2, high NH_4^+), suggest that anammox bacteria is at least one of the sources of BHT II in benthic microbial mats in Lake Fryxell. that being the case, this study corroborates the use of BHT II as a biomarker for anammox bacteria in geological archives. Since the biosynthetic pathway of BHT II has yet to be elucidated, it is not possible to unambiguously state that anammox bacteria are a source of BHT II in Lake Fryxell or that any other BHT II producers exist. Metagenomic data for Lake Fryxell mats are available (Dillon, 2018) and may be further investigated when the biosynthetic pathway for BHT II is determined.

In order to extend the interpretation of BHT II as a proxy for marine oxygen minimum zones (OMZ) it is imperative that we consider the BHT II ratio, as previously described. The average BHT II ratio in cuspate pinnacle mats collected from 9-9.3 m depth in the upper oxic zone (Fig. 2) was 0.044 (*SD*= 0.003; *n*= 4). The BHT II ratio increased with depth as oxygen content decreases. Consistent with previous studies of BHT II in marine oxygen minimum zones (OMZ; Sáenz et al., 2011; Wakeham et al., 2012; Matys et al., 2017), the highest value (*mean*= 0.098; *SD*= 0.009; *n*= 3) was identified at the chemocline, immediately above the oxic-anoxic transition (approx. 9.8 m) and where NH_4 becomes available (8-13 µg/L), in mats of the ridge-pit morphology at 9.7 m depth. The BHT II ratio remained elevated in the upper anoxic zone (9.9 m; *mean*= 0.094; *SD*= 0.017; *n*= 3) before decreasing (*mean*= 0.043; *SD*= 0.008; *n*= 5) in the flocculent mat (10.6- 11 m depth).

Compared to OMZ systems, the BHT II ratios described here (0.03-0.11) are very low (Fig. 5). This is likely due to the dilution of the BHT II signal in benthic microbial mats in Lake Fryxell by an abundance of organisms that produce BHT. Anammox bacteria in Lake Fryxell are likely limited by seasonal changes in O_2 concentration and NH_4^+. However, it is difficult to compare the absolute abundances of BHP in these environments due to inconsistencies in sampling procedures (ng BHP/mg TOC vs. ng BHP/L). Nevertheless, even the highest BHT II ratio values measured in Lake Fryxell (0.2) are substantially lower than BHT II ratio values measured in modern OMZ systems (Sáenz et al., 2011; Matys et al., 2017; Fig. 5) which are often 0.6-0.8. As a result, we suggest that the presence of BHT II may indicate anammox activity, while only BHT II ratio values ≥0.3 may reflect OMZ influence.

5.5 Conclusions

We have observed a high abundance and diversity of bacteriohopanepolyols in benthic microbial mats from Lake Fryxell, an ice-covered lake in the McMurdo Dry Valleys, Antarctica. This study contributes to the dearth of BHP research in Polar Regions and corroborates biomarkers developed in low-latitude environments. BHP diversity varies with benthic microbial mat morphology, with significant differences between those mat morphologies present in oxic and suboxic/anoxic environments. Of particular interest is the presence of bacteriohopanetetrol isomer (BHT II). The BHT II ratio (BHT II/total BHT) has been proposed as a proxy for past changes in the relative importance of anammox and fluctuations in nitrogen cycling in response to ocean redox changes through the geological record. Our results suggest that the presence of BHT II in benthic microbial mats may indicate the presence of anammox bacteria although additional sources may be possible. However, BHT II ratios <0.3 may suggest the presence of anammox bacteria in benthic microbial mats or sediments while values >0.3 may indicate influence from marine oxygen minimum zones and other environments supporting intense anammox activity.

5.6 Acknowledgements

We would like to acknowledge the United States Antarctic Program and Antarctica New Zealand for logistical support.

5.7 Funding

The collection of field data was supported by the National Science Foundation Division of Polar Programs (grant number 1115245), the McMurdo Long Term Ecological Research project. Work undertaken at MIT was supported by an award (NNA13AA90A) from the NASA Astrobiology Insitute. DYS and TM were supported by NASA Astrobiology through grant NN13AI60G. EDM and RES also thank the MIT-NZ MISTI Global Seed Funds grant program for additional support.

5.8 References

Bisseret, P., Zundel, M., Rohmer, M., 1985. Prokaryotic triterpenoids 2. 2β -Methylhopanoids from Methylobacterium organophilum and Nostoc muscorum, a new series of prokaryotic triterpenoids. European Journal of Biochemistry 150, 29– 34.

Bligh, E.G., Dyer, W.J., 1959. A rapid method of total lipid extraction and purification. Canadian Journal of Biochemistry and Physiology 37, 911–917.

Blumenberg, M., Berndmeyer, C., Moros, M., Muschalla, M., Schmale, O., Thiel, V., 2013. Bacteriohopanepolyols record stratification, nitrogen fixation and other biogeochemical perturbations in Holocene sediments of the central Baltic Sea. Biogeosciences 10, 2725–35.

Brocks, J.J., Pearson, A., 2005. Building the Biomarker Tree of Life. Reviews in Mineralogy and Geochemistry 59, 233-258.

Castañeda, I.S., Schouten, A., 2011 A review of molecular organic proxies for examining modern and ancient lacurine environments. Quaternary Science Reviews 1-41.

Cooke, M.P., Talbot, H.M., Farrimond, P., 2008. Bacterial populations recorded in bacteriohopanepolyol distributions in soils from Northern England. Organic Geochemistry, 39, 1347–1358.

Cook, M.P., van Dongen, B.E., Talbot, H.M., Semiletov, I., Shakhova, N., Guo, L., Gustafsson, Ö., 2009. Bacteriohopanepolyol biomarker composition of organic matter exported to the Arctic Ocean by seven of the major Arctic rivers. Organic Geochemistry 40, 1151-1159.

Dillon, M., 2018. The phylogenetic metabolic structure of the benthic microbial mats in Lake Fryxell, Antarctica: Effects of photosynthetically active radiation and oxygen concentration. Ph.D. Dissertation, University of California Davis

Fischer, W.W., Summons, R.E., Pearson, A., 2005. Targeted genomic discovery of biosynthetic pathways: anaerobic synthesis of hopanoids by Geobacter sulfurreducens. Geobiology 3, 33-40.

Hawes, I., Schwarz, A.–M., 2000. Absorption and utilization of irradiance by cyanobacterial mats in two ice-covered Antarctic lakes with contrasting light climates. Journal of Phycology 37, 5-15.

Howard-Williams, C., Schwarz, A.-M., Hawes, I., Priscu, J.C., 1998. Optical properties of the McMurdo Dry Valley lakes, Antarctica. Antarctic Research Series 72, 189-203.

Jessen, G.L., Lichtschlag, A., Ramette, A., Pantoja, S., Rossel, P.E., Schubert, C.J., Struch, U., Boetius, A., 2017. Hypoxia causes preservation of labile organic matter and changes seafloor microbial community composition (Black Sea). Science Advances 3:e1601897.

Jungblut, A.D., Hawes, I., Mackey, T.J., Krusor, M., Doran, P.T., Sumner, D.Y., … Goroncy, A.K., 2016. Microbial Mat Communities along an Oxygen Gradient in a Perennially Ice-Covered Antarctic Lake. Applied and Environmental Microbiology 82, 620-630.

Kharbush, J.J., Ugalde, J.A., Hogle, S.L., Allen, E.E., Aluwihare, L.I., 2013. Composite bacterial hopanoids and their microbial producers across oxygen gradients in the water column of the California Current. Appl Environ Microbiol 79:7491– 7501.

Lawson, J., Doran, P.T., Kenig, F., Des Marais, D.J., Priscu, J.C., 2004. Stable carbon and nitrogen isotopic composition of benthic and pelagic organic matter in lakes of the McMurdo Dry Valleys, Antarctica. Aquatic Geochemistry 10, 269-301.

Laybourn-Parry, J., James, M.R., McKnight, D.M., Priscu, J., Spaulding, A.S., Shield, R., 1996. The microbial plankton of Lake Fryxell, southern Victoria Land, Antarctica during the summers of 1992 and 1994. Polar Biology 17, 54-61.

Mackey, T.J., Sumner, D.Y., Jungblut, A.D., 2017. Morphological signatures of microbial activity across sediment and light microenvironments of Lake Vanda, Antarctica. Sedimentary Geology 361, 82-92.

Matys, E.D., Sepúlveda, J., Pantoja, S., Lange, C.B., Caniupan, M., Lamy, F., Summons, R.E., 2017. Bacteriohopanepolyols along redox gradients in the Humboldt Current System off northern Chile. Geobiology 15, 844-857.

Matys, E.D., Mackey, T., Grettenberger, C., Mueller, E., Sumner D.Y., Hawes, I., Summons, R.E. submitted. Bacteriohopanepolyols in benthic microbial mats across environmental gradients in Lake Vanda, Antarctica. Geobiology.

Pearson, A., Page, S.R.F., Jorgenson, T.L., Fischer, W.W., Higgins, M.B., 2007. Novel hopanoid cyclases from the environment. Environ. Microbiology 9, 2175–88

Pearson, A., Rusch, D.B., 2009. Distribution of microbial terpenoid lipid cyclases in the global ocean metagenome. ISME Journal 3, 352–363.

Peiseler, B. and Rohmer, M. (1992) Prokaryotic triterpenoids of the hopane series. Bacteriohopanetetrols of new side-chain configuration from Acetobacter species. Journal of Chemical Research, 288-289.

Peters, K.E., Moldowan, J.M., Walters, C.C., 2005. Biomarkers and Isotopes in the Environment and Human History. Cambridge, UK: Cambridge Univ. Press

Rashby, S.E., Sessions, A.L., Summons, R.E., Newman, D.K. 2007 Biosynthesis of 2-methylbacteriohopanepolyols by an anoxygenic phototroph. PNAS 104, 15099-15104.

Ricci, J.N., Coleman, M.L., Welander, P.V., Sessions, A.L., Summons, R.E., Spear, J.R., Newman, D.K., 2014. Diverse capacity for 2-methylhopanoid production correlates with a specific ecological niche. The ISME Journal 8, 675–684.

Ricci, J.N, Michel, A.J., Newman, D.K., 2015. Phylogenetic analysis of HpnP reveals the origin of 2-methylhopanoid production in Alphaproteobacteria. Geobiology 13, 267–77.

Ricci, J.N., Morton, R., Kulkarni, G., Summers, M.L., Newman, D.K., 2017. Hopanoids play a role in stress tolerance and nutrient storage in the cyanobacterium Nostoc punctiforme. Geobiology 15, 173-183.

Rohmer, M., Bouvier-Nave, P., Ourisson, G., 1984. Distribution of hopanoid triterpenes in prokaryotes. Journal of General Microbiology 130, 1137–1150.

Rush, D., Sinninghe Damsté, J.S., Poulton, S. W., Thamdrup, B., Garside, A.L., Acuña González, J., ... Talbot, H.M., 2014. Anaerobic ammonium-oxidising bacteria: A biological source of the bacteriohopanetetrol stereoisomer in marine sediments. Geochimica et Cosmochimica Acta 140, 50-64.

Sáenz, J.P., Wakeham, S.G., Eglinton, T.I., Summons, R.E., 2011. New constraints on the provenance of hopanoids in the marine geologic record: Bacteriohopanepolyols in marine suboxic and anoxic environments. Organic Geochemistry 42, 1351-1362.

Sumner, D.Y., Hawes, I., Mackey, T., Jungblut, A.-D., Doran, P.T., 2015. Antarctic microbial mats: A modern analog for Archean lacustrine oxygen oases. Geology 43, 887-890.

Sumner, D.Y., Hawes, I., Andersen, D.T., Jungblut, A.-D., Mackey, T., Wall, K., 2016. Growth model for microbial pinnacles in Lake Vanda, Antarctica. Geobiology 14, 556-574.

Talbot, H.M., Watson, D.F., Murrell, J.C., Carter, J.F., Farrimond, P., 2001. Analysis of intact bacteriohopanepolyols from methanotrophic bacteria by reversed-phase high-performance liquid chromatography-atmospheric pressure chemical ionization mass spectrometry. Journal of Chromatography A 921, 175-185.

Talbot, H.M., Summons, R.E., Jahnke, L., Farrimond, P., 2003. Characteristic fragmentation of bacteriohopanepolyols during atmospheric pressure chemical ionisation liquid chromatography/ion trap mass spectrometry. Rapid Communications in Mass Spectrometry 17, 2788-2796.

Talbot, H.M., Rohmer, M., Farrimond, P., 2007. Structural characterization of unsaturated bacterial hopanoids by atmospheric pressure chemical ionization liquid chromatography/ion trap mass spectrometry. Rapid Communications in Mass Spectrometry 21, 1613-1622.

Talbot, H.M., Summons, R.E., Jahnke, L.L., Cockell, C.S., Rohmer, M., Farrimond, P., 2008. Cyanobacterial bacteriohopanepolyol signatures from cultures and natural environmental settings. Organic Geochemistry 39, 232-263.

Vincent, W.F., 1982. Production strategies in Antarctic inland waters: phytoplankton eco-physiology in a permanently ice-covered lake. Ecology 62, 1215–1224.

Wakeham, S.G., Turich, C., Schubotz, F., Podlaska, A., Li, X.N., Varela, R., ... Hinrichs, K.-U., 2012. Biomarkers, chemistry and microbiology show chemoautotrophy in a multilayer chemocline in the Cariaco Basin. Deep-Sea Research I 63, 133-156.

Welander, P.V., Coleman, M., Sessions, A.L., Summons, R.E., Newman, D.K., 2010. Identification of a methylase required for 2-methylhopanoid production and implications for the interpretation of sedimentary hopanes. PNAS 107, 8537–8542.

Welander, P.V., Doughty, D.M., Wu, C.-H., Mehay, S., Summons, R.E., Newman, D.K., 2012. Identification and characterization of Rhodopseudomonas palustris TIE-1 hopanoid biosynthesis mutants. Geobiology 10, 163-177.

Welander, P.V., Summons, R.E., 2012. Discovery, taxonomic distribution, and phenotypic characterization of a gene required for 3-methylhopanoid production. PNAS 109, 12905-12910.

Wharton, R.A.Jr., Parker, B.C., Simmons, G.M., 1983. Distribution, species composition and morphology of algal mats in Antarctic dry valley lakes. Phycologia 22, 355-365.

Wu, C.-H., Kong, L., Bialecka-Fornal, M., Park, S., Thompson, A.L., Kulkarni, G., … Newman, D.K., 2015 Quantitative hopanoid analysis enables robust pattern detection and comparison between laboratories. Geobiology 13, 391–407.

Zhang, L., Jungblut, A.D., Hawes, I., Andersen, D.T., Sumner, D.Y., Mackey, T.J., 2015. Cyanobacterial diversity in benthic mats of the McMurdo Dry Valley Lakes, Antarctica. Polar Biology 38, 1097-1110.

Zhao, N., Berova, N., Nakanishi, K., Rohmer, M., Mougenot, P., Ju¨rgens, U.J., 1996. Structures of two bacteriohopanoids with acyclic pentol side-chains from the cyanobacterium Nostoc PCC 6720. Tetrahedron 52, 2777–2788.

Zundel, M., Rohmer, M., 1985. Prokaryotic triterpenoids. 3. The biosynthesis of 2 β-methylhopanoids and 3 β-methylhopanoids of Methylobacterium organophilum and Acetobacter pasteurianus ssp. pasteurianus. Eur J Biochem 150, 35–39.

5.9 Figures

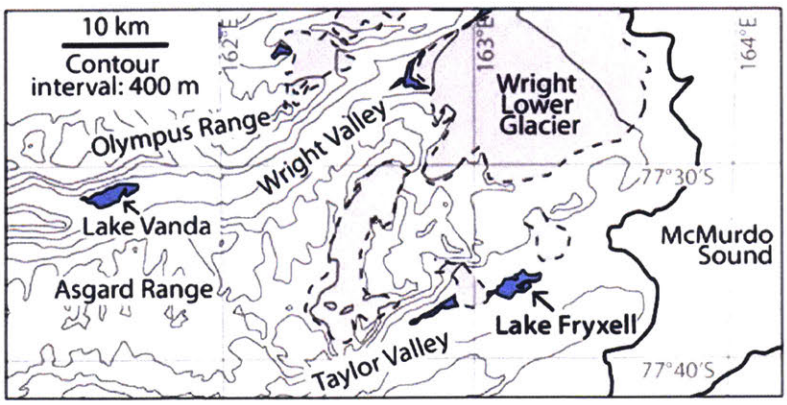

Figure 1. Map of the McMurdo Dry Valleys, including Lake Fryxell

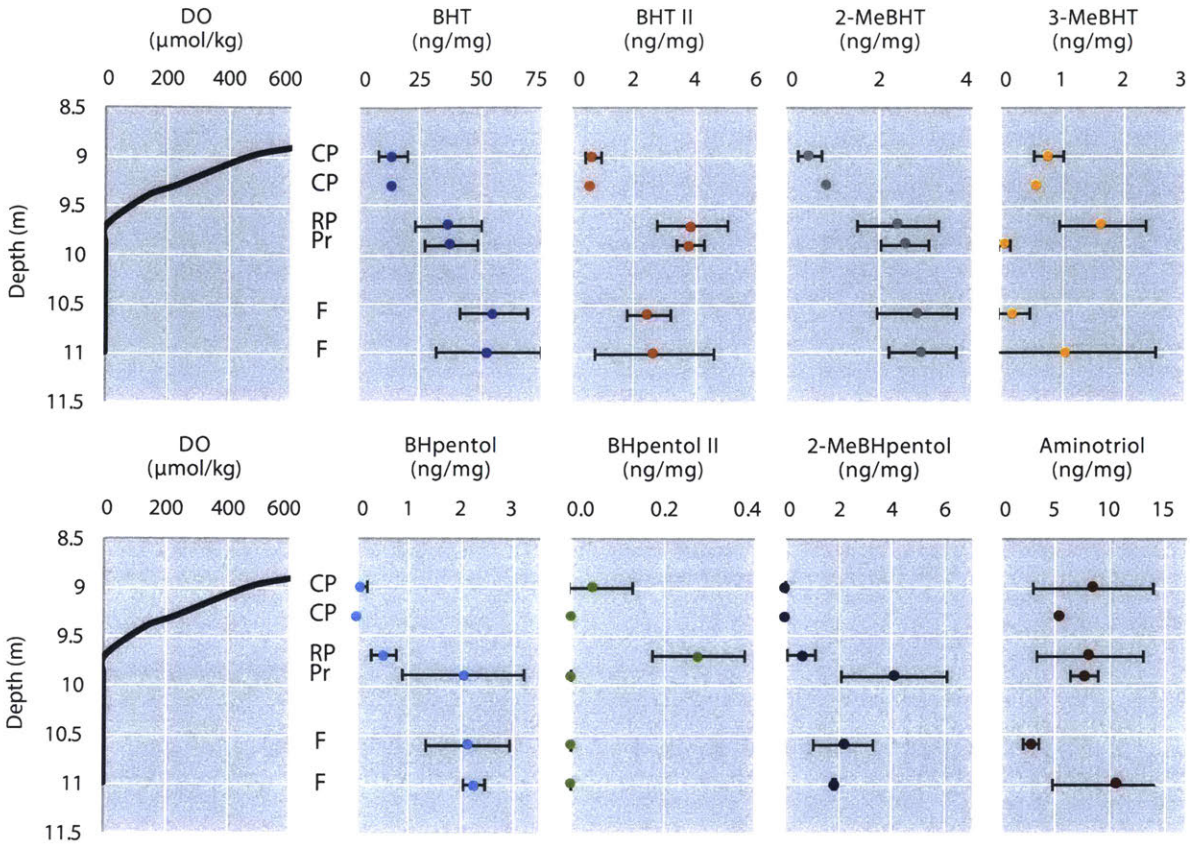

Figure 2. Dissolved oxygen (DO) profiles and corresponding mat morphologies (CP: cuspate pinnacles; RP: ridge-pit; Pr: prostrate; F: floculent) and bacteriohopanepolyols (BHPs; ng BHP/mg total organic carbon) in whole mat samples in Lake Fryxell, Antarctica. Error bars indicate ±1 standard deviation.

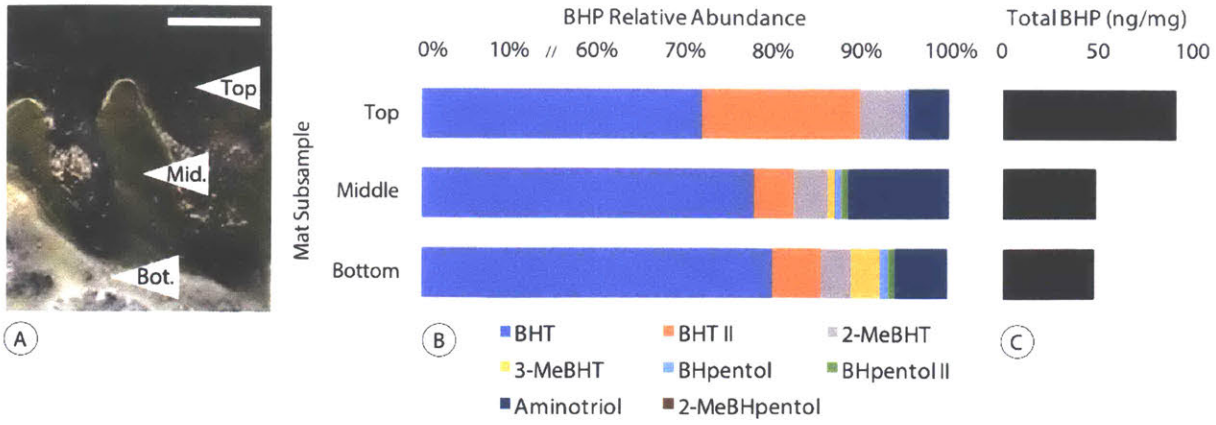

Figure 3. Relative abundance (B) of bacteriohopanepolyols (BHP) and total BHP (C) in ridge-pit benthic microbial mats (A) from 9.4 m depth in Lake Fryxell, Antarctica. White arrows indicate pigmented zones sampled for analysis: Top, Middle (Mid.), and Bottom (Bot.). Scale bar signifies 10 mm.

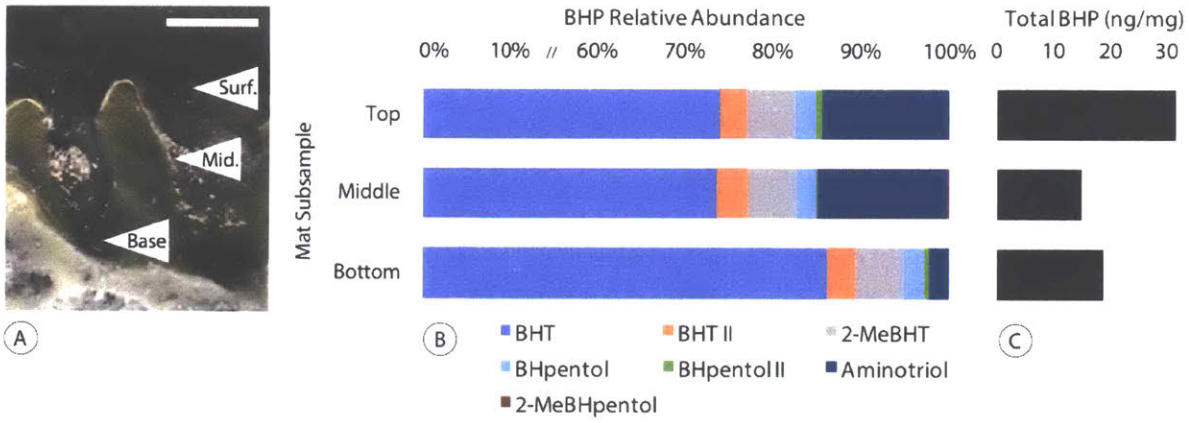

Figure 4. Relative abundance (B) of bacteriohopanepolyols (BHP) and total BHP (C) in ridge-pit benthic microbial mats (A) from 9.5 m depth in Lake Fryxell, Antarctica. White arrows indicate mat features sampled for analysis: photosynthetic upper surface (Surf.), dark pigmented base (Base), and beige material in between (Mid.). Scale bar signifies 10 mm.

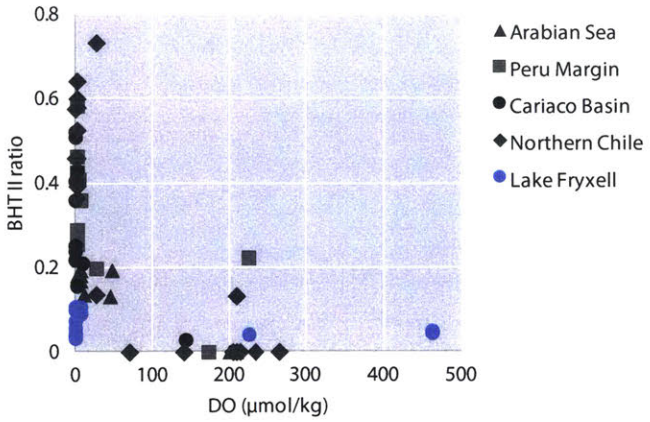

Figure 5. Bacteriohopanetetrol (BHT) II ratio (BHT/BHT + BHT II) vs. dissolved oxygen (DO) concentration measured in marine oxygen minimum zones (Arabian Sea, Peru Margin, Cariaco Basin, and Northern Chile) and Lake Fryxell, Antarctica (adapted from Matys et al., 2017.

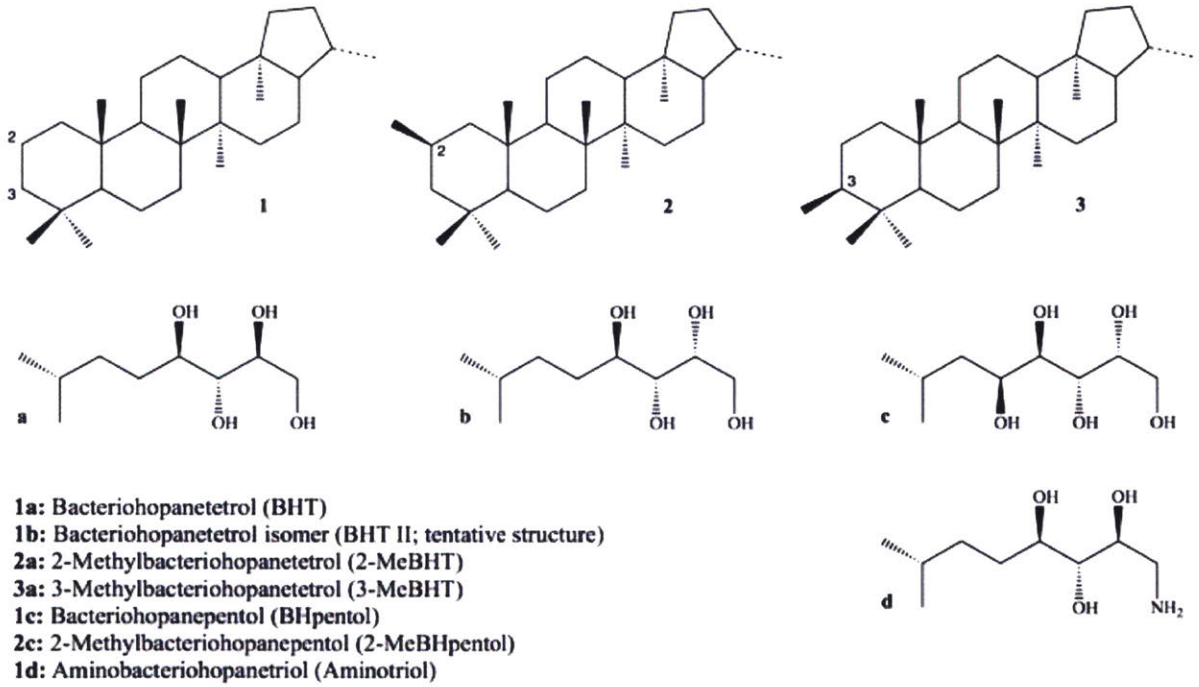

1a: Bacteriohopanetetrol (BHT)
1b: Bacteriohopanetetrol isomer (BHT II; tentative structure)
2a: 2-Methylbacteriohopanetetrol (2-MeBHT)
3a: 3-Methylbacteriohopanetetrol (3-MeBHT)
1c: Bacteriohopanepentol (BHpentol)
2c: 2-Methylbacteriohopanepentol (2-MeBHpentol)
1d: Aminobacteriohopanetriol (Aminotriol)

Supplementary Figure 1. Bacteriohopanepolyols identified in this study. The illustrated stereochemistry for BHT II is tentative, based on Peiseler and Rohmer (1992).

5.10 Tables

Table 1. Environmental conditions in Lake Fryxell (from Jungblut et al., 2016)

DEPTH (m)	EC (mS/cm)	DO (mg/L)	DO (µmol/kg)	IRRADIANCE (% surface)	pH	DIC (mg/L)	DRP (µg/L)	NH4N (µg/L)	NO2+NO3N (µg/L)
8.9	2.98	20.4	622	0.74	7.5	15.5	2	<1	1
9	3.04	15.2	463	0.82	7.47	14.4	2	<1	1
9.3	3.15	7.4	226	0.44	7.46	16.1	1	<1	1
9.4	3.33	4.5	137	0.36	7.44	18	2	<1	1
9.7	3.54	0.2	6	0.26	7.48	20.2	3	8	1
9.9	3.61	0	0	0.27	7.49	20.9	3	13	1
10.2	3.9	0	0	0.22	7.47	21.6	39	100	1
10.6	4.25	0	0	0.18	7.51	23.2	53	120	1
11	4.61	0	0	0.12	7.52	26	70	280	2

EC: electrical conductivity; DO: dissolved oxygen; DIC: dissolved inorganic carbon; DRP: dissolved reactive phosphorus
<1: below limit of detection

Table 2. Bacteriohopanepolyols identified in benthic microbial mats from Lake Fryxell, Antarctica.

MAT MORPHOLOGY		DEPTH (m)	TOC (%)	BHT 655.49 (ng/mg)	BHT II 655.49 (ng/mg)	2-MeBHT (ng/mg)	3-MeBHT (ng/mg)	BHpentol (ng/mg)	BHpentol II (ng/mg)	Aminotriol (ng/mg)	2-MeBHpentol (ng/mg)	*TOTAL (ng/mg)*
WHOLE MAT SAMPLES												
Cuspate pinnacles		9	25.2	9.9	0.5	0.3	0.6	0.0	0.0	10.3	0.0	*21.6*
Cuspate pinnacles		9	22.0	11.7	0.5	0.4	0.6	0.0	0.0	12.8	0.0	*26.1*
Cuspate pinnacles		9	14.4	21.0	1.0	0.8	1.0	0.2	0.1	2.2	0.0	*26.4*
Cuspate pinnacles		9.3	19.3	13.6	0.6	0.9	0.6	0.0	0.0	5.4	0.0	*21.0*
Ridge-pit		9.7	10.4	21.2	2.6	1.4	0.9	0.4	0.2	2.6	0.5	*29.7*
Ridge-pit		9.7	8.6	46.6	4.8	2.8	1.7	0.8	0.4	11.4	1.2	*69.5*
Ridge-pit		9.7	12.9	42.3	4.3	3.0	2.3	0.4	0.3	10.5	0.2	*63.2*
Prostrate		9.9	8.2	28.0	3.3	2.0	0.0	1.2	0.0	8.8	2.6	*46.0*
Prostrate		9.9	4.4	49.4	4.0	3.0	0.2	3.4	0.0	8.1	6.3	*74.3*
Prostrate		9.9	7.4	36.9	4.1	2.6	0.0	1.5	0.0	6.3	3.3	*54.8*
Floculent		10.6	8.0	40.2	1.9	1.9	0.0	1.5	0.0	3.6	1.4	*50.4*
Floculent		10.6	8.2	59.1	2.4	3.2	0.5	1.9	0.0	2.1	1.7	*70.8*
Floculent		10.6	8.3	67.4	3.2	3.5	0.1	3.0	0.0	2.8	3.5	*83.5*
Floculent		11	5.7	38.0	1.3	2.4	0.0	2.1	0.0	14.6	1.8	*60.2*
Floculent		11	7.4	68.3	4.0	3.5	2.1	2.4	0.0	6.5	1.9	*88.7*
SUBSAMPLED PROSTRATE MAT												
Prostrate	Top	9.4	21.1	65.2	16.1	4.7	0.0	0.4	0.0	4.2	0.2	*90.7*
Prostrate	Middle	9.4	20.8	37.6	2.2	1.8	0.3	0.4	0.4	5.5	0.1	*48.3*
Prostrate	Bottom	9.4	12.5	38.2	2.6	1.6	1.5	0.5	0.4	2.8	0.2	*47.7*
DISSECTED HONEYCOMB STRUCTURE												
Ridge-pit	Top	9.5	3.3	19.7	0.9	1.5	0.0	0.6	0.2	4.1	0.0	*27.0*
Ridge-pit	Top	9.5	6.2	25.9	1.1	2.0	0.0	0.7	0.3	8.3	0.0	*38.4*
Ridge-pit	Top	9.5	5.1	24.8	0.9	1.8	0.0	0.8	0.3	1.1	0.0	*29.7*
Ridge-pit	Middle	9.5	4.5	11.6	0.5	0.8	0.0	0.3	0.0	0.5	0.0	*13.7*
Ridge-pit	Middle	9.5	3.8	12.0	0.6	1.0	0.0	0.4	0.1	3.8	0.1	*18.0*
Ridge-pit	Middle	9.5	2.8	9.1	0.5	0.6	0.0	0.2	0.0	2.3	0.0	*12.7*
Ridge-pit	Pit	9.5	3.3	18.4	0.8	1.3	0.0	0.5	0.2	0.4	0.0	*21.5*
Ridge-pit	Pit	9.5	6.2	16.0	0.5	1.0	0.0	0.4	0.0	0.3	0.0	*18.2*
Ridge-pit	Pit	9.5	5.1	14.2	0.5	0.9	0.0	0.4	0.1	0.5	0.0	*16.6*

TOC: total organic carbon

Chapter 6.

Concluding Remarks

This thesis describes advances in bacterial membrane lipid biomarker research through the investigation of environmental controls on the distribution of bacteriohopanepolyols (BHPs). Chapters 2-5 of this thesis discuss the application of BHPs and their stable degradation products, hopanes, as valuable phylogenetic and environmental biomarkers.

Findings from Chapters 2 and 3 consider the production of 2-methylhopanoids (2-MeBHP) by cyanobacteria and implications for the interpretation of 2-methylhopanes in the rock record. Chapter 2 describes the abundance and diversity of 2-MeBHP in ice-covered Lake Vanda, Antarctica. The results of this study suggest that cyanobacteria, the sole source of 2-MeBHP in Lake Vanda, produce 2-MeBHP in abundance, possibly in response to this low light environment. For example, the relative abundance of 2-MeBHP (i) increased with depth into benthic microbial mats where irradiance decreased and (ii) is inversely correlated with photosynthetically active radiation in isolated mat layers across a shading gradient, where other environmental parameters would have varied only slightly. This correlative data was further investigated in Chapter 3. Chapter 3 describes the production of 2-MeBHP over des-methyl counterparts in response to photosynthetic stress (limited diurnal light duration) in two types of filamentous cyanobacteria, *Phormidium luridum* and *Nostoc punctiforme*. *P. luridum* likely employed 2 strategies for adjusting membrane lipid composition in response to photosynthetic stress, including the modification of pre-existing lipid structures and *de novo* synthesis. Surprisingly, *N. punctiforme* did not differentiate into akinetes, known to produce an abundance of 2-MeBHP as the light duration approached limiting values. As a result, we conclude that decreased light cycles result in the modification of vegetative cell membrane lipids to include a higher abundance of 2-MeBHP in relation to their desmethyl counterparts, as seen in *P. luridum*. When unable to produce 2-MeBHP, *N. punctiforme hpnP* mutants produce an abundance of two isomers of bacteriohopanepentol (BHpentol). While structurally dissimilar, 2-MeBHPs and BHpentol may perform similar functions in adapting to environmental stressors, such as photosynthetic light limitation. Although 2-MeBHP localization has been addressed in vegetative cells of *N. punctiforme*, we suggest that future studies isolate and characterize the hopanoid contents of cytoplasmic, thylakoid, and outer

membrane fractions of *Phormidium luridum* in order to further examine the role of 2-MeBHP in a comprehensive suite of cyanobacteria.

Chapters 4 and 5 discuss the distribution of BHPs across oxic/anoxic transitions in a marine oxygen minimum zone and an ice-covered lake in Antarctica. An isomer of bacteriohopanetetrol (BHT II) has been associated with anaerobic ammonium oxidation (anammox) bacteria and suboxic to anoxic marine environments. However, little is known about the scope, distribution, and preservation of this biomarker. Chapter 4 reports that BHT II abundance increased as oxygen content decreased in the water column, consistent with previous results from Perú, the Cariaco Basin and the Arabian Sea, and in line with previous microbiological evidence, which indicates intense anammox activity in OMZ waters of this region. The BHT II signature is transported from the water column to surface sediments, and preserved in older sediments, where the relative abundance of BHT II correlates with $\delta^{15}N$ values of bulk sediment during a glacial-interglacial transition. This suggests that the production, transport, and preservation of BHT II in oxygen-deficient marine settings offers a proxy for past changes in the relative importance of anammox, and fluctuations in nitrogen cycling in response to ocean redox changes through the geological record. However, it is essential that the scope of BHT II be critically evaluated in order to confidently interpret BHT II records in sedimentary archives. As such, in Chapter 5, the distribution and possible source organisms of BHT II in benthic microbial mats from Lake Fryxell, Antarctica are described. We find that BHT II abundance in microbial mats also increased as oxygen content decreased in the water column, consistent with the results previously described. While anammox bacteria are a likely source of BHT II in this environment, alternate sources cannot be ruled out. Nonetheless, we suggest that the presence of BHT II in sedimentary archives may indicate the presence of anammox bacteria. However, we urge that the BHT II ratio is essential for interpretations of this compound in sediments. We propose that BHT II ratios <0.3 may indicate the presence of anammox bacteria in benthic microbial mats or sediments while values >0.3 may indicate influence from marine oxygen minimum zones and other environments supporting intense anammox activity.

While this thesis describes advances in bacterial membrane lipid biomarker research, there are still many questions that remain concerning the use of bacteriohopanepolyols and hopanes as biomarkers in modern and ancient sediments. It is essential that scientists continue to screen diverse environments for hopanoids and source organisms, consider environmental controls on the production of particular hopanoids, and test hypotheses through laboratory experiments with diverse organisms. Finally, standardization of laboratory procedures (lipid

extraction, analysis, and quantification) is essential if we are to generate high quality data that may be compared across laboratories, in order to fully appreciate the scope and environmental controls on hopanoid production in modern and ancient environments.